UNIVERSITÀ DEGLI STUDI DI
CASSINO E DEL LAZIO MERIDIONALE

Corso di Dottorato in
Metodi, modelli e tecnologie per l'ingegneria

curriculum Ingegneria Civile e Ambientale
Ciclo XXXIII

Simultaneous removal of carbon, nitrogen and phosphorus from municipal wastewater through continuous-flow oxygen-controlled moving bed biofilm reactors

SSD: ICAR/03, ICAR/02

Coordinatore del Corso
Chiar.mo Prof. Wilma Polini

Dottorando
Francesca Iannacone

Supervisore
Chiar.mo Prof. Giovanni Esposito

Supervisore
Chiar.mo Prof. Rudy Gargano

Abstract

Eutrophication is an imbalance of aquatic system functioning due to an uncontrolled discharge of nutrients, i.e. nitrogen (N) and phosphorus (P), in water bodies. European legislation has defined discharge limits for BOD_5, COD and TSS for wastewater treatment plants (WWTPs) serving >2000 population equivalent (PE). Moreover, stringent nutrient-discharge limits have been set for treated effluents from WWTPs larger than 10000 PE discharging into sensitive areas. Nevertheless, for small communities (below 2000 PE), the current national directive (D. Lgs. n°152/2006) and European legislation does not oblige to respect the discharge limits required for larger communities, although strict purification values can be set at local level, mainly depending on the receiving water body (e.g. lake or river). Italy is characterized by the existence of a huge amount of low-populated locations, as almost 44% of the municipalities count less than 2000 inhabitants. Centralised wastewater treatment is not always feasible or the most cost-effective option for all sites due to geographical conditions and dispersed settlements.

The aim of this doctoral thesis was to study a compact solution for the removal of C, N and P for the treatment of low- and medium-strength municipal wastewater that may help small communities to implement efficient and low-cost wastewater treatment. The combined removal of carbon and nutrients via simultaneous nitrification and denitrification (SND) coupled to P removal in moving bed biofilm reactors (MBBRs) was chosen as a potentially advantageous system for the scope as biofilm reactors enable the formation of a stratified biofilm with different microbial families depending on wastewater composition and operating conditions. Although satisfactory removal efficiencies have been achieved by operating single-stage MBBR as sequencing batch reactors (SBR) alternating anaerobic and aerobic/anoxic conditions, the MBBR-SBR technology is best suited to treat industrial wastewater, being discontinuously produced during the day, while a continuous-mode operation would be more suitable for municipal wastewater treatment.

In this PhD work, SND coupled to P removal was investigated in continuous-flow single-stage MBBRs adopting different aeration strategies, i.e. stable microaerobic conditions and intermittent aeration (IA) conditions. The microaerobic conditions were

set by maintaining a dissolved oxygen (DO) of 1.0 (±0.2) mg L^{-1}, resulting in a simultaneous removal of COD, total inorganic nitrogen (TIN) and dissolved phosphorus ($P\text{-}PO_4^{3-}$) with average efficiencies of 87%, 58% and 66% respectively, at feed C/N ratio of 4.2. At feed C/N ratio of 2.7, average TIN RE was 46% due to lack of electron donor for denitrification. At the same time, at feed C/N ratio of 5.6, excess overgrowth of heterotrophic aerobic bacteria (HAB) led to poor nitrification, determining an average TIN RE of 51%. Subsequently, aeration strategy was shifted from a continuous aeration mode to a microaerobic/aerobic IA condition. SND process and P removal were studied in a continuous-flow IAMBBR under different DO regimes (0.2–2, 0.2–3 and 0.2–4 mg L^{-1}). Simultaneous removal of dissolved organic carbon (DOC), TIN and $P\text{-}PO_4^{3-}$ removal efficiencies of 100%, 62% and 75% were achieved at DO range at 0.2–3 mg L^{-1} and at feed C/N ratio of 3.6. The bacterial community composition of the IAMBBR biofilm was investigated by Illumina sequencing, revealing the coexistence of nitrifiers (*Nitrosonomas* and *Nitrospira*) and denitrifiers with P-accumulating ability indicated as putative PAO (*Hydrogenophaga*), which were abundantly detected throughout the entire study. As last step, the feasibility of coupling a simultaneous partial nitrification and denitrification (SPND) to P removal were studied in two continuous-flow IAMBBRs. The effect of feeding two different carbon sources, i.e. ethanol and acetate, on the reactor performances and microbial community composition was also investigated. The inhibition of *nitratation* phase ($NO_2^- \rightarrow NO_3^-$) allowed to reach average DOC, TIN and $P\text{-}PO_4^{3-}$ REs of 100%, 81–88% and 83–86% at DO range of 0.2–3 mg L^{-1} and feed C/N ratio of 3.6. Finally, the effect of different feed C/P ratios (22 and 11) on P removal and microbial community of both biofilm and suspended biomass was studied. Illumina sequencing displayed the presence of putative PAOs such as *Hydrogenophaga* and *Acidovorax*, while typical NOB were never detected. MBBRs performing combined SPND and P removal achieved a 20% higher TIN RE compared to previous SND process under similar DO and C/N conditions.

This work shows that efficient, simple and low-cost C, N and P removal can be achieved in MBBR by controlling the aeration pattern and at certain C/N/P ratios. Therefore, microaerobic/aerobic MBBRs are proposed as an interesting solution for implementing wastewater treatment in small communities.

TABLE OF CONTENTS

List of Figures

List of Tables

Abbreviations

AGS	Aerobic Granular Sludge
ANAMMOX	Anaerobic Ammonium Oxidation
ANN	Artificial Neural Network
AOB	Ammonia Oxidizing Bacteria
BDP	Biodegradable Polymers
BNR	Biological Nitrogen Removal
CAS	Conventional Activated Sludge
CFD	Computational Fluid Dynamics
COD	Chemical Oxygen Demand
CSTR	Complete stirred tank reactor
DNB	Denitrifying Bacteria
DO	Dissolved Oxygen
DOC	Dissolved Organic Carbon
EBPR	Enhanced Biological Phosphorus Removal
EPS	Extracellular Polymeric Substances
FA	Free Ammonia
FBBR	Fluidized Bed Biofilm Reactor
FNA	Free Nitrous Acid
GAO	Glycogen Accumulating Organisms
HAB	Heterotrophic Aerobic Bacteria
HDPE	High-Density Polyethylene
HRT	Hydraulic Retention Time
IAMBBR	Intermittent Aeration Moving Bed Biofilm Reactor
IFAS	Integrated Fixed-film Activated Sludge
mMBBR	Microaerobic Moving Bed Biofilm Reactor
MBBR	Moving Bed Biofilm Reactor
MBR	Membrane Bioreactor
MLP	Multilayer Perceptron
NAR	Nitrite Accumulation Rate
NOB	Nitrite Oxidizing Bacteria

PAO	Phosphorus Accumulating Organisms
PBS	Poly Butanediol Succinate
PCL	Polycaprolactone
PE	Polyethylene
PHA	Poly-hydroxyalkanoates
PHB	Poly-3-hydroxybutyric acid
PLA	Polylactic Acid
PN	Protein
PP	Polypropylene
PS	Polysaccharide
PU	Polyurethane
RE	Removal
RF	Random Forest
SBR	Sequencing Batch Reactor
sCOD	Soluble Chemical Oxygen Demand
SGV	Superficial Gas Velocity
SHARON	Single reactor system for High Ammonium Removal Over Nitrite
SND	Simultaneous Nitrification and Denitrification
SNDPR	Simultaneous Nitrification-Denitrification and Phosphorus Removal
SPND	Simultaneous Partial Nitrification and Denitrification
SRT	Sludge Retention Time
TIN	Total Inorganic Nitrogen
TN	Total Nitrogen
TOC	Total Organic Carbon
TSS	Total Suspended Solids
VFA	Volatile Fatty Acid
VSS	Volatile Suspended Solids
WWTP	Wastewater Treatment Plant

CHAPTER 1.

Introduction

1.

In the last decades, an increasing attention from the scientific community has been given to the phenomenon of eutrophication in surface waters (rivers, estuaries and lakes) [1]. Eutrophication is an imbalance of aquatic ecosystems functioning, triggered by an increase of N and P loadings. The intensity of the phenomena depends on environmental factors, such as high temperatures, long residence time in water bodies and high exposition to light. Generally, eutrophication is characterized by an excess growth of plants and algae (e.g. phytoplankton and macrophytes), adapting to the new environmental conditions and replacing the initial species [2]. These new proliferations generate a large amount of biodegradable organic matter for bacteria. Their degradation by bacteria leads to further oxygen consumption, depleting dissolved oxygen (DO) and smothering aquatic organisms [3]. These events can disrupt aquatic biota and determine toxic emissions (CO_2, H_2S and CH_4). In addition, some type of algal blooms are known to release a variety of toxic compounds (such as saxitoxins, brevotoxins and domoic acid) which may result in serious health effects on both humans and animals [4,5].

Major N and P sources in aquatic systems are: (1) agriculture activities, such as animal manure and chemical fertilizers not fully used by plants; (2) inadequate wastewater treatment plants; (3) fertilizers and detergents containing high percentage of P; (4) stormwater carrying pollutants from rooftops, sidewalks, and roads, into local wastewater; (5) combustion of fossil fuels that increase the amount of P in the air. In addition, P is considered a non-renewable resource obtained mainly from rocks (e.g. phosphorite) located in a few world regions. Hence, during recent years, particular attention has been given to new technologies enhancing the performance of wastewater treatment plants to limit nutrient discharge in water bodies but also to recover and recycle the nutrients present in sewage [6,7] (**Fig. 1.1**).

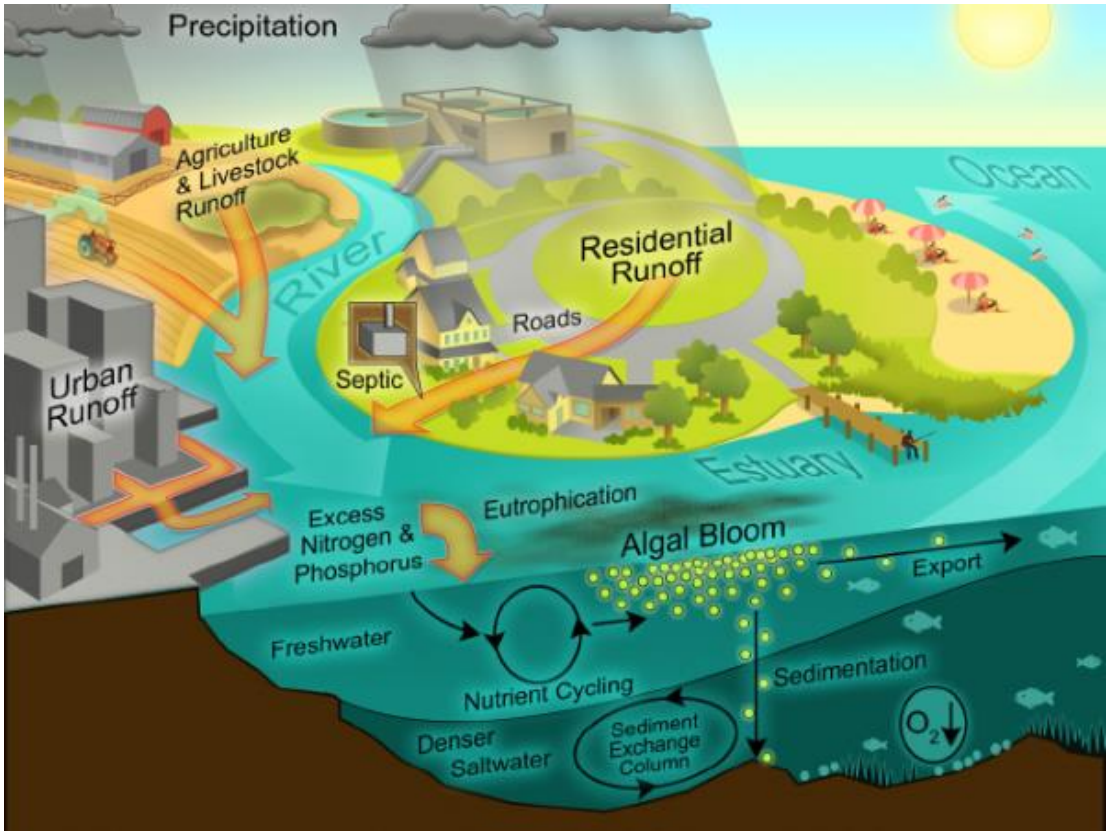

Figure 1.1 - Nutrients sources https://projecteutrophication.weebly.com/sources-of-cultural-eutrophication.html

1.1 Nitrogen and phosphorus removal: overview of treatment technologies

Up to date, nutrient removal can be achieved through chemical, physico-chemical or biological techniques [8]. Crystallization of magnesium ammonium phosphate ($MgNH_4PO_4 \cdot 6H_2O$), being also known as struvite, is a chemical process for the simultaneous removal of ammonium nitrogen ($N\text{-}NH_4^+$) and P. Struvite precipitation is usually obtained by adding magnesium salt (Mg^{2+}) to concentrated streams containing P concentrations higher than 50 mg L^{-1} [9]. Chemical precipitation of struvite can remove up to 80–90% of the soluble PO_4^{3-} and 20–30% of the soluble NH_4^+ from wastewater. However, fertilizers based on struvite are more expensive than conventional fertilizers [10]. Chemical P precipitation can also be achieved by the addition of calcium (Ca^{2+}), aluminum (Al^{3+}) or iron (Fe^{3+}) salts. Aluminum and iron salts are not commonly used, as aluminum is toxic for most plant while iron makes P less available for future recovery [11].

Physico-chemical methods include adsorption, stripping, ion exchange and membrane filtration. Ion exchange has the advantage of operating at a wide range of temperatures. However, this process requires high investment cost and the addition of chemicals to regenerate the adsorbent [10]. Natural zeolite (e.g. clinoptilolite) is one of the most used adsorbent [12] and is characterized by a porous structure with a high cation exchange ability, especially with NH_4^+ and potassium (K^+), since natural zeolite is characterized by a negatively charged surface [13]. Recently, biochar has received widespread attention as an adsorbent that adsorbs N and P. Biochar is a stable carbon-rich product formed by thermal decomposition of biomass (agricultural and forestry wastes) under anoxic conditions [14]. Membrane systems generate highly concentrated product including N, P and Mg, suitable for agronomically product. However, membrane presents fouling problem due to accumulation of salts and contaminants [15].

Biological methods typically include nitrification, denitrification, enhanced biological phosphorus removal (EBPR), being commonly applied in WWTP, and microalgae systems, in which microalgae cultivated in photobioreactors absorb organic and inorganic matter and nutrients [10]. Biological methods will be discussed in depth in Chapter 2. Conventional biological N removal include two sub-processes: (1) nitrification and (2) denitrification. Nitrification involves autotrophic nitrifiers, which oxidize ammonia (NH_4^+) to nitrate (NO_3^-) under aerobic condition. Not all NH_4^+ is oxidized, but part is used for cell growth as N source and carbon dioxide (CO_2) is used as carbon source [16]. Denitrification is carried out by denitrifying bacteria (DNB) which reduce NO_3^- to nitrogen gas (N_2) in four steps under strictly anoxic conditions [17], since DO can inhibit the enzymes involved in denitrification steps [18]. Today, the approach for N removal in municipal WWTPs foresees a pre-denitrification cycle, which denitrification and organic removal is carried first, followed by aerobic nitrification [19].

EBPR is carried out by polyphosphate accumulating organisms (PAOs) taking up phosphate from wastewater in excess compared to growth requirement (*luxury uptake*) , under anaerobic and aerobic/anoxic alternating conditions [20]. Under anaerobic conditions, volatile fatty acids (VFAs) are taken up and stored as intracellular polyhydroxyalkanoates (PHAs). PAOs gain the energy from the hydrolysis of intracellular polyphosphate (poly-P) stored during the aerobic phase, releasing phosphates in the bulk liquid. Under subsequent aerobic condition and in absence of extra organic carbon, PAOs use the stored PHAs as carbon and energy source for growth, while phosphate is taken up from the bulk liquid and stored in the form of intracellular poly-P [21,22]. Because the amount of PO_4^{3-} released during the anaerobic phase is lower than the amount taken up during the aerobic or anoxic phase, net phosphorus is achieved by

organisms, and P can be removed readily from the wastewater by wasting P-rich sludge. The schemes for EBPR are based on alternating phases providing at the same time nitrification and denitrification phases for N removal. A downstream aerobic phase can be foreseen in the sludge line for P recovering from sludge [23].

1.2 Thesis scope and objective

In Italy, more than 9000 WWTPs are reported to treat wastewater from small communities with population equivalent (PE) <2000. Small residential communities are financially unprofitable to be connected to centralized WWTPs [24,25]. Falletti et al. [25] reported that plants that treat less than 2000 PE are often characterized only by primary treatment, while most plants in the range of 2000–10000 PE have also secondary treatment. Small plants can be upgraded by implementing advanced technology requiring minimal additional space or by converting existing reactors. The current national and European legislation does not oblige small communities (<2000 PE) to respect the discharge limits applied to larger communities as less stringent purification values can be set at regional level through Source Water Protection Plans (SWP), with permissible discharge limits depending on the receiving water body (sea, lake, river, or soil, where it is allowed). The negative environmental impacts of wastewater discharge from small communities necessitate research for improved wastewater treatment technologies. The main aim of this doctoral thesis is to study a compact and low-cost treatment solution that may help small communities struggling with the implementation of secondary treatment in WWTPs.

In this PhD research, the following objectives were addressed:

- Investigate the optimal conditions to achieve simultaneous removal of carbon (C), N and P in continuous-flow moving bed biofilm reactors (MBBRs):
    - Testing different aeration strategy (continuous mode and intermittent aeration).
    - Evaluating the impact of different feed C/N ratios on performance removals.
    - Investigating the microbial community structure and the key microorganisms involved in N and P removal.
- Investigate the feasibility to couple simultaneous partial nitrification and denitrification and P removal in continuous-flow MBBRs:

- Testing different carbon source (i.e. ethanol and acetate) on both nutrients removal efficiency and microbial community.
- Investigating the effect of different feed C/P ratios on both P removal and microbial community of biofilm and suspended biomass.

1.3 Thesis outline

This doctoral thesis is composed by 6 chapters (**Fig. 1.2**).

Chapter 1 is a general introduction on the main topics of the thesis. The structure of thesis is also described.

Chapter 2 proposes a comparative analysis of the parameters affecting simultaneous nitrification and denitrification (SND) and the most used biofilm reactor configurations, such as moving bed biofilm reactors (MBBRs), sequencing biofilm batch reactors (SBBR) and aerobic granular sludge (AGS).

Chapter 3 investigates the impact of feed C/N ratio on simultaneous nitrogen and phosphorus removal in a continuous flow MBBR under stable microaerobic conditions (1.0 ± 0.2 mg L^{-1}).

Chapter 4 investigates the removal efficiencies of carbon, nitrogen and phosphorus in a continuous-flow MBBR alternating microaerobic and aerobic conditions. The SND process coupled with phosphorus removal was studied under different DO ranges and feed C/N ratios. Finally, biofilm evolution was investigated by means of Illumina sequencing analysis.

Chapter 5 investigates the feasibility of shortcut SND coupled to phosphorus removal in a continuous-flow MBBR under microaerobic/aerobic alternating conditions and the impact of different feed carbon sources on the process.

Chapter 6 is a general discussion of the results obtained during the doctoral studies. This chapter also provides recommendations and perspectives for future research.

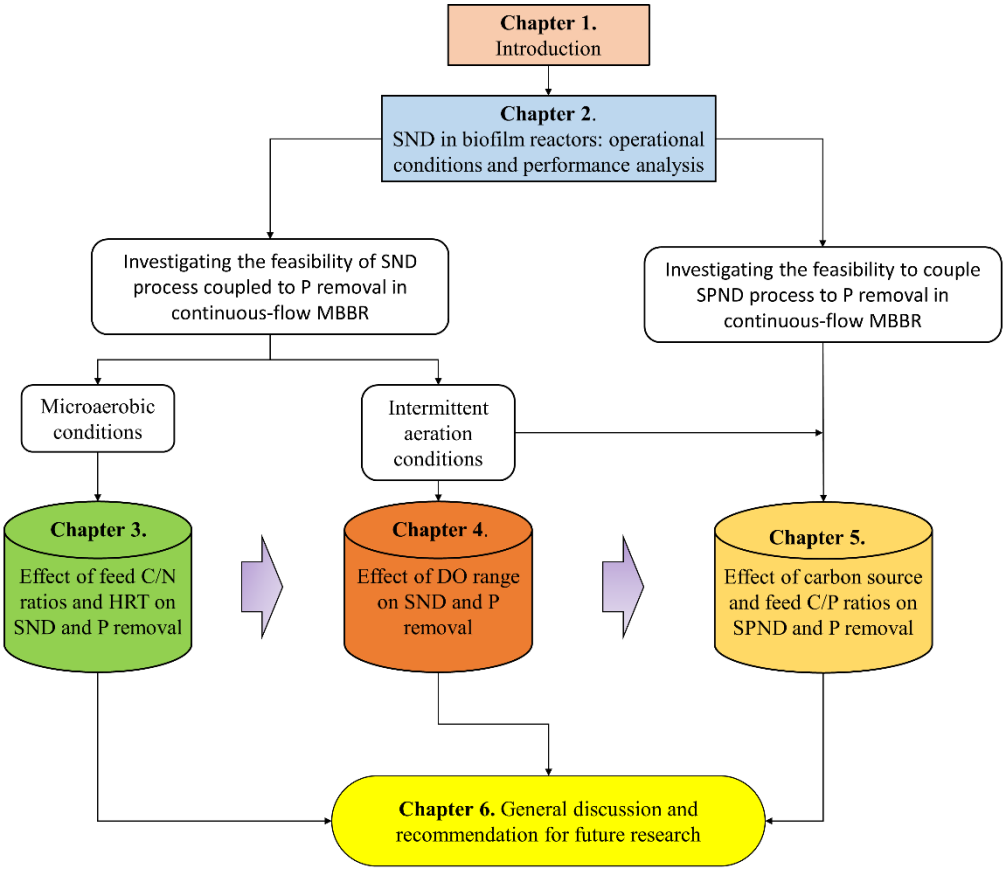

Figure 1.2 - Flow scheme describing the structure of the doctoral thesis

1.4 Reference

[1] P.J.T.M. van Puijenbroek, A.H.W. Beusen, A.F. Bouwman, Global nitrogen and phosphorus in urban waste water based on the Shared Socio-economic pathways, *J. Environ. Manage. 231* (2019) 446–456.

[2] R.A. Camacho, J.L. Martin, B. Watson, M.J. Paul, L. Zheng, J.B. Stribling, Modeling the factors controlling phytoplankton in the St. Louis Bay estuary, Mississippi and evaluating estuarine responses to nutrient load modifications, *J. Environ. Eng.* 141 (2015) 1–17.

[3] X. Mao, P.H. Myavagh, S. Lotfikatouli, B.S. Hsiao, H.W. Walker, Membrane bioreactors for nitrogen removal from wastewater: a review, *J. Environ. Eng.* 146 (2020) 03120002.

[4] S. Rahimi, O. Modin, I. Mijakovic, Technologies for biological removal and recovery of nitrogen from wastewater, *Biotechnol. Adv.* 43 (2020) 107570.

[5] M. Le Moal, C. Gascuel-odoux, A. Ménesguen, Y. Souchon, C. Étrillard, A. Levain, F. Moatar, A. Pannard, P. Souchu, A. Lefebvre, G. Pinay, Eutrophication: a new wine in an old bottle?, *Sci. Total Environ.* 651 (2019) 1–11.

[6] Z. Song, X. Zhang, H. Hao, W. Guo, P. Song, Y. Zhang, Zeolite powder based polyurethane sponges as biocarriers in moving bed biofilm reactor for improving nitrogen removal of municipal wastewater, *Sci. Total Environ.* 651 (2019) 1078–1086.

[7] J. Yin, P. Zhang, F. Li, G. Li, B. Hai, Simultaneous biological nitrogen and phosphorus removal with a sequencing batch reactor-biofilm system, *Int. Biodeterior. Biodegradation. (*2015) 1–6.

[8] P.S. Kumar, L. Korving, M.C.M. Van Loosdrecht, G.-J. Witkamp, Adsorption as a technology to achieve ultra-low concentrations of phosphate: research gaps and economic analysis, *Water Res. X.* 4 (2019) 100029.

[9] S. Salehi, K.Y. Cheng, A. Heitz, M.P. Ginige, Simultaneous nitrification, denitrification and phosphorus recovery (SNDPr) - an opportunity to facilitate full-scale recovery of phosphorus from municipal wastewater, *J. Environ. Manage.* 238 (2019) 41–48.

[10] M.C. Chrispim, M. Scholz, M. Antunes, Phosphorus recovery from municipal wastewater treatment: critical review of challenges and opportunities for developing countries, *J. Environ. Manage.* 248 (2019) 109268.

[11] Z. Yuan, S. Pratt, D.J. Batstone, Phosphorus recovery from wastewater through microbial processes, *Curr. Opin. Biotechnol.* 23 (2012) 878–883.

[12] S. He, G. Xue, H. Kong, X. Li, Improving the performance of sequencing batch reactor (SBR) by the addition of zeolite powder, *J. Hazard. Mater.* 142 (2007) 493–499.

[13] Y. Zhao, D. Liu, W. Huang, Y. Yang, M. Ji, L.D. Nghiem, Q.T. Trinh, N.H. Tran, Insights into biofilm carriers for biological wastewater treatment processes: current state-of-the-art, challenges, and opportunities, *Bioresour. Technol.* 288 (2019) 121619.

[14] Y. Dai, W. Wang, L. Lu, L. Yan, D. Yu, Utilization of biochar for the removal of nitrogen and phosphorus, *J. Clean. Prod.* 257 (2020) 120573.

[15] A.G. Capodaglio, P. Hlavínek, M. Raboni, Physico-chemical technologies for nitrogen removal from wastewaters: a review, *Rev. Ambient. Água.* 10 (2015).

[16] F. Jaramillo, M. Orchard, C. Muñoz, M. Zamorano, C. Antileo, Advanced strategies to improve nitrification process in sequencing batch reactors - a review, *J. Environ. Manage.* 218 (2018) 154–164.

[17] B.E. Rittmann, P.L. McCarty, Environmental biotechnology: principles and applications, McGraw Hill Education, 2012.

[18] F. Di Capua, F. Pirozzi, P.N.L. Lens, G. Esposito, Electron donors for autotrophic denitrification, *Chem. Eng. J.* 362 (2019) 922–937.

[19] M. Fabbricino, F. Pirozzi, Designing and upgrading model of pre-denitrification systems, *Clean Technolody Environ. Policy*. 6 (2004) 213–220.

[20] S.Y. Gebremariam, M.W. Beutel, D. Christian, T.F. Hess, Research advances and challenges in the microbiology of enhanced biological phosphorus removal — a critical review, *Water Environ. Res.* 83 (2011) 195–219..

[21] M. Stokholm-Bjerregaard, S.J. Mcilroy, M. Nierychlo, S.M. Karst, M. Albertsen, P.H. Nielsen, A critical assessment of the microorganisms proposed to be important to enhanced biological phosphorus removal in full-scale wastewater treatment systems, *Front. Microbiol*. 8 (2017) 718.

[22] M. Pijuan, A. Guisasola, J.A. Baeza, J. Carrera, C. Casas, J. Lafuente, Net P-removal deterioration in enriched PAO sludge subjected to permanent aerobic conditions, *J. Biotechnol.* 123 (2006) 117–126.

[23] Y. Chen, C. Peng, J. Wang, L. Ye, L. Zhang, Y. Peng, Effect of nitrate recycling ratio on simultaneous biological nutrient removal in a novel anaerobic/anoxic/oxic (A2/O) -biological aerated filter (BAF) system, *Bioresour. Technol.* 102 (2011) 5722–5727.

[24] G. Libralato, A.V. Ghirardini, F. Avezzù, To centralise or to decentralise: an overview of the most recent trends in wastewater treatment management, *J. Environ. Manage.* 94 (2012) 61–68.

[25] L. Falletti, L. Conte, A. Zaggia, Small wastewater treatment plants in Italy: situation and case studies of upgrading with advanced technologies, *Desalin. Water Treat.* 51 (2013) 2402–2410.

CHAPTER 2.

Simultaneous nitrification and denitrification in biofilm reactors: operational conditions and performance analysis

2.

2.1 Introduction

Nitrogen (N) and phosphorus (P) are essential nutrients for all living forms [1]. However, excessive discharge of N and P in surface waters can determine an abnormal growth of algae and, consequently, a depletion of dissolved oxygen (DO) [2,3]. This phenomenon is known as eutrophication and represents a serious problem affecting water quality in rivers, lakes and estuaries around the world [4–6]. The main source of N in surface waters is represented by the run-off from agricultural land and industrial activities [7], while P contamination occurs primarily from industry, households and livestock manure [8]. The exponential growth of urbanization in the last years has led to an increase in nutrient-rich wastewater production [9]. The European Council Directive 271/91 EEC and the European Water Framework Directive 60/2000/EC focused their attention to the protection of sensitive areas at risk of eutrophication by setting limitations for total phosphorus (TP) and total nitrogen (TN) concentrations in treated effluents from WWTPs larger than 10000 population equivalent (PE). Discharge limits for chemical oxygen demand (COD), biochemical oxygen demand (BOD_5) and total suspended solids (TSS) are also provided for agglomerations larger than 2000 PE. However, for small communities (below 2000 PE), the current national and European legislation does not oblige to respect the discharge limits required for larger communities as less stringent purification values can be set at local level, with permissible discharge limits based on receiving water bodies. Therefore, one of the keys challenges for the achievements of discharge requirements is to identify the most feasible and cost-effective technologies for the treatment of wastewater from small communities that contribute to eutrophication phenomenon.

As an example, Italy is characterized by the existence of a huge amount of low-populated locations, as almost 44% of the municipalities count less than 2000 inhabitants (ISTAT, 2019). Lijó et al. [10] reported over 9000 wastewater treatments plants (WWTPs) in Italy being designed for 2000 PE or less. The centralized treatment of wastewaters from small communities is not always feasible or the most cost-effective option due to geographical conditions and dispersed settlements [11].

Biological nitrogen removal (BNR) is known to remove N compound from wastewaters and is recognized as the most economical process to reach the stringent limit discharge with higher cost-effectiveness compared to physicochemical processes [12,13]. Simultaneous nitrification and denitrification (SND) is capable to completely remove N

within the same bioreactor under specific operating conditions, which differentiate this process from conventional nitrification/denitrification being carried out in separate bioreactors [12,14,15]. Moreover, in the last years the SND process was also coupled with enhanced biological phosphorus removal (EPBR), resulting in the so-called simultaneous nitrification-denitrification and phosphorus removal (SNDPR) process [16]. Recently, SNDPR has gained increasing attention as a doorway to remove nutrients (i.e. N and P) in a single system and simultaneously reducing both carbon and oxygen requirements [17,18].

Up to date, many researchers have studied the effect of various factors on SND, including the feed C/N ratio, DO concentration, hydraulic retention time (HRT) and aeration pattern. In this chapter, a comprehensive review of SND applications in biofilm reactors is presented. Also, the fundamental mechanisms of SND are investigated and critical knowledge gaps identified.

2.2 Overview of nitrogen removal bioprocesses

The nitrification process is carried out under aerobic conditions and consists of two consequential steps of oxidation (**Fig. 2.1**). In the first step, ammonia oxidizing bacteria (AOB) oxidize NH_4^+ to nitrite (NO_2^-) by consuming 1.5 mol of oxygen. In this reaction, the enzymes ammonia monooxygenase (AMO) and then hydroxylamine oxidoreductase (HAO) are involved, along with hydroxylamine (NH_2OH) as intermediate product; in the second step, nitrite oxidizing bacteria (NOB) convert NO_2^- to NO_3^- by consuming 0.5 mol of oxygen. In this case nitrite oxidoreductases (NXR) are the enzymes involved [19,20] (**Fig. 2.1**). AOB and NOB use only inorganic carbon sources, consuming almost 7.1 mg $CaCO_3$ for each mg N-NH_4^+ oxidized [21,22]. During nitrification, nitrous oxide (N_2O), a potent greenhouse gas [23], may be produced by AOB via two main pathways: reduction of NO_2^- as terminal electron acceptor to N_2O (pathway known as nitrifier denitrification) and incomplete oxidation of hydroxylamine (NH_2OH), which is first chemically decomposed to NO and then biologically reduced to N_2O (known as hydroxylamine pathway) [24]. AOB genera include *Nitrosospira*, *Nitrosomonas*, *Nitrosovibrio* and *Nitrosococcus*, while *Nitrospira*, *Nitrobacter*, *Nitrospina* and *Nitrococcus* are identified as NOB [25,26]. Under anoxic conditions, the reduction of NO_3^- to NO_2^- and then to N_2 is carried out by denitrifying bacteria (DNB), by generally using organic carbon as electron donor and producing alkalinity. Similar to nitrification, incomplete denitrification can lead to the emission of N_2O, being a process intermediate [23,27]. Bacteria belonging to *Thaurea*, *Flavobacterium*, *Acidovorax*, *Hydrogenophaga*,

Rhizobium, *Pseudomonas* and *Acinetobacter* are reported as denitrifiers frequently observed in WWTPs [28,29]. The dominant phylum in activated sludge is commonly represented by *Proteobacteria*, followed by *Bacteroides*, *Chloroflexy* and *Actinobacteria* [20].

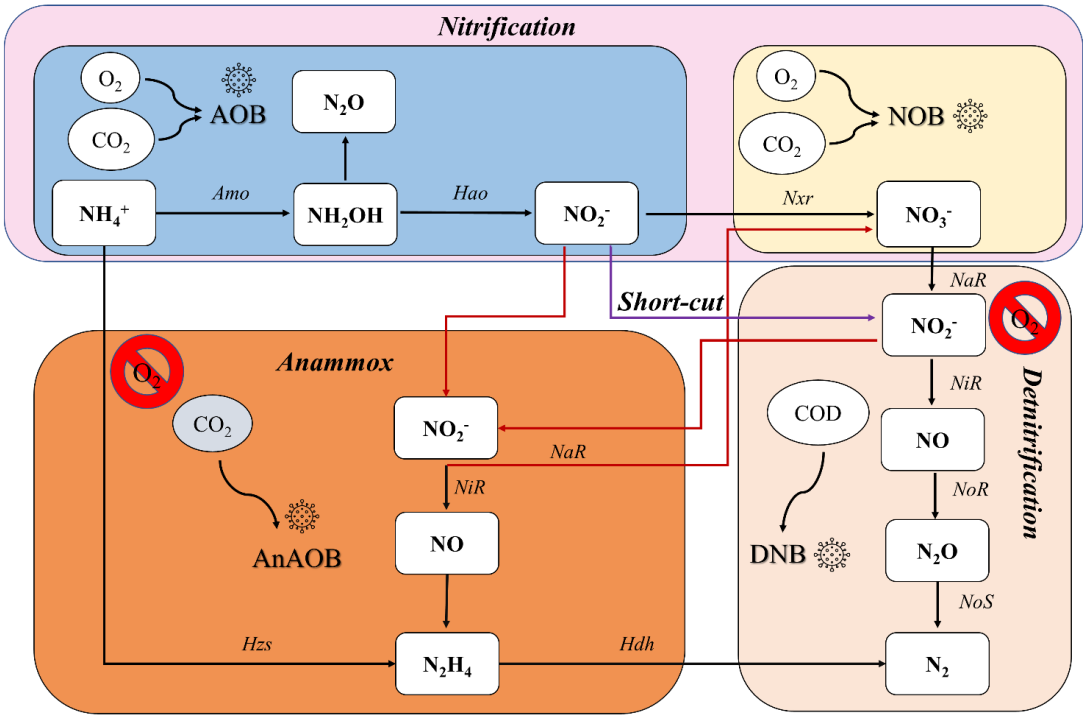

Figure 2.1 - Major biological processes of the nitrogen cycle. AOB, ammonium oxidizing bacteria; NOB, nitrite oxidizing bacteria; DNB, denitrifying bacteria; AnAOB, anaerobic ammonium oxidizing bacteria; Amo, ammonia monooxygenase; Hao; hydroxylamine oxidoreductase; Nxr, nitrite oxidoreductases; Hzs, hydrazine hydrolase; Hdh, hydrazine-oxidizing enzyme; NaR, nitrate reductase; NiR, nitrite reductase; NoR, nitric oxide reductase; NoS, nitrous oxide reductase.

BNR through nitrification and denitrification is mainly accomplished within the conventional activated sludge (CAS) system. Generally, nitrogen removal is achieved by means of a pre-denitrification cycle, with provides for an heterotrophic denitrification phase followed by an aerobic phase for combined oxidation of organics and ammonium [30]. However, CAS is often unsustainable for the treatment of wastewater produced in small communities due to large structural footprints and high energy demand and sludge production [14].

In recent years, novel biological processes, i.e. Anaerobic AMMonia Oxidation (Anammox) and simultaneous nitrification denitrification (SND), have been increasingly investigated with the aim to limit nitrogen discharge in water bodies by reducing the operating costs of WWTPs.

Anammox is defined as an autotrophic process for complete N-NH_4^+ removal, since Anammox bacteria oxidize NH_4^+ directly to N_2 obtaining energy for growth from the oxidation of NO_2^- to NO_3^- [31] (**Fig. 2.1**). Nitrite can be produced by partial nitrification (*nitritation*) of NH_4^+ or through partial denitrification (DN or *denitritation*) of NO_3^-. The advantages connected to *nitritation* are: (1) reduced energy consumption thanks to a 60% lower oxygen requirement because only 50% of ammonia needs to be partially oxidized to NO_2^- instead that to NO_3^-; (2) no need of external carbon source to obtain a complete nitrogen removal, because partial nitrification and then Anammox are both autotrophic processes; (3) reduced CO_2 and N_2O emission; (4) reduced sludge production due to slow growth of Anammox bacteria [20,29,32]. Despite these advantages, the Anammox process presents limitations: (1) the specific growth rate of Anammox organisms is low (0.069 d^{-1}), resulting in long enrichment and start-up periods [33]; (2) excess discharge of nitrate in effluent might require a post-denitrification phase to achieve the standards; (3) anammox bacteria requires high temperature (i.e. 30–40°C) and a strict temperature and pH control, showing strong sensitivity to operational conditions; (4) the presence of organic matter generates a competition for NO_2^- between denitrifying and anammox bacteria determining a lower ammonium removal; (5) organic compounds can inhibit anammox activity completely or partially [20,29,32].

2.3 Simultaneous nitrification denitrification (SND)

The SND process can be considered a promising alternative to conventional pre-denitrification cycle in WWTP for the simultaneous removal of C and N from municipal wastewater as it offers several advantages: (1) carbon demand and sludge production are reduced by over 30% [34,35], (2) alkalinity supply by denitrification helps to maintain a circumneutral pH, (3) there is no need of NO_3^- recirculation, (4) less energy for aeration is required [36], (5) small footprint [37]. Potential disadvantages of the SND process are (1) lower nitrogen removal efficiencies compared to separate denitrification and nitrification, (2) significant nitrous oxide (N_2O) accumulation [38] and (3) process instability due to competition among the different microbial families coexisting in the system.

Fig. 2.2 shows the number of publications on SND process during the last 30 years. As can be seen from the upper right graph, since 1990 nearly 1400 scientific contributions have been published on SND process with various engineered systems. Most studies have been carried out at laboratory scale using different types of biofilm and suspended-growth systems. Generally, technologies based on biofilm systems have different advantages

over CAS system: (1) higher biomass concentration; (2) lower space requirements; (3) reduced hydraulic retention time (HRT) and sludge production; (4) performance more stable [39]. In addition, biofilm systems allow the coexistence of different microbial species involved in nutrients removal on a support media being fixed or floating in the bioreactor, which makes these systems perfectly suitable for the SND process. Biofilm reactors that have been applied for SND includes moving bed biofilm reactor (MBBR) (**Table 2.1**), sequencing batch biofilm reactor (SBBR) (**Table 2.2**), membrane biofilm bioreactor (**Table 2.3**), aerobic granular sludge (AGS) reactor (**Table 2.4**) and fluidized bed biofilm reactor (FBBR).

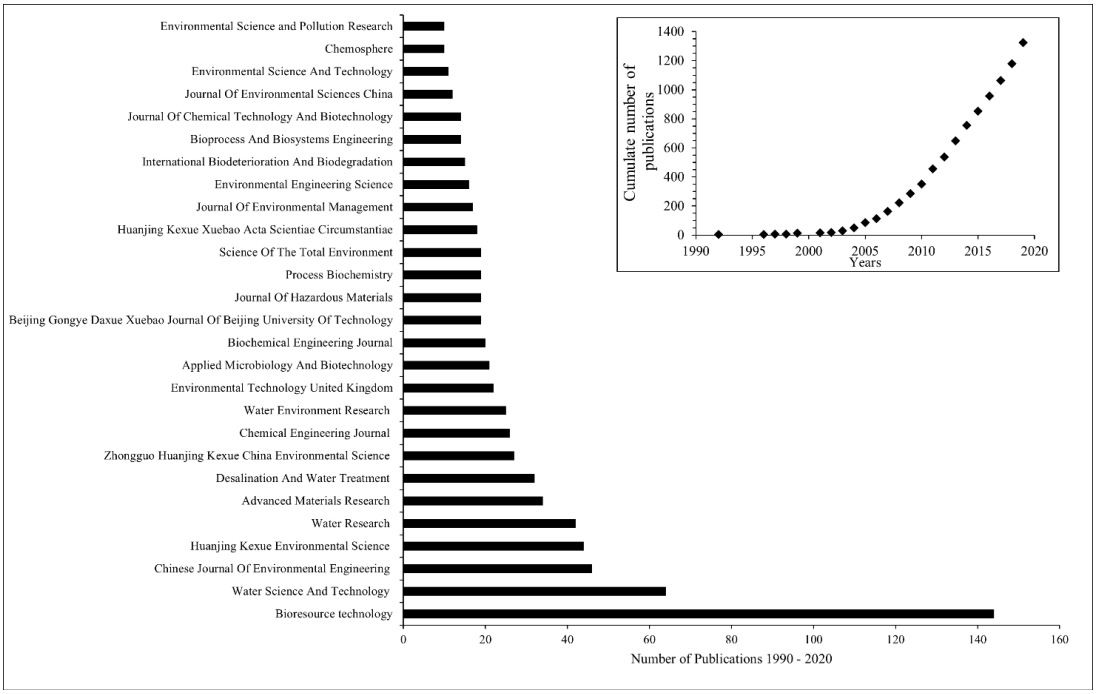

Figure 2.2 - Number of publications on SND since 1990 until 2020 (Source: Scopus).

2.4 Factors influencing SND process in biofilm reactors

The key for a successful SND process is to balance the coexistence between bacteria involved in nitrification (AOB, NOB) and denitrification (DNB). Each group of bacteria has its optimal living environment [40,41]. Up to date, researchers have focused their attention on studying the parameters affecting SND during bioreactor operation. Besides environmental factors (pH and temperature), which regulate the activity of the bacterial species involved, the SND process is impacted by operating parameters such as DO, HRT, feed C/N ratio, diffusion limitations inside biofilm, microbial competition and type of influent wastewater.

2.4.1 Environmental factors

Environmental factors such as pH and temperature can affect both the efficiency and pathways of nitrification. It is well known that AOB and NOB are sensitive to these parameters [13]. It has been reported that AOB can outcompete NOB at temperatures > 25°C, while NOB grow much faster at lower temperatures. T. Liu et al. [42] evaluated the SND performance of a MBBR operated under three different temperatures (23°C, 18°C and 13°C). The optimal value of temperature was 23°C, while lower temperatures were unbeneficial due to slow growth of AOB. When the temperature decreased from 23°C to 13°C, TN REs decreased from 55.3% to 28.9% due to lower nitrifying activity [42]. pH values in the bioreactor are determined by bacterial activity. During the nitrification process, AOB and NOB bacteria consume almost 7.13 mg $CaCO_3$ for each mg of $N\text{-}NH_4^+$ oxidized due to release of H^+. However, denitrification supplies alkalinity which helps to keep a circumneutral pH [43,44].

Temperature and pH are also keys parameters affecting the *nitritation* process. For instance, pH affects the AOB and NOB activities directly by modifying the enzymatic reaction mechanism or indirectly via inhibition by free ammonia (FA) and free nitrous acid (FNA). The suggested pH to inhibit NOB is reported to be between 7.5–8.5 [26]. *Nitritation* combined with SND process will be discussed in **Section 2.5**.

2.4.2 Operational parameters

- ***DO concentration***

DO concentration in the bioreactor impacts the microbial physiology and community composition within the biofilm [14]. As is well known, the SND process is based on the co-existence of AOB, NOB and DNB inside the biofilm, being possible thanks to DO concentration gradients generated by diffusional limitations [45]. Specifically, the DO concentration in the bulk liquid can be manipulated to create a gradient determining the formation of an anoxic micro-environment where denitrification can occur, while nitrifying bacteria thrive on the external region of the biofilm were DO is more abundant [46–48].

In the literature, the suitable DO concentration for maintaining the SND process varies in a wide range (0.8–7 mg L^{-1}) and is affected by a number of factors, e.g. carbon source availability, reactor configuration and operation, granule size or biofilm thickness and carrier type (**Tables 2.1**–**2.4**). The set DO concentration must ensure a balance between microbial families and the production and consumption of NO_x. Penetration depth of DO influences the SND performance, as high values of DO concentration in the bulk liquid

can limit the formation of the anoxic zone, while low DO concentrations can limit nitrification [49–52]. Cao et al. [7] investigated the effect of DO on SND in a MBBR by means of microelectrode measurements and real time polymerase chain reaction (PCR). Five DO concentrations ranging from 1.5 to 5.5 mg L^{-1} were tested in five identical moving bed SBRs (MBBR-SBRs) (**Table 2.2**). After an acclimatization period, the highest TN removal efficiency (RE) was observed at a DO concentration of 2.5 mg L^{-1} (84%), while COD REs were > 90% in all systems (**Table 2.2**). Higher DO concentration (3.5–5.5 mg L^{-1}) inhibited denitrification due to the increased DO penetration in the MBBR biofilm, while the relative abundance of AOB and NOB increased. Low DO concentration (1.5 mg L^{-1}) limited the nitrifying activity, resulting in lowest relative abundance of AOB in the biofilm and in a significant increase of N-NH_4^+ concentration in the effluent (up to 13.8 mg L^{-1}). Based on these results, it clear that DO is a very important parameter and must be strictly controlled to maximize TN RE.

In another study, Liu et al. [45] studied the effects of three different DO concentration (2.5 ± 0.5 mg L^{-1}, 1.5 ± 0.5 mg L^{-1} and 0.8 ± 0.3 mg L^{-1}) in a continuous-flow MBBR. Results showed that a DO lower than 1 mg L^{-1} is beneficial for SND performance (TN RE up to 53%) with high N-NH_4^+ RE (85%). At DO over 1.5 ± 0.5 mg L^{-1}, N-NH_4^+ RE reached 98% corresponding to TN RE of almost 30% due to limited denitrification activity. Recently, the microaerobic operation of continuous-flow MBBRs at DO levels of 1.0 ± 0.2 mg L^{-1} showed promising SND performances [26,42] (**Table 2.1**). However, under oxygen-limited conditions AOB may compete with NOB and HAB for DO [53]. The basic problem in nitrification lies in the fact that nitrifying bacteria (NOB and AOB), which oxidize NH_4^+ and NO_2^-, have much lower growth rate and higher affinity constant of oxygen compared to HAB, which can easily outcompete them under limiting DO conditions.

Applications of AGS systems showed that DO concentrations in the range of 1.5–3.0 mg L^{-1} generally tend to increase SND performances [49,54]. However, high DO concentrations are required inside AGS reactors to ensure long-term stability of the bioreactor. Long term stability is maintained by high shearing force affected mainly by aeration, which also determines nitrification and denitrification efficiencies [55–57]. Yan et al. [55] studied the effect of three DO concentration ranges (6–7, 4–5, 2–3 mg L^{-1}) on AGS performances and dynamic changes in sludge particle size. With the decrease of DO concentration and air shear force the percentage of particle size with diameter less than 0.5 mm increased by 0.9-6.4%, which means that higher DO levels (6–7 mg L^{-1}) determined an appropriate hydrodynamic shear force for a stable operation, while lower DO values led to partial break-up of the granules [55,58]. However, low TIN REs with

an average value of 21% were achieved at the highest DO concentration range of 6–7 mg L^{-1}, while higher REs (i.e. 38%) were observed under DO concentrations of 2–3 mg L^{-1}. TN REs was probably affected also by the low feed C/N of 1, which could not provide sufficient organic electron donor for denitrification activity and growth of microorganism [55].

Intermittent aeration (IA) can be a suitable choice for the SND process, as it can promote the activities of both nitrifying and denitrifying bacteria coexisting in the biofilm [44,59]. In addition, IA can significantly limit the expenses for wastewater treatment, as aeration accounts for more than 50% of the energy costs of a municipal WWTP [44,60].

- ***Feed C/N ratio***

Municipal wastewaters are generally characterized by low C/N ratios, which may result in low nitrogen removal efficiency due to lack of organic electron donor for denitrification [61,62]. As a result, additional carbon source such as methanol, glucose or sodium acetate is often needed [61,63]. In the same way, low SND performance in biofilm systems is often linked to the lack of electron donors for denitrification [49,64]. The outer space of biofilm is generally occupied by HAB, for which it is easier to get food from the bulking solution than for DNB, which occupy the inner anoxic zone. During the process of organic substance diffusion from the bulking solution to the aerobic zone and further to the anoxic zone, a large amount of organics is consumed by HAB and the remaining organics may not meet the requirement for denitrification. F. Wang et al. [65] used an AGS to treat real domestic wastewater through SND process. The SBR showed average COD and TP REs of 80% and 71%, respectively. Nitrification efficiency reached values up to 92%, however TN RE was about 52% due to low feed C/N ratios (0.4–2.3), lower than the theoretical value of 2.9 for complete nitrogen removal. Later, Wang et al. [66] studied the effects of three different COD/TN ratios (20, 10, 4) on an SNDPR process using AGS. TN REs decreased from 95% to 75% due to carbon deficiency, being the result of reduced COD/TN ratio following the increase of effluent N-NO_3^- from 0.2 to 14.6 mg L^{-1}.

Possible solutions to overcome the lack of carbon source in real municipal wastewater are: (1) addition of liquid carbon sources, such as ethanol, methanol or acetic acid; (2) addition of solid carbon source, such as biodegradable polymers (BDPs) [45,67–69]. Wang et al. (2009) observed a 30% improvement of TN RE when the volumetric loading rate (VLR) was increased from 0.7 to 3.41 kg m^{-3} d^{-1} adding sodium acetate in batch experiments with aerobic granules due to more carbon source being available for denitrification. The second solution is the use BDPs, such as poly-3-hydroxybutyric acid (PHB), polycaprolactone (PCL), polylactic acid (PLA) and poly butanediol succinate

(PBS) [39]. BDPs can be hydrolyzed by extracellular enzymes secreted by specific microorganisms, and then hydrolysis products can be utilized by HAB and DNB as sources of organic carbon [63,70,71]. BDPs are identified as slow-release carriers and are used in various application as electron donor/nutrient sources but also as biofilm carriers [39]. Han et al. [63] compared the nitrogen removal performance of a conventional MBR (C-MBR) to that of an MBR with a novel biocarrier composed of polyester-urethane sponge with a PBS granule wrapped inside the sponge. The PBS was used as external carbon source and also as biofilm carriers treating low feed C/N ratio (below 1.0) wastewater (**Table 2.2**). After biofilm formation and the consequent enrichment of bacteria able to disintegrate the PBS material, the effluent $N\text{-}NO_3^-$ decreased from 22.2 to 4.6 mg L^{-1}, resulting in an increased TN RE from 62% to 92% [63]. The MBR with modified carriers achieved TN RE value 80% higher compared to that of C-MBR (12%). However, BDPs are characterized by high costs, being 2 - 7 fold higher than ethanol or methanol and similar to that of acid acetic [39,67]. Low-cost alternatives to BDPs are other natural biopolymers such as starch or lignocellulose. Feng et al. [72] used a biodegradable support made in rice husk and lignocellulosic materials mainly composed of biodegradable cellulose, branched hemicelluloses and recalcitrant lignin.

Although positive effects have been highlighted, increase of feed C/N ratio in SND systems should be controlled. Several studies pointed out that excess organic carbon feeding may limit nitrification and denitrification efficiencies. Under high biodegradable COD loadings, HAB characterized by high growth rates and biomass yields will outcompete AOB and NOB for DO and NH_4^+ and DNB for organic carbon and NO_x. Fu et al. [73] investigated the effect of five C/N ratios (4.3–13.4) on the SND process under strictly aerobic conditions (DO = 3.0–4.0 mg L^{-1}) in three MBBRs filled with polyethylene (PE) carriers. During experimental activities, ammonia concentrations in the three MBBRs has been gradually increased to a final concentration of 100 mg L^{-1}, corresponding to a C/N ratios between 4.5 and 13.4. The results demonstrated nearly complete denitrification at a C/N ratio of 4.5–13.4, while nitrification efficiency was relatively low (41–2%) probably due to the competition between nitrifiers and HAB for DO [51,73] (**Table 2.1**). FISH analysis showed an increase of AOB and NOB abundances linked to a decrease of COD loading rate, which indicates that a lower supply of carbon source determined a decrease in the abundance of heterotrophic bacteria within the biofilm while making more DO available for nitrifying bacteria.

2.5 Short-cut SND

The short-cut SND process (also known as SND via nitrite or simultaneous partial nitrification denitrification, SPND) involves the incomplete oxidation of NH_4^+ to NO_2^- by AOB (*nitritation*) followed by the complete reduction of NO_2^- to N_2 by DNB (*denitritation*) (**Fig. 2.1**). The *nitritation* process implies the NOB activity suppression to stop NO_2^- oxidation and allow *denitritation*. Short-cut SND is a feasible technology to treat wastewater with low C/N ratio, as it results in lower carbon consumption compared to complete SND. SND via nitrite, or shortcut SND, is proposed by several studies adopting different pathway to inhibit NOB growth [15,62,74–77].

In order to allow the AOB growth and simultaneously inhibit the NOB activity and avoid their proliferation, it is essential to maintain specific operational conditions, e.g. pH between 7.5 and 8.5 [26], DO levels below 1.5 mg L^{-1} [13,19], temperature >25°C [20,75], SRT or reaction time below 5 days [29], real time control of anoxic and aerobic alternation conditions [74], inhibitory FA and FNA concentrations. The main advantages related to short-cut SND compared to conventional nitrification and denitrification are: (1) 25% oxygen reduction during aerobic phase, implying saving almost 60% of energy costs; (2) reduction of almost 40% of carbon requirements for denitrification [14,19,29,78]. Jia et al. [53] reported a decrease of theoretical oxygen consumption and required COD from 2 to 1.5 mol O_2/mol NH_4^+ and from 40 to 24 mg COD/mol NH_4^+, respectively, compared to conventional nitrification and denitrification. Furthermore, NO_2^- reduction rate is reported to be 1.5–2 folds higher than NO_3^- reduction, which should accelerate nitrogen removal [20,78].

FA and FNA inhibit both AOB and NOB and their concentrations in the bioreactors are determined by those of NH_4^+ or NO_2^- concentration. Threshold limits of inhibition for AOB and NOB are different, being NOB more sensitive than AOB to both FA and FNA. AOB is inhibited by FA with concentrations between 10–605 mg N L^{-1}, while values between 0.1–5 mg N L^{-1} are sufficient to inhibit NOB [26]. In particular, high concentrations of FA inhibit the NXR enzyme located on NOB [19]. FNA concentrations that inhibit AOB lie between 0.42–1.72 mg N L^{-1}, while NOB inhibition was observed already at concentrations of 0.011–0.07 mg N L^{-1}. Concentrations between 0.026–0.22 mg N L^{-1} could completely inhibit NOB activity [26,53].

It is widely known that at temperatures lower than 20°C the maximum specific growth rate of NOB is higher than the growth rate of AOB and temperatures higher than 25°C are required for AOB to outgrow NOB and ensure nitrite accumulation [75]. Based on this concept, a new process, namely SHARON (Single reactor system for High activity Ammonium removal Over Nitrite), was proposed. The SHARON process enables to achieve a controlled *nitritation*, although it is not suitable for municipal wastewater due

to its strict operational conditions. Indeed, the SHARON process runs at HRT of 1–3 days and temperature between 30 and 40°C [26,74]. Due to high specific heat of water (4.183 Kj Kg^{-1}, 20°C), it is not economical feasible to increase the temperature of municipal wastewater [19]. Hence different strategies to enhance the activity of AOB over NOB have to be found [79]. In addition, maintaining a stable *nitritation* in system treating real wastewater characterized by low C/N ratio and low N-NH_4^+ concentrations (< 50 mg L^{-1}) (such as municipal wastewater) is complicated, also due to influent fluctuations, especially during continuous operation [13,19]. Another important issue to consider is the potential discharge of high concentrations of nitrite in water, which is toxic for human. Further investigation of SND via nitrite coupled phosphorus removal are required in order to understand the potential inhibitory effects of nitrite on polyphosphate accumulating organisms (PAOs) [13,20].

- ***DO limitation***

DO is the terminal electron acceptor in the oxidation-reduction respiratory chains for both AOB and NOB. Oxygen half saturation constant for AOB ($K_{O, AOB}$) falls in the range of 0.2–0.4 mg O_2 L^{-1}, being lower than that for NOB ($K_{O, NOB}$), i.e. 0.7–2.0 mg O_2 L^{-1}, which means that AOB have a higher affinity for oxygen than NOB [26]. This implies that NOB are often at a disadvantage when competing with AOB for DO [20,26,61,80]. However, recent studies reported that NOB affinity for oxygen significantly increased after long-term operation with low DO concentration, making NOB better competitors for DO than AOB [81,82].

Tan et al. [76] studied the effect of three COD/N ratios (1.8, 5.0 and 10.5) on the shortcut SND process in a SBR-MBBR equipped with PU carrier (dimensions: 20x20x20 mm, porosity: 50% and pore radius 1.5 mm) (**Table 2.1**). TN RE of 79% was achieved under a COD/N ratio of 10.5, while lower TN RE (55%) was observed under the lowest C/N ratio (1.8) [76]. The authors attributed the low denitrification efficiency under COD/N ratio of 1.8 to the lack of organic carbon in the synthetic influent, which is congruent with the observation of Feng et al. [72]. However, the nitrite accumulation ratio (NAR), evaluated as the ratio between effluent nitrite and the sum of effluent nitrite and nitrate (NO_x) was high (87–95 %) under each COD/N ratio. Hence, they concluded that the factor that affected shortcut SND was mainly related to the low DO concentrations during the process (< 1.0 mg L^{-1}). Low DO concentration affected the oxidation of ammonium when the COD/TN ratio increased from 5.0 to 10.5 due to DO consumption for the decomposition of the organic substrate [76] and probably caused sludge filamentous bulking problems [13]. Peng and Zhu [19] suggested a DO range of 1.0–1.5

mg L^{-1} to obtain a successful *nitritation*. The authors suggested also a real time control to regulate DO concentrations in reactors.

In recent years, different authors have reported that alternating anoxic and aerobic conditions may induce *nitritation* [83]. One of the NOB suppression mechanisms that has been attributed to IA is the establishment of a lag-phase in NOB activity after the transition from the anoxic to the aerobic period [13,83,84]. NOB are inhibited under periodic alternation due to the inactivation of NXR enzyme under anoxic conditions and the reactivation under the subsequent aerobic phase. However, under aerobic condition AOB recovered faster than NOB. Gilbert et al. (2014) indicated that 15 min was the minimum duration of anoxic phase able to generate a lag-phase in NO_2^- oxidation (up to 13 min). The length of this lag-phase was longer for NOB compared to AOB and was shown to depend on DO levels experienced by the biomass during cultivation and air flow rate during the aerobic period. Lag-phase in biomass cultivated at higher DO levels was distinctively longer than in biomass adapted to lower DO levels. Increasing air flow rate decreased the delay in NO_3^- production. In contrast, anoxic periods longer than 15–20 min and temperature did not affect the length of the lag-phase.

Yang and Yang [74] achieved SND process via nitrite in an intermittently aerated membrane MBBR without a strict control of SRT. The authors shifted from a condition with continuous aeration to a condition with alternating aerobic and non-aeration conditions. In the membrane MBBR, TN RE increased from 68% under continuous aeration condition to 88% with an aeration phase of 2 min and a mixing phase of 4 min under a constant COD/TN ratio of 5.0. Meanwhile, the NAR increased from 5% to 79%. The microbiological analysis revealed the presence of AOB, which accounted for about 54% and of NOB for almost 26%. The authors concluded that NOB could be inhibited under intermittent condition but not totally washed out from reactor.

Because SBR reactors are often operated under multiple aerobic/anoxic periods, they are well suited for SND via nitrite. Recently, Campo et al. [62] used AGS-SBR technology to threat real domestic wastewater with low COD/N ratio (2.8–3.8). The authors reached high effluent quality with COD, TP and TN REs of 84%, 96% and 71%, respectively, and estimated that about 56% of nitrogen was removed via-nitrite and 44% via nitrate. The SPND process permitted to save the aeration requirement for nitrification (14%) and almost 22% in COD for denitrification [62]. The strategies adopted were: (1) maintaining low DO concentration during aerobic phase (1.4–1.6 mg L^{-1}), (2) maintaining a low DO/NH_4^+ ratio and (3) maintaining a low SRT of biomass flocs (8–10 days) that determined a washout of NOB biomass.

- ***Salinity***

Saline wastewaters are widely common because of industrial or agricultural discharges. High salt content (> 3.5%) has negative effect on nutrient removal, although lower salinity values were reported to improve nitrogen removal [85]. NOB are more sensitive to salt than AOB, as a value of 9.0 g NaCl L^{-1} could inhibit NOB activity while enhancing AOB activity. Stable *nitritation* was achieved also at 6.5 g NaCl L^{-1} [15]. The nitrogen removal pathway could shifted from SND via nitrate to a SND via nitrite when salinity increased from 1.0% to 2.0% [85,86]. Huang et al. [15] studied the effect of the duration of the anaerobic (AN) and aerobic (O) phases on short-cut SND in a hybrid biofilm SBR (HSBBR) under low salinity (1.2%) and COD/TN ratio of 10. Higher TN RE average values over 92% was achieved at AN/O ratio of 1/5.5 h, 1.5/5 h and 2/4.5 h. Microbial community analysis on suspended biomass and biofilm revealed the presence of the NOB *Nitrospira* with a relative abundance of 0.1% only in the suspended sludge and when the duration of the AN/O cycle was 0/6.5h. Later, Xia et al. [85] reported that SND via nitrite became the main nitrogen removal pathway under salinity between 1.6% and 2.4%. The TN REs achieved were 78 (±3) %, 83 (±4) % and 74 (±4) % at the salinity of 0.8%, 1.6% and 2.4%, respectively. Under the highest salinity (2.4%), the authors registered also the highest accumulation of nitrite, revealing also an inhibition of denitrifying bacteria in this condition [85]. At the end of the study, *Nitrospira* genus was the only NOB bacteria detected, with low percentage abundance (0.1–0.2%). When salinity increased from 2.5% to 3.0%, the activity of ammonium oxidizers, nitrite oxidizers, nitrite reductase and dehydrogenase were inhibited [77]. On the other hand, salinity higher than 2% let to deterioration of phosphorus removal in AGS performing SND coupled with biological phosphorus removal. Nitrogen removal was not affected by salinity, while phosphorus removal was completely deteriorated due to the inhibitions of phosphorus uptake and release under aerobic and anaerobic conditions [86].

2.6 SND coupled to phosphorus removal

Phosphorus removal can be achieved by means of physical, chemical or biological methods [87]. Physical methods, including ion exchange and osmosis, are expensive and inefficient, removing only 10% of the total phosphorus [88]. Chemical phosphorus removal can be achieved by adsorption and precipitation. Precipitation involves the use of addition of calcium (Ca^{2+}), aluminum (Al^{3+}) or iron (Fe^{3+}) forming insoluble precipitates with PO_4^{3-} which can be removed in decantation basins. The main disadvantages of precipitation are the high cost of chemicals and variability of pH influent, which may influence the phosphorus RE [1,87]. On the other hand, adsorption

is rarely used in municipal WWTPs due to the high costs of the adsorbent and regeneration process [89]. Additionally, chemical techniques lead to high sludge production in addition to expensive purchase of chemicals [90]. P can be chemically precipitated as magnesium ammonium phosphate (MAP), also known as struvite, which can be used as a fertilizer. However, struvite precipitation commonly requires P concentrations in the liquid phase above 50 mg L^{-1} [91], while domestic wastewater is characterized by low concentrations of phosphorus (6–8 mg L^{-1}) [1]. A more suitable approach for P recovery from wastewater is to concentrate P in waste streams, mainly using biological processes and then apply other technologies for its recovery [1].

The EPBR process is up to date a cost effective and environmentally sustainable alternative to physicochemical methods for phosphorus removal. Several biological treatments have been developed, such as the five-stage Bardenpho process (anaerobic/anoxic/oxic/anoxic/oxic), the anaerobic/anoxic/oxic (A^2O) process and the University of Cape Town (UCT) process [92]. The most widely used process is the A^2O, a single-stage suspended growth system incorporating anaerobic, anoxic and oxic zones in sequence [3]. All biological strategies aim to generate a concentrated stream of P trough the metabolic activity of polyphosphate (poly-P) PAOs. PAOs are able to store more phosphorus than the amount needed for growth when exposed to alternating organic substrate and oxygen concentrations conditions. This net P uptake is known as luxury P-uptake. The conventional cycle for PAO development includes an anaerobic phase, during which low-weight organic molecules such as volatile fatty acids (VFAs) are generated and stored intracellularly by PAOs as poly-hydroxyalkanoates (PHA). The energy for this process is provided by the hydrolysis of internally stored poly-P granules, resulting in the release of orthophosphate in bulk liquid. Under the following anoxic or aerobic phase, PHA accumulated under anaerobic phase are oxidized by means of an available electron donor (DO or nitrate) and the released energy is used to uptake phosphate in higher amount than that released in the previous anaerobic phase [87,93]. Up to date, different putative PAOs have been identified in EPBR system. *Candidatus Accumulibacter* is the most commonly abundant PAO in EPBR system [94]. Many putative PAOs have been discovered until now, including members of the genera *Pseudomonas*, *Paracoccus*, *Comamonas*, *Acidovorax*, *Hydrogenophaga*, and *Aquaspirillum* [95]. Although the anaerobic phase is commonly foreseen to trigger PAO metabolism recent studies have highlighted that net phosphorus uptake can be established when the electron donor (substrate) and the electron acceptor (nitrate or oxygen) are present simultaneously under aerobic conditions [94]. Pijuan et al. [94] studied the behaviour of PAO enriched biomass under aerobic conditions and presence of acetate. As

reported by different works, two phases can be observed (feast and famine) [93]. In the first phase (feast phase), PAOs have a similar behaviour as under anaerobic conditions, namely, acetate is consumed and PHA produced while glycogen is degraded and $P\text{-}PO_4^{3-}$ is released. Depletion of organic substrate triggers the second phase (famine), during PAO consume PHA, glycogen is formed and phosphate is uptaken [93,94]. Recently, Yadav et al. [96] investigated the EPBR performance of a bacterial consortium (including *Acinetobacter*, *Pseudomonas* and *Bacillus*) in continuous stirred tank reactor (CSTR) under aerobic conditions (2–3 mg O_2 L^{-1}) and reached TP REs between 30% and 90% with influent TP concentrations of 1.4–40 mg L^{-1}. The authors supposed that TP removal was achieved by the synergistic activity between individual strains of phosphate solubilizing and accumulating microbes that easily consumed the solubilized phosphate, both added in the CSTR. Bioaugmentation with consortia bacteria with proven phosphate accumulating abilities accelerated the EPBR process, resulting in high TP removal without providing anaerobic/anoxic zones in the CSTR [96,97].

- ***Competition for carbon source.***

In EPBR system, particular attention should be placed on the competition between glycogen accumulating organisms (GAOs) and PAOs. GAOs, such as *Candidatus Competibacter*, have a similar metabolic behavior of PAOs. Under anaerobic conditions, GAOs store VFAs produced from the fermentation of organic substrate as PHAs, gaining the energy for storage from the oxidation of internally stored glycogen [87,98]. Different studies reported that under high feed COD/P ratios (> 50), GAOs grow more rapidly than PAOs, while lower C/P ratios favor the enrichment of PAOs [16,66]. He et al. [16] studied the effects of feed C/P ratios between 16 and 50 on AGS reactor performing SNDPR. TP RE increased from 86% to 96% with the decreasing C/P ratios, while a minimal impact was observed on nitrogen removal. Overdosage of carbon led to decline of phosphorus removal due to limited carbon source. Analysis of key functional groups involved in nitrogen and phosphorus removal revealed that the decrease of feed C/P ratio was favourable to the enrichment of GAOs, whereas the PAOs relative abundance decreased from 26% to 9.4% [16]. In another study, Wang et al. [66] studied the effects of C/N ratio on SNDPR using an AGS reactor. The authors reported that a decreasing feed C/N ratio (from 20 to 4) was surely favourable for the enrichment of GAO, in according to He et al. [16]. In the meantime, the increasing of influent nitrogen was favourable for the proliferation of denitrifying PAO (DNPAOs) (such as *Pseudomonas* and *Dechloromonas*), determining a stable TP removal during the study [66]. However, low C/N ratio increased the competition for carbon source between PAOs, GAOs and DNB with consequence on TN removal [99,100].

2.7 SND in biofilm reactors

SND has been investigated under various operational conditions and reactor configurations (**Tables 2.1**-**2.4**).Biofilm system ensure efficient removal of C, N and P due to layered structure and formation of anaerobic, anoxic and aerobic zones [12,62]. The major operational parameters influencing SND in biofilm reactors vary according to the reactor type. In this section, the configurations and key features of the most used biofilm reactors for SND are critically described with the scope to provide guidelines for successful and cost-effective operation.

2.7.1 Moving bed biofilm reactor

MBBR has been widely applied for nutrient removal from wastewater [59,66]. The presence of mobile carriers moving in the reactor enables the formation of a stratified biofilm with a bacterial community composition influenced by wastewater composition and operating conditions [101]. Substrates are transported from the bulk into biofilm trough diffusion mechanisms which allow the formation of anaerobic, anoxic and aerobic layers in the MBBR biofilm [102]. Compared to fixed-bed biofilm systems, the MBBR does not suffer clogging or channeling issues and no periodical backwashing is needed [71]. In recent years, the effect of various factors, i.e. carrier type, C/N ratio, DO concentration and filling ratio, on the SND process has been investigated in MBBR systems. **Table 2.1** lists the performance and operating conditions of continuous flow MBBRs applied for the SND process.

- ***Impact of carrier type.***

Carrier material, surface area and roughness have a key role in determining the performance of a MBBR since these characteristics affect both microbial adhesion and growth [6,39,48]. Additionally, the development, thickness and geometry of the biofilm on the carrier can significantly influence the diffusion of several parameters, e.g. DO, and modulate gradients with positive effects on nitrogen removal. The carrier used for MBBR operation can be classified in three major groups based on the nature the material used: inorganic materials (zeolite, ceramics or activated carbon), inert organic materials (PVA) and reactive materials (bamboo fiber, alginate) [39].

The choice of the appropriate support media for the SND process is nowadays the subject of several studies. Up to date, various biofilm carriers have been applied to support SND in MBBRs, including K-series AnoxKaldnes^{TM} made in PE, polyurethane (PU) sponge, high density polyethylene (HDPE) carriers, ceramic carrier or zeolite powders combined with PU sponge (Z-PU) (**Table 2.1**). Zinatizadeh and Ghaytooli [36]

compared the performance of two MBBRs equipped with two different types of carrier (i.e. ring-shaped form and Kaldnes-3) made of high-density PE and characterized by different form but equal specific surface (500 m^2/m^3). At DO concentrations of 2.5–3.0 mg L^{-1}, the maximum TN REs were 50% and 46% for the systems equipped with ring-shaped carriers and Kaldens-3, respectively. The lower nitrate concentration (below 12 mg L^{-1}) in the effluent of MBBR equipped with ring-shaped form indicates that the establishment of the anoxic layer was favoured by the geometric structure of the rings. Biofilm growing on Kaldnes-3 was likely exposed to higher DO concentrations due to smaller holes compared to that attached on ring-shaped carriers. However, scanning electron microscopy (SEM), used to study the morphology of the biofilms, showed a higher concentration of biomass in Kaldnes-3 compared to ring form carriers [36].

Of all carrier types, sponges feature the largest specific surface area (**Table 2.1**) and a high porosity (> 97%) useful for microbial growth, which determines also a limited diffusion of DO in the cubic biofilm being advantageous for the SND process [6,103]. The high specific surface area of sponges promotes biofilm development while porosity allows to reduce clogging [104]. Sandip and Kalyanraman [105] compared the SND performance of a MBBR filled with PU foam carriers (280m^2/m^3) to that observed in a MBBR containing conventional PE carrier media similar in shape to AnoxKaldnes K1 (500 m^2/m^3) (**Table 2.1**). A maximum TN RE of 59% was achieved in the MBBR filled with PU foam carriers, being 17% higher than the average TN RE observed in the MBBR filled with PE carriers. This difference was mainly due to the higher nitrifying activity observed with PU foam carriers, being 11% higher than the average $N\text{-}NH_4^+$ RE observed in the MBBR with PE carriers. The authors attributed this result to the higher biofilm-liquid contact area of PU foam compared to PE carriers, since increased nitrifying activity has been observed in the MBBRs. The effect of foam size was investigated by Lim et al. [106]. The authors investigated TN RE in four MBBR operated in parallel with foam cubes of 8-, 27-, 64- and 125-mL and resulting in TN REs of 37%, 31%, 24% and 19%, respectively (**Table 2.2**). Larger PU foam cubes were not fully covered by biomass which limited TN RE, while a robust biofilm developed on smaller cubes [106]. For comparison, an SBR was operated without carrier addition. TN RE was only 15% due to poor denitrification as a result of high DO and low COD concentrations in the bulk, while for MBBRs the occurrence of DO gradient inside the foam coupled to the storage of carbon in the deep biofilm layers allowed the denitrification during the SND process. Carbon storage and the occurrence of denitrification were confirmed by batch tests, revealing the occurrence of $N\text{-}NO_x^-$ reduction without the addition of carbon source.

Table 2.1 - SND performance and operating conditions of continuous flow MBBRs treating municipal wastewater.

Carrier type	Specific surface (m^2/m^3)	Materials	Filling ratio (%)	HRT (h)	DO (mg L^{-1})	Carbon source	Feed TP (mg L^{-1})	Feed TN (mg L^{-1})	Feed C/N ratio	COD RE (%)	TN RE (%)	TP RE (%)	Reference
Novel carrier	560 – 600	PE – PQAS 10 – Fe_2O_3	30	8	0.6 – 0.8	BOD_5 Glucose	n.a.	30 – 70	≤5[c]	79 – 86	62 – 76	n.a.	[45]
Conventional carrier	560 – 600	PE	30	8	0.6 – 0.8	BOD_5 Glucose	n.a.	30 – 70	≤5[c]	n.a.	45 – 72	n.a.	
Novel carrier	560 – 600	PE – PQAS 10 – Fe_2O_3	35	8	0.75	Glucose	6	40	5-9[c]	86 – 91	45 – 78	n.a.	[42]
Conventional carrier	560 – 600	PE	35	8	0.75	Glucose	6	40	5-9[c]	85	43 – 62	n.a.	
PE plastic	500	PE	20, 30, 40	5	3.0	Glucose	10	40 ± 10	5	81	34 – 42	n.a.	[105]
PU foam	280	PU	20, 30, 40	5	3.0	Glucose	10	40 ± 10	5	83	47 – 59	n.a.	
Zeolite powder based polyurethane sponges	0.846[b]	PU – zeolite (SiO_2)	10	12	5.0 – 6.5	n.a.	2.7 – 3.5	28 – 33	3.5	>94[a]	84	n.a.	[6]
Sponges biocarriers	0.846[b]	PU	10	12	5.0 – 6.5	n.a.	2.7 – 3.5	28 – 33	3.5	>94[a]	75	n.a.	
Bio-carriers	1200	n.a.	30	10	n.a.	Glucose	5.7	51	6.3[c]	< 90	≤ 30	≤ 30	[59]
Cubic-shaped sponges	n.a.	PU	10, 20, 30	12	5.0-6.5	Glucose	2.7 – 3.5	16	7.1	94[a]	85 – 95	n.a.	[107]
Cubic-shaped sponges	0.846[b]	PU	10, 20, 30	12	5.0 – 6.5	Glucose	2.7 – 3.5	13 – 18	6.5-10	94-96[a]	77 – 87	n.a.	[103]
Kaldnes-3	500	PE	50	4 – 12	2.0 – 4.0	BOD_5	2 – 4	n.a.	5[c]	50-88	26 – 46	0-38	[36]
Ring R2	500	PE	50	4 – 12	2.0 – 4.0	BOD_5	2 – 4	n.a.	5[c]	54-85	26 – 50	0-38	
PUF carrier	1120	PU	20, 30,40	5 – 7	4.0 – 6.0	Glucose	5	25(±3)	~11[c]	81	25 – 54	11 – 24	[108]
PU carrier	900	PU	20	14	160 – 180 L h^{-1}	Glucose	3.2	44(±5)	3.7[c], 8.1[c]	90[a]	20 – 55	n.a.	[70]
Biodegradable polymer	0.346[b]	PCL	16.7	14	160 – 180 L h^{-1}	Glucose	3.2	44(±5)	3.7[c], 8.1[c]	72[a]	59	n.a.	
Biodegradable polymer	0.37[b]	PCL	11.3	18.5	2.8 – 3.7	Glucose	5.0	58(±13.1)	0.7[c]	>86[a]	74.6	n.a.	[71]
Polyethylene carriers	500	PE	30	10	2.0 – 4.0	n.a.	COD:N:P 100:5:1	100	4.5-13.4	94-96	26-51	n.a.	[73]

n.a. = not available.
[a] measured as total organic carbon (TOC).
[b] reported as m^2g^{-1}
[c] available as COD/N

Song et al. [6] combined zeolite powders with PU sponge as biofilm carrier. Zeolite is a non-metallic material and a porous mineral with a high ion-exchange affinity for N-NH_4^+ [40] due to its negatively charged surface [39]. In previous works, zeolite was used for the enhancement of RE in ammonium rich wastewater [109]. Song et al. [6] compared the SND performances of two continuous-flow MBBRs filled with different carrier elements (PU and zeolite-PU sponge) with DO concentrations between 5.0 and 6.5 mg L^{-1}. The zeolite powder entered in the pores of PU sponges by physical rotation, improving the specific surface area useful for biofilm attachment. The authors reported a biofilm attachment ratio for Z-PU of 0.47(±0.13) g/g carrier, being 1.3 times higher than that of conventional sponge carriers. The pore size was reduced by zeolite powders resulting in a block of oxygen diffusion. Due to decrease of DO concentrations in the inner zones of the biofilm, the DNB growth could gradually increase improving TN RE [6,103,108]. An average TN RE of 84 (±5) %was achieved in the MBBR with Z-PU sponges, being almost 10% higher than that observed in the MBBR with PU sponge. The efficiency of nitrification was basically the same, hence the difference in terms of TN RE was mainly related to denitrification activity.

Carriers made by recycling waste material have attracted the interest of the researchers in recent years, being a cost-effective and environmental friendly solution for MBBR operation. Massoompour et al. [48] proposed a new carrier composed of waste activated carbon (AC) and PE carriers mixed trough a chemical and thermal process. The authors compared the performance of two parallel reactors filled with two different carriers, i.e. conventional PE carriers and modified PE with AC carriers (**Table 2.2**). The analysis revealed a specific surface area of the modified carriers 10.9 times higher than that of conventional carriers and an increase of attached biomass up to 20% on the modified carriers. The speed of microbial adhesion and growth in the bioreactor with modified PE carriers was 26% higher than that observed with conventional carriers enhanced by the hydrophobic nature of AC [48]. The hydrophobicity, the charged surface as well as the high porosity provide a favorable condition for microbial adhesion. TN RE was improved by almost 17% for MBBR equipped with modified carriers due to the development of a larger anoxic area in the modified carriers, being nitrification efficiencies similar in both MBBRs. Again, improvement of denitrification was the main mechanisms for achieving higher TN REs by using novel carriers, which allowed to modulate DO gradient and establish larger anoxic conditions within the biofilm.

Table 2.2 - SND in SBR–MBBR systems.

Carrier type	Specific surface (m^2/m^3)	Materials	Filling ratio (%)	Cycle Length (min)	Cycle phase	AN phase (min)	O phase (min)	A phase (min)	Settling(min)	Idle (min)	Discharge (min)	Range DO (mg L^{-1})	Carbon source	Feed TP (mg L^{-1})	Feed TN (mg L^{-1})	Feed C/N ratio	COD RE (%)	TN RE (%)	TP RE (%)	Reference
PU foam	n.a.	PU	30	–	–	–	600	–	–	120	–	1.5 – 5.5	$C_6H_{10}O_5$	n.a.	25	~12[c]	92	42 – 85	n.a.	[51]
AC CBMC	2.70[b]	AC, PE	40, 55	360	–	–	350	–	–	–	5	6.0	Acetate	18	55	5[c]	82 – 94	68 – 88	n.a.	[48]
Conventional carrier	0.2478[b]	PE	40, 55	360	–	–	350	–	–	–	5	6.0	Acetate	18	55	5[c]	82 – 94	59 – 76	n.a.	
Combined fibers	n.a.	PP	n.a.	–	–	175	90	175	30	–	5	2.0	Glucose	n.a.	100	3.8[c]	94	73	n.a.	[61]
Novel carrier	650	PE –PQAS 10– Fe_2O_3	30	240	A/O	–	200	40	–	–	–	1.0–1.5	n.a.	n.a.	50	5[C]	81 – 84	78 – 80	n.a.	[110]
Conventional	650	PE																		
PUF foam	n.a.	PU	30.	600, 480	AN/ O	–	–	–	–	–	–	0.5 – 1.5	Acetate	23	89	~4.5[c]	85	60	n.a.	[111]
HX9KL, BIOMASTER BCN 012KLS	500	PE	40, 60	240, 360	–	–	90, 50	150, 90	0, 10	–	0, 3	0.8 – 1.1	n.a.	2.9 4.0	35(±7) 47(±6)	5.5[c] – 6[c]	78 – 95	50 – 76	n.a.	[43]
Biodegradable rice	n.a.	Rice husk		720	–	–	240, 60	480, 60*	–	–	30	0.1 – 2.0	Acetate, yeast, sucrose	n.a.	35(±4)	7.6[c], 5.6[c] 1.8[c]	64 – 83	41 – 89	n.a.	[72]
Carrier Filler	382	PU	15.8	720	–	–	240, 60	480, 60*	–	–	30			n.a.	35(±3.9)					
Foam carrier	n.a.	PU	30.	720	–	–	600	–	–	120	–	1.5, 2.5, 3.5, 4.5, 5.5	$C_6H_{10}O_5$	5.7	22 – 31	~10.2[c]	> 90	42 – 84	n.a.	[7]
Plastic fiber	n.a.	n.a.	12	720	AN/ O/A	50	190 – 270	380– 460	–	–	–	1.5 – 2.2	Glucose	10	50	1 – 4[c]	50–90	83 – 98	6 – 27	[112]
Cylindrical carrier	n.a.	PP	30	–	–	90	210	90	30	40	–	0.2 – 2.5	n.a.	13	35	11.4[c]	95	94	97	[99]
PU foam	1621	PU	n.a.	360	–	–	297	–	50	–	–	0.1 – 0.9	Glucose	4.6	227 – 65	1.8[c], 5.0[c], 10.5[c]	n.a.	55, 74, 79	n.a.	[76]
PU foam	n.a.	PU	8	–	–	60	60	–	90	570	–	0 – 7	Peptone, sucrose, acetate	40	48	5[c]	65	57 – 100	n.a.	[113]
PU foam	412 – 455	PU	8	–	–	–	600	120	90	570	–	0 – 7	Peptone, sucrose, acetate	40	48	4.1[c]	70	19 – 37	n.a.	[106]
Bio–carrier K3	500	PE	30	480	–	60	240	120	30	–	–	n.a.	Acetate	12	35	15.7[c]	n.a.	71.5	92	[114]

AN = Anaerobic phase.
O = Aerobic phase
A = Anoxic phase.
n.a. = not available.
[a] measured as total organic carbon (TOC).
[b] reported as m^2g^{-1}
[c] available as COD/N

One of the drawback of inert organic material, such as polypropylene (PP) and PE, is the low bio-affinity and hydrophilicity, which may cause biofilm detachment [39]. Pure PP, PE and HDPE carriers are characterized by negative charge surface similar to the surface charge of biofilm, which can hamper the biofilm formation on carriers due to repulsions between microbes and carriers. Hence, novel carriers with an enhanced bio-affinity due to a hydrophilically or electrophilically modified surface have been proposed [42,45,110,115]. T. Liu et al. [42,45] proposed a surface-modified carrier made of PE with polyquaternium-10 (PQAS-10), Fe_2O_3 and 2 wt% clinoptilolite, characterized by a strong ammonium adsorption capacity, which benefited the enrichment of nitrifying bacteria. The water contact angle was reduced from 92.0 (±3.4) ° to 60.2 (±2.3) ° compared with traditional carriers made in PE thanks to the addition of PQAS-10 (positively charged materials). In this way the problem of the repulsions between microbes and carrier surface in PE, PP and HDPE is reduced. Surface-modified carriers help to accelerate biofilm formation during start-up and determined higher REs compared to traditional PE carriers [42,115] (**Table 2.1**). The authors reported a material cost of the surface-modified carrier similar to that of conventional carriers, although the step of dispersing the materials (i.e. clinoptilolite) into PE powder by mechanical stirring require a non-negligible consume of energy [116].

- ***Filling ratio***

MBBRs are usually operated with filling ratios between 20% and 70% [117]. Values below 70% are recommended in order to assure an adequate mixing, while ratios above 20% guarantee sufficient concentration of attached-growth biomass [22]. The choice of the filling ratio affects both the bioreactor performance and operational costs, i.e. energy consumption and the purchase of carriers. Quan et al. [108] evaluated the effect of three PUF carrier filling ratios (20%, 30% and 40%) on SND in three parallel MBBRs with an aeration zone and a settling zone. TN RE in the reactor filled with 40% of PUF carriers was 2 times higher than in the reactor with 20% filling ratio (**Table 2.1**). The filling ratio also affected both biofilm structure and nitrification activity. The structures of the biofilms attached to PUF carriers in the three MBBRs were different. Biofilm in the MBBR 20% filling ratio was thick and dense, while in the other two MBBRs the carriers looked hollow with a thin biofilm. Microprofiles analysis revealed that dense biofilm can block DO from being transported into inner layer as well as nitrifier growth, which can explain the poorer performance of the MBBR with 20% filling ratio. The microbial community analysis showed that the relative abundance of nitrifying bacteria such as *Nitrosomonas* and *Nitrospira*, in MBBRs with filling ratios of 30% and 40% packing rate reactor were higher than those of MBBR with 20% filling ratio, which limited the

nitrification performance. Similarly, Ferrentino et al. [43] investigated the performance of a SBR-MBBR, characterized initially by a filling ratio of 40% and then increased to 60%, in terms of COD and TN REs. The increase of filling ratio from 40% to 60% determined an increase of nitrification activity with a decrease of $N\text{-}NH_4^+$ concentration from 20 (±4) mg L^{-1} to 10 (±2) mg L^{-1} and, consequently, an increase of TN RE from an average value of 50% to 66%.

Several studies have observed an influence of the filling ratio on bacterial abundance. Lim et al. [113] used 8-mL PUF foam to pack three batch reactors with 20%, 30% and 40% filling ratio and the TN REs achieved were 86%, 100% and 96%, respectively. The authors reported a negative trend of the pseudo-zero-order rate constant parallelly to the decrease of suspended growth biomass. The authors supposed that suspended growth biomass had a huge influence on $N\text{-}NH_4^+$ RE.

Zhang et al. [107] conducted a study on SND process in MBBRs filled with PUF foam with filling ratios of 10%, 20% and 30%, in which average TN REs of 77%, 86% and 87% were observed, respectively (**Table 2.1**). The highest ammonium oxidation and denitrification rates were achieved in the reactor filled by 30% with carriers, being 2.2 mg $N\text{-}NH_4^+$ g biomass^{-1} h and 5.1 mg $N\text{-}NO_3^-$ g biomass^{-1} h (**Table 2.1**). Based on the TN REs, there was no difference between the two MBBRs filled at 20% and 30% of PUF foam. The concentration of attached biomass was similar for MBBR filled at 10% and 20%, higher than that of the MBBR filled at 30%, while the total biomass in the reactors increased with the increase of filling ratios. Recently, Massoompour et al. [48] investigated the SND process by employing new carrier based on AC, as described in the previous section. The authors investigated TN REs by decreasing filling ratio at stable aeration conditions. The decrease of filling ratio from 55% to 45% led to a decrease of COD and TN REs from 93% to 89% and from 80% to 68%, respectively. The decrease of performance removals was coupled to the decrease in concentration of attached-growth biomass from 2881 to 2480 mg L^{-1}.

- ***Hydraulic retention time***

Changes of HRT can lead to short- and long-term effects on SND performance. Zinatizadeh and Ghaytooli [36] operated a continuous-flow MBBR removing C and N from municipal wastewater through SND process. They increased the HRT and DO from 4 to 8 h and from 2 to 3 mg L^{-1}, respectively. Subsequently, growth and activity of AOB and NOB increased which determined an higher biofilm thickness resulting in more favorable anoxic conditions for DNB and higher TN REs. Quan et al. [108] observed the increase of HRT from 5 h to 7 h led to improvement of TN REs from 25% to 54%, from 53% to 49% and from 34% to 52% in three MBBRs filled with 20%, 30% and 40% of

PUF carriers. The change of HRT in the three reactors did not affect the COD RE, which remained stable at 81%, but affected the N-NH_4^+ RE, which increased after prolonged time operation from 40–60% to 95% in the reactor filled with 20% of PUF carriers. In the reactor filled with 30% of PUF carriers, the N-NH_4^+ RE increased from 60% to 95%, while in the MBBR filled with 40% of PUF carriers N-NH_4^+ RE remained stable at 96% under both HRT values.

However, literature lacks information of the effect of HRT on the evolution of the microbial community in the MBBR, which should be investigated.

2.7.2 Hybrid biofilm systems

- ***Sequencing batch MBBR (SBR-MBBR)***

The SBR system is characterized by a compact structure and flexible operation. However, an obvious drawback is that efficient nitrogen and phosphorus removal is difficult to achieve due to the presence of nitrifying and denitrifying bacteria and PAOs completely mixed in the SBR that compete with each other. In contrast, a biofilm system provides different micro zones where different bacteria can find the ideal conditions to grow [99,118]. In light of this, a hybrid system combining SBR and a biofilm system, such as the MBBR, has generated much interest in recent years. Combining SBR with biofilm systems allows to maximize the SRT (sludge retention time) of the bioreactor and allow the simultaneous growth of AOB, NOB, DNB, PAO and DNPAO, being characterized by different growth rates [99,114].

Table 2.2 lists the performance and operating conditions of combined SBR and MBBR systems (SBR-MBBRs) applied for the SND process. The conventional SBR system is characterized by a sequence of operational steps organized as follow: feeding step, reaction step, settling step, drainage step and often an idle step. The cycle format can be optimized and configured to combine nitrification and denitrification in one reactor [106]. In the SBR-MBBR studied until now, the reaction step could be composed by an aeration step only [48,106], by intermitted aeration [113] or by anaerobic/aerobic (A^2) processes and aerobic-aerobic-anoxic (A^2O) processes as carried out by Yin et al. [99] and Lo et al. [114] (**Table 2.2**).

Yin et al. [99] started up an SBR-MBBR system with two phases, an A^2 and an A^2O, in order to enrich the biofilm and suspended activated sludge with PAOs and DNPAOs. The operational cycles were adjusted in order to obtain high performance on treatment of urban wastewater. The experimental activity was carried out by individually optimizing the anaerobic, aerobic and anoxic phases. Extended anaerobic phase (higher than 90 min)

would consume more organic matter as well as inhibit the growth of aerobic microorganisms. The duration of the aerobic phase time was chosen in order to meet the requirement for nitrification and phosphorus removal. The authors chose a duration of 210 min since the COD was almost exhausted and could limit phosphate uptake under aerobic conditions. On the other hand, the duration of the anoxic phase time was chosen in order to have a reduction of NO_x^- and a further phosphate uptake. The authors reached TN, TP and COD REs of 94%, 97% and 95%, respectively (**Table 2.2**) and showed how DNPAOs played a key role for phosphate uptake and denitrification activity under anoxic and aerobic conditions. Most of the carbon fed to the reactor was indeed converted to PHB and then used for denitrification and phosphate uptake under anoxic and aerobic conditions [99].

- ***Hybrid MBR***

MBR combined with biofilm reactor (hybrid MBR) can improve the system performance and in some case reduce the effect of suspended solids on membrane fouling [63,64,118]. One of the main problems of the MBR system is biofouling, that reduces membrane permeability and increases transmembrane pressure (TMP) as well as the operational costs due to frequent chemical cleaning or replacement [39,64,119]. The overgrowth of filamentous bacteria can enhance the production of a high quantity of extracellular polymeric substances (EPS), which worsened membrane fouling [120]. EPS are sticky materials secreted by bacteria and are mainly composed by polysaccharides (PS), protein (PN), nucleic acids, humic-like substances and lipids [121]. EPS can adsorb and also store temporally ammonia, nitrite and nitrate in wastewater, affecting in this way nitrogen removal [55]. **Table 2.3** lists the performance and operating conditions of hybrid MBRs applied for the SND process.

Yang et al. [122] proposed a MBR filled with carriers (30% v/v) to study and compare the SND efficiencies to conventional MBR. Hybrid MBRs operated in continuous mode revealed a higher membrane fouling compared to conventional MBR due to the formation of a tick cake layer without pores [122]. Both reactors showed good COD REs higher than 95%, while TN REs efficiencies reached values up to 89% and 43% for hybrid MBR and conventional MBR, respectively. However, the hybrid MBR showed an improvement of AOB, NOB and HAB activities, and a stable response to variations of COD/TN ratio during experimental activities (**Table 2.3**).

Table 2.3 - Hybrid biofilm-MBR for SND of municipal wastewater.

Carrier type	Specific surface (m^2/m^3)	Materials	Filling ratio (%)	Type	Material	Pore size (μm)	Surface Area (m^2)	HRT (h)	DO (mg L^{-1})	Carbon source	Feed TN (mg L^{-1})	Feed C/N ratio	COD RE (%)	TN RE (%)	TP RE (%)	Reference
Biocarrier made	28000─32000	polyvinyl formal, AC	2─8	n.a.	Polyvinyl idene difluoride	0.1	0.1	8	2.0	n.a.	34.4	20─6.7	98	72─94	n.a.	[64]
Sponge, PBS granules	8000─10000	polyester–urethane	30	Hollow fiber	n.a.	0.2	0.085	24	0.5─0.8	Acetate	60	1.7[c]	> 90	94	n.a.	[63]
Nonwonens carriers	900	n.a.	30	Hallow fiber	PP	0.1	0.4	12	n.a.	Sucrose	20	22.1─8.9[c]	96	65─76	n.a.	[122]
Nonwonens carriers	900	n.a.	30	Hallow fiber	PP	0.1	0.4	─	n.a.	Acetate	33─77	12.9─5[c]	94	83	97	[118]
Nonwonens carriers	900	n.a.	30	Hallow fiber	PP	0.1	0.4	12	n.a.	Acetate	42.5─58	3.7─5.6[c]	93	88	n.a.	[74]

n.a. = not available.
[a] measured as total organic carbon (TOC).
[b] reported as m^2g^{-1}
[c] available as COD/N

It has been demonstrated that the SBR operation mode of hybrid MBRs compared to continuous mode can alleviate membrane fouling since filamentous bacteria are restrained in the reactor [63,64,118]. K. M. Wang et al. [64] showed that adding static biocarriers improved nitrification and denitrification while reducing the relative abundance of *Sphingobacterials_unclassified*, *Ohtaekwangia* and *Rhodocyclaceae_unclassified*, responsible of EPS secretion and consequent membrane fouling problem. Meanwhile, the authors observed also an improvement by almost 8% for TN removal in the hybrid MBR compared to the conventional MBR due to better denitrification, which was attributed to the formation of anoxic and aerobic microenvironments in the biocarriers. In the same way, Han et al. [63] reported a slower increase of TMP in a hybrid MBR seeded with biocarrier (sponge coupled with PBS granules) compared to a conventional MBR, corresponding to an operation time of hybrid MBR 1.5 times longer than that of conventional MBR. The authors did not exclude that the reduction of cake layer may be also attributed to physical clearance mechanism of biocarriers, e.g. the frictional force carried out by biocarriers on submerged membrane, back-transport effect from membrane surface to bulk solution due to turbulence of suspended carriers or impact of biocarriers on membrane with consequent shaking of this [63].

Although interesting performances have been highlighted, the operation of MBR-MBBR would be rather expensive due to high cost of membranes and carriers and, therefore, a cost-effectiveness analysis would be needed [123].

2.7.3 Aerobic granular sludge

Aerobic granular sludge (AGS) is a technology developed in the 90's and has been widely applied for the treatment of wastewater with low and medium C/N ratios but also for industrial wastewaters [124]. AGS combines the characteristics of activated sludge and biofilm systems due to presence of suspended microbial aggregates without any supporting carrier and a structure similar to biofilm, with the formations of aerobic, anoxic and anaerobic zones [65]. Aerobic granules are described as biomass microspheres that grow under aerobic conditions without a carrier material and are generated during wastewater treatment. These granules appear denser and heavier than regular CAS flocks [125]. EPS play an essential role in the composition and structure of AGS, contributing to cell adhesion and microbial matrix [66]. As reported previously, EPS are mainly composed by PS and PN, nucleic acids, humic-like substances and lipids [121]. The PS/PN ratio is an important parameter for evaluating the stability of AGS as values below 0.6 have been reported to be not suitable for stable granulation [121].

The biological processes that are involved in AGS are the same as activated sludge and are carried out by the same types of bacteria. The difference is that processes occur in distinct zones of the granules and often occur simultaneously [54]. Up to date, AGS have been recognized as a promising and emerging technology for wastewater treatment as alternative to CAS thanks to several advantages, such as excellent settleability, small footprint, high biomass retention and the ability to remove simultaneously carbon, nitrogen and phosphorus [12,58,126]. **Table 2.4** lists the operational parameters and SND performance of AGS reactors. The most common option for enrichment of aerobic granules for SND and for maximizing carbon, nitrogen and phosphorus removal is to apply AGS in a SBR (**Table 2.4**) [54,127]. Many studies about AGS-SBR were established successfully in lab-scale with a height/diameter ratio (H/D) between 5 and 10 (**Table 2.4**).

Despite the excellent TN REs trough SND process, in long term operation the stability of aerobic granules represents the serious problem being determined by granules desegregation into filamentous fraction [66,121]. The long term stability is affected by: (1) feed C/N ratio; (2) aeration intensity and (3) organic loading rate [57]. A possible solution to ensure a long stability is to enrich the bacterial community with slow growing microorganisms (metabolic selection), such as PAOs and GAOs, characterized by higher granulation properties [62]. In addition, HAB proliferation is suppressed due to lack of carbon source under aerobic conditions, stored by GAOs and PAOs under previous anaerobic conditions [127]. Hence, SBR cycles generally include an anaerobic period followed by an aerobic period. Recently anaerobic/aerobic/anoxic cycles have been used, aiming to improve the SNDPR performances (**Table 2.4**). Lab-scale studies on SND with AGS have been mainly conducted using VFAs as organic carbon source. If the growth of PAOs and GAOs is crucial for the formation of stabile granules, the granulation may be hampered during the treatment of real municipal wastewater containing low VFAs concentrations [49,128]. Sarma and Tay [125] reported VFA concentrations in real municipal wastewater between 22–92 mg COD L^{-1}, while non-diffusible organic carbon represents almost 50% of the total COD influent.

Table 2.4 - SND in AGS reactors

Cycle length (h)	Cycle	AN (min)	O (min)	A (min)	Settling (min)	Discharge (min)	Granule diameter (mm)	H/D	DO (mg L^{-1}) (O)	Carbon source	Feed TP (mg L^{-1})	Feed TN (mg L^{-1})	Feed C/N ratio	COD RE (%)	TN RE (%)	TP RE (%)	Reference
3 – 6	AN–O	20 – 60	30 – 250	–	13.3 – 25	3.3 – 6.7	1.5	18.75	1.0 – 2.5	BOD_5	7.2 – 1.8	31 34	~ 5[c]	69 – 84	31 – 71	59 – 96	[62]
6	AN–O–A	120	90	144	2	–	–	–	n.a.	Acetate, Succinate (1:1, 1:3, 3:1)	3	20	~ 10[c]	90	~80	~90	[12]
5.6 h	AN – O	90	240	–	5	1	> 0.3	8.4	2	Acetate – propionate – BOD_5	3.2 – 5.4	30 – 43	11 – 26[c]	83 – 93	45 – 77	64 – 96	[128]
4	AN – A – O, AN/O, O	0 – 45 – 55	104 – 220	0 – 30	10	–	0.2	10	8 – 10	Acetate, propionate	20 – 25	100	6.5 – 1.6	98 – 91	75 – 19	59 – 16	[129]
6	AN–O	54	270 – 285	–	20 – 5	1	1.5 – 0.7	10	n.a.	Acetate, Glucose, Ethanol	10	110	~ 6[c]	87 – 96	34 – 78	18 – 53	[130]
5.2	AN–O–A	120	90 – 120 – 150	144 – 114 –84	2	–	–	–	7.75 –2 – 1.25	Acetate	4	50	4.0[c]	n.a.	63 – 85	n.a.	[57]
6	AN–O–A	120	90	144	2	–	–	5.2	7–8	Acetate	3	2 – 55	20[c] – 10[c] – 4[c]	95 – 94	95 – 75	98	[66]
3.6 h	O	–	150	–	20	40	0.09 – 0.4	n.a.	2	BOD_5	20	91	~ 14.7[c]	92	87	95	[131]
6	AN–O–A	120	90	144	2	–	–	5	5	Acetate	4 – 8 – 12.5	20	~ 10[c]	89.2	88.5	96 – 86	[16]
6	AN–O–A	120	90	144	2	–	–	5	0.8 – 1.2	Acetate, glucose	3	20	~ 10[c]	91– 81	94 – 81	95 – 70	[100]
6	AN–O–A	120	90	144	2	–	1.4 ± 0.6 1.8 ± 0.9	5	3.5 – 4.5/ 0.8 – 1.2	Acetate	3	20	~ 10[c]	95	64 – 94	97	[56]
6	AN–O–A	120	90	144	2	–	–	5	5	Acetate	3.3	19	10.7[c]	94	94	98	[132]
8	AN–O–A	180	180–140	90–148	20–2	–	1.0 – 0.6	6.3	5	Acetate	8 – 14	40 – 50	~ 7[c]	80 – 90	88 – 97	74 – 87	[133]
8	AN–O–A	180	180 – 150	90–138	20–2	–	1.2	5.2	5	Acetate	6	15	~ 10[c]	87	97	79	[134]
6	AN – O	130	160	–	60	–	1.6 – 0.3	4.25	0.8 – 1.6	Acetate	36	50	~ 16[c]	n.a.	65	93	[135]

AN = Anaerobic phase.
O = Aerobic phase
A = Anoxic phase.
n.a. = not available.
[a] measured as total organic carbon (TOC).
[b] reported as m^2g^{-1}
[c] available as COD/N

Table 2.4 - SND in AGS reactors (Continued)

Cycle length (h)	Cycle	AN (min)	O (min)	A (min)	Settling (min)	Discharge (min)	Granule diameter (mm)	H/D	DO (mg L^{-1}) (O)	Carbon source	Feed TP (mg L^{-1})	Feed TN (mg L^{-1})	Feed C/N ratio	COD RE (%)	TN RE (%)	TP RE (%)	Reference
4	O	–	180	–	5	2	0.5 – 1.7	8	> 4.0	Acetate	n.a.	250 – 330	~1[c]	100	33 – 77	n.a.	[136]
4	AN – O	10– 20	184 – 219	–	35 – 10	–	0.5	9.7	n.a.	BOD_5	n.a.	83	~7[c]	92	61	n.a.	[137]
6.5 – 3	AN – O – A	–	300 – 60	n.a.	30	–	>0.2	n.a.	1.8 – 2.5	BOD_5	6.7	50	~ 10[c]	87	86	87	[138]
3	O	–	162 – 167	–	2 – 7	6	> 1.5	11.1	7 – 8	Acetate	n.a.	154 – 77.2	8 – 16	> 90	> 90	n.a.	[139]
3 – 4	O	–	164 – 224	–	15	0.5	0.3 – 0.7	22.2	243 – 275 L h^{-1}	BOD_5	n.a.	76 – 91	4.7 – 11.2[c]	78 – 92	66 – 97	n.a.	[69]
3	AN – O	60	112	–	3	5	0.9 – 1.1	n.a.	50 – 40 – 30%	Propionate	20	50	8 – 1.2[c]	100	40 – 95	88 – 98	[140]
6	AN – O – A	45 – 100	35 – 160	3 – 40	2 – 40	–	0.2	n.a.	2	BOD_5 + Acetate	9	67	~5[c]	100	75 – 84	93 – 99	[141]
5.4	O	–	114	–	3	3	2.4	7.2	6 – 8	Sucrose, acetate, propionate	10	40	~ 10[c]	>80	>75	45 – 70	[142]
4	A – O	–	213	10	2	5	1.5 – 0.7	20	2	n.a.	5	60	~ 10[c]	85 – 80	68 – 96	n.a.	[143]
4	O	–	167 – 130	–	8 – 45	5	0.8	5	8	BOD_5	n.a.	60	~ 16.7[c]	80	50	n.a.	[144]
2.5 – 4	A – O	90	240	5	–	–	–	3.2	2 – 3	Acetate – BOD_5	3.8, 1–7	35, 43 – 147	0.4 – 2.3	64 – 89	47	60 – 96	[65]
n.a.	AN – O – A	30	90	30	–	–.	> 1.0	n.a.	0.2 – 0.4 L min^{-1}	Acetate	10	60	2.5	~ 100	~ 100	~ 100	[145]
6	AN – O	90	120	–	0.5	–	1.0	n.a.	2 – 5	Acetate	10	60	~ 10[c]	~ 100	~ 100	~ 100	[146]
3	O	–	169	–	3	5	1.0	n.a.	100 – 50 – 40 – 20 – 10%	Acetate	n.a.	n.a.	8.3[c]	n.a.	8 – 45	n.a.	[147]
4 – 6	O, AN – O, AN – A	0 – 120	230	0 – 120	2	4	0.4 – 1.9	13.3	2.0 – 0.5	Ethanol	n.a.	25 – 150	3 – 5[c]	92	20 – 40	n.a.	[148]

* Non–aeration phase
AN = Anaerobic phase.
O = Aerobic phase
A = Anoxic phase.
n.a. = not available.
[a] measured as total organic carbon (TOC).
[b] reported as m^2g^{-1}
[c] available as COD/N

- ***Granules diameter and organic carbon***

The diameter of granules sludge is a factor influencing the nitrogen removal in SND process [149]. Generally, after few months the size of granules is 0.5 mm while dimensions of 2.0 mm are generally achieved after few years [128,137]. The size of the granules together with the DO penetration depth determines the extension of the anoxic zone. Limited anoxic zones in smaller granules affect the SND performance compared to larger granules [49]. We et al. (2020) reported that granule diameters of 0.9 mm could significantly improve TN RE, while smaller size granules (0.25–0.63 mm) did not favor SND [144,150]. In order to achieve an appropriate development of anoxic and aerobic zone, the optimal average diameter of aerobic granules should be around 2.0 mm [62,151]. Successful granulation can be linked to: (1) the diffusibility of organic substrate and its availability; (2) the microbial community composition.

Rollemberg et al. [130] studied the effects of three different carbon source (acetate, ethanol and glucose) on SND process performance. The acetate favored the formation of large granules with average diameter of 1.5 mm, while average diameters of AGS fed with ethanol and glucose were 1.2 mm and 0.7 mm, respectively. The AGS fed with acetate achieved a TN RE (i.e. 72%), higher of 20% and 30% compared to that achieved by the AGS fed with ethanol and glucose, respectively. High effluent concentrations of $N\text{-}NO_x$ (> 10 mg L^{-1}) may suggest that partial denitrification occur in AGS fed with ethanol and glucose. On the other hand, granules growing on acetate can reached diameter higher than 3 mm and break after long term operation.

Derlon et al. [150] pointed out that typical granule size developed with real municipal wastewater varied between 0.2 and 1.3 mm (**Table 4**). These values are smaller than that observed in granules cultivated with synthetic wastewater, usually reported to be higher than 2.0 mm. The authors evaluated the formation of aerobic granules for the treatment of low strength real wastewater through SND process. The authors did not observe the occurrence of SND due to small size of granules ($0.25 < d < 0.63$ mm). The limited denitrification can be explained by the limited anoxic zone in aerobic granules or by limited availability of organic substrate in anoxic zone [65,137,144]. F. Chen et al. [143] reported an increase of TN RE from 68% to 72% with the increase of the granules size from 0.7 to 1.5 mm.

Layer et al. [128] used 4 different influent compositions characterized by increasing non-diffusible organic carbon to study how diffusible and non-diffusible substrate influence the SND process and the granulation process under anaerobic/aerobic conditions. Higher is the diffusibility of organic substrate (i.e. VFAs) and higher is the growth promoted in the deep layers leading to the formation of dense and large granules

(d = 1–3 mm). The reactors fed with real municipal wastewater were characterized by slower start-up, lower granule fractions, small granules diameter (0.25–0.63mm) and the presence of 20–40% of flocs in the reactors. The non-diffusible of organic substrate hampered the granulation process. Under anaerobic conditions only a part of non-diffusible substrate is converted through hydrolysis being a very slow process. Under aerobic conditions the organic carbon available is present in different forms: stored by PAOs/GAOs, soluble form but not fermented or in particulate form not hydrolyzed under aerobic form. Organic carbon in particulate form cannot diffuse in granule, so the high availability of organic substrate in the aerobic phase support the growth of HAB. The growth of HAB lead to filamentous and floc formations determining poorer settling properties of granules and overall lower nutrients removal. During start-up period (400 days), the reactor fed with 100% of VFA showed a TN RE of 77% via SND, while the other effluents were characterized by large accumulation of $N\text{-}NO_3^-$ (> 10 mg L^{-1}) corresponding to TN REs between 45% and 60%. Since full nitrification was observed in each reactor, the authors concluded that the higher effluent concentrations of $N\text{-}NO_3^-$ results from a lower denitrification activity inside anoxic zone. To improve TN REs other approaches must be considered, such as pre o post-denitrification or optimizing the aeration strategy. An intermittent aeration during subsequent anaerobic phases could be implemented to increase TN RE, however transient DO conditions were reported to favor filamentous growth and breakage of granules [49]. Campo et al. [62] proposed an aeration phase composed by two sub-phases to achieve high TN RE trough SND: (1) DO controlled phase; (2) DO not controlled phase. During the second sub-phase the oxygen is progressively depleted enhancing the NO_x^- reduction by extending the anoxic zone in granules (**Table 4**). However, real influent wastewater used by Campo et al. [62] was characterized by an higher biodegradable soluble COD (COD_{BS}) and total COD ratio compared to that of previous works [49,128,150], with values between 20% and 40%. In this way, the COD_{BS}, being almost a 60% of total COD, was stored under anaerobic conditions by PAOs/GAOs and no soluble organic substrate was available during aerobic condition for HAB growth. The high availability of COD_{BS} may determine a better granulation and overall removal efficiencies (**Table 4**).

Further elaboration on factors limiting SND process during the treatment of real municipal wastewaters with AGS should be addressed.

- ***Shear force***

As mentioned in **Section 2.4.2**, to maintain the stability of granules one of the main factor to control is the hydraulic shear force, which is mainly affected by air flow or mixing and reactor H/D ratio [55,57]. Shear stress arise from liquid/gas flows and attrition

between particles [54]. When exposed to high shear stress (2.5 cm s^{-1}), aerobic granules become more compact and stable, while low superficial gas velocity (SGV) is always accompanied by larger volume of granules but with a less compact structure and low settling velocity [127,152–154]. It's important emphasize the relation between aeration and DO. Limiting air flow can lead to insufficient nitrification and improve denitrification [147].

Zhang et al. [153] combined low strength wastewater (i.e. COD/TN = 8) with a SGV of 0.55 cm s^{-1} obtaining small and stable granular (d = 0.8 mm) under anaerobic/aerobic/anoxic alternating conditions. After the maturation of granules, simultaneous removal of nitrogen and carbon was achieved, with TN RE and COD RE up to 99% and 90%. Although, low SGV comported saving energy during the operation of WWTP. He et al. [56] studied the effect of three low SGV (0.17–0.11–0.04 cm s^{-1}) treating low feed C/N ratio (i.e. 3.3) domestic wastewater through SND process. The granules size increased from 1.5 (±0.5) mm to 1.5 (±0.6) mm and 1.8 (±0.9) mm while the settling velocity decreased from 58 (±0.2) to 40 (±0.2) m h^{-1}. However the system remained stable without showing sludge bulking or flock desegregation [56], despite the decrease of the PN/PS ratio from 0.41 to 0.18. In the opposite way TN RE increased from 64% to 94% when decreasing the SGV due to an improvement of performance during anoxic phase, although more time was required to achieve complete nitrification [57]. The authors recommended combining medium aeration intensity with the right length of aeration phase to improve SND performance.

2.7.4 Fluidized bed biofilm reactor

The fluidized bed biofilm reactor (FBBR) is characterized by a solid biomass carrier material which is fluidized in the reactor by high liquid or gas flow rates [155]. FBBRs can be operated in up-flow mode or also in down-flow mode, depending on the direction of the flow inside the reactor, and with several carrier materials [119]. FBBRs have been applied for the treatment of wastewater characterized by high $N\text{-}NH_4^+$ concentrations [26] due to the high biomass concentration in the reactor bed. Due to its particular shape the FBBR can treat small quantities of wastewater and, therefore, it has been mainly applied for the treatment of industrial wastewater. Few studies are reported on FBBR treatment of municipal wastewater characterized by low medium C/N ratio for the removal of nitrogen. Besides, potential disadvantages of this system are: (1) high pumping cost to maintain an upward velocity and fluidize the bed; (2) limitations on reactor sizes to maintain the height/diameter ratio required; (3) deterioration of carriers due to friction forces [155].

Wen et al. [156] used a bench-scale FBBR with a diameter of 70 mm and height of 1.5 m to achieve SND process. The biocarrier used was a fragmentized rubber (d = 3 mm; 1.10 g cm^{-3}). The small size of biocarriers allowed to have a high specific surface area for biomass attachment and growth [156]. The authors achieved an NH_4^+ RE up to 80%, however low TN removal of 50% was reported with a DO concentration of 3 mg L^{-1}. TN REs reached values up to 60–70% once DO concentrations dropped below 3.0 mg L^{-1}.

2.8 References

[1] M.C. Chrispim, M. Scholz, M. Antunes, Phosphorus recovery from municipal wastewater treatment: critical review of challenges and opportunities for developing countries, *J. Environ. Manage.* 248 (2019) 109268.

[2] R.W. Butcher, Studies in the ecology of rivers: VII. The algae of organically enriched waters, *J. Ecol.* 35 (2016) 186–191.

[3] Y. Chen, C. Peng, J. Wang, L. Ye, L. Zhang, Y. Peng, Effect of nitrate recycling ratio on simultaneous biological nutrient removal in a novel anaerobic/anoxic/oxic (A2/O) -biological aerated filter (BAF) system, *Bioresour. Technol.* 102 (2011) 5722–5727.

[4] P.J.T.M. van Puijenbroek, A.H.W. Beusen, A.F. Bouwman, Global nitrogen and phosphorus in urban waste water based on the Shared Socio-economic pathways, *J. Environ. Manage.* 231 (2019) 446–456.

[5] J.H. Janse, J.J. Kuiper, M.J. Weijters, E.P. Westerbeek, M.H.J.L. Jeuken, M. Bakkenes, R. Alkemade, W.M. Mooij, J.T.A. Verhoeven, GLOBIO-Aquatic, a global model of human impact on the biodiversity of inland aquatic ecosystems, *Environ. Sci. Policy*. 48 (2014) 99–114.

[6] Z. Song, X. Zhang, H. Hao, W. Guo, P. Song, Y. Zhang, Zeolite powder based polyurethane sponges as biocarriers in moving bed biofilm reactor for improving nitrogen removal of municipal wastewater, *Sci. Total Environ.* 651 (2019) 1078–1086.

[7] Y. Cao, C. Zhang, H. Rong, G. Zheng, L. Zhao, The effect of dissolved oxygen concentration (DO) on oxygen diffusion and bacterial community structure in moving bed sequencing batch reactor (MBSBR), *Water Res.* 108 (2017) 86–94.

[8] F. Di Capua, F. Pirozzi, P.N.L. Lens, G. Esposito, Electron donors for autotrophic denitrification, *Chem. Eng. J.* 362 (2019) 922–937.

[9] EEA, EEA Signals 2018 - Water Is Life. Copenhagen, Denmark., 2018.

[10] L. Lijó, S. Malamis, S. González-García, F. Fatone, M.. T. Moreira, E. Katsou, Technical and environmental evaluation of an integrated scheme for the co-treatment of wastewater and domestic organic waste in small communities, *Water Res.* 109 (2016) 173–185.

[11] G. Libralato, A.V. Ghirardini, F. Avezzù, To centralise or to decentralise: an overview of the most recent trends in wastewater treatment management, *J. Environ. Manage.* 94 (2012) 61–68.

[12] Q. He, J. Song, W. Zhang, S. Gao, H. Wang, J. Yu, Enhanced simultaneous nitrification, denitrification and phosphorus removal through mixed carbon source by aerobic granular sludge, *J. Hazard. Mater.* 382 (2020) 121043.

[13] S. Ge, S. Wang, X. Yang, S. Qiu, B. Li, Y. Peng, Detection of nitrifiers and evaluation of partial nitrification for wastewater treatment: a review, *Chemosphere*. 140 (2015) 85–98.

[14] L. Yan, S. Liu, Q. Liu, M. Zhang, Y. Liu, Y. Wen, Z. Chen, Improved performance of simultaneous nitrification and denitrification via nitrite in an oxygen-limited SBR by alternating the DO, *Bioresour. Technol.* 275 (2019) 153–162.

[15] W. Huang, Z. She, M. Gao, Q. Wang, C. Jin, Y. Zhao, L. Guo, Effect of anaerobic/aerobic duration on nitrogen removal and microbial community in a simultaneous partial nitrification and denitrification system under low salinity, *Sci. Total Environ.* 651 (2019) 859–870.

[16] Q. He, J. Zhou, Q. Song, W. Zhang, H. Wang, L. Liu, Elucidation of microbial characterization of aerobic granules in a sequencing batch reactor performing simultaneous nitrification, denitrification and phosphorus removal at varying carbon to phosphorus ratios, *Bioresour. Technol.* 241 (2017) 127–133.

[17] C. Li, S. Liu, T. Ma, M. Zheng, J. Ni, Simultaneous nitrification, denitrification and phosphorus removal in a sequencing batch reactor (SBR) under low temperature, *Chemosphere*. 229 (2019) 132–141.

[18] Y. Chen, Q. Wang, S. Zhao, W. Yang, H. Wang, W. Jia, Removal of nutrients and emission of nitrous oxide during simultaneous nitrification, denitrification and phosphorus removal process with metal ions addition, *Int. Biodeterior. Biodegrad.* 142 (2019) 143–150.

[19] Y. Peng, G. Zhu, Biological nitrogen removal with nitrification and denitrification via nitrite pathway, *Appl. Microbiol. Biotechnol.* 73 (2006) 15–26.

[20] S. Rahimi, O. Modin, I. Mijakovic, Technologies for biological removal and recovery of nitrogen from wastewater, *Biotechnol. Adv.* 43 (2020) 107570.

[21] C.Z. Correa, K.V.M.C. Prates, E.F. de Oliveira, D.D. Lopes, A.C. Barana, Nitrification/denitrification of real municipal wastewater in an intermittently aerated structured bed reactor, *J. Water Process Eng.* 23 (2018) 134–141.

[22] A. di Biase, M.S. Kowalski, T.R. Devlin, J.A. Oleszkiewicz, Moving bed biofilm reactor technology in municipal wastewater treatment: a review, *J. Environ. Manage.* 247 (2019) 849–866.

[23] F. Sabba, C. Picioreanu, R. Nerenberg, Mechanisms of nitrous oxide (N2O) formation and reduction in denitrifying biofilms, *Biotechnol. Bioeng.* 114 (2017) 2753–2761.

[24] F. Sabba, C. Picioreanu, J. Pérez, R. Nerenberg, Hydroxylamine diffusion can enhance N_2O emissions in nitrifying biofilms: a modeling study, *Environ. Sci. Technol.* 49 (2015) 1486–1494.

[25] S. Zhang, Z. Huang, S. Lu, J. Zheng, X. Zhang, Nutrients removal and bacterial community structure for low C/N municipal wastewater using a modified Anaerobic/Anoxic/Oxic (mA2/O) process at north areas of China, *Bioresour. Technol.* 243 (2017) 975–985.

[26] X. Liu, M. Kim, G. Nakhla, M. Andalib, Y. Fang, Partial nitrification-reactor configurations, and operational conditions: performance analysis, *J. Environ. Chem. Eng.* 8 (2020) 103984.

[27] G. Mannina, M. Capodici, A. Cosenza, D. Di Trapani, V. Armando, H. Ødegaard, Nitrous oxide from moving bed based integrated fixedfilm activated sludge membrane bioreactors, *J. Environ. Manage.* 187 (2017) 96–102.

[28] R. Pishgar, J.A. Dominic, Z. Sheng, J.H. Tay, Denitrification performance and microbial versatility in response to different selection pressures, *Bioresour. Technol.* 281 (2019) 72–83.

[29] L. Miao, G. Yang, T. Tao, Y. Peng, Recent advances in nitrogen removal from landfill leachate using biological treatments – a review, *J. Environ. Manage*. 235 (2019) 178–185.

[30] S.-P. Sun, C. Pellicer i Nàcher, B. Merkey, Q. Zhou, S.-Q. Xia, J.-H. Sun, B.F. Smets, Effective biological nitrogen removal treatment processes for domestic wastewaters with Low C/N ratios: a review, *Environ. Enginnering Sci.* 27 (2010) 111–126.

[31] Z. Hu, H.J.C.T. Wessels, T. Alen, M.S.M. Jetten, B. Kartal, Nitric oxide-dependent anaerobic ammonium oxidation oxidation, *Nat. Commun.* 10 (2019) 1244.

[32] I. Sancho, E. Licon, C. Valderrama, N. De Arespacochaga, S. López-Palau, J.L. Cortina, Recovery of ammonia from domestic wastewater effluents as liquid fertilizers by integration of natural zeolites and hollow fibre membrane contactors, *Sci. Total Environ.* 585 (2017) 244–251.

[33] K. Bernat, D. Kulikowska, M. Zielinska, A. Cydzik-Kwiatkowska, I. Wojnowska-Baryła, Nitrogen removal from wastewater with a low COD/N ratio at a low oxygen concentration, *Bioresour. Technol.* 102 (2011) 4913–4916.

[34] Y.Z. Li, Y.L. He, D.G. Ohandja, J. Ji, J.F. Li, T. Zhou, Simultaneous nitrification–denitrification achieved by an innovative internal-loop airlift MBR: comparative study, *Bioresour. Technol.* 99 (2008) 5867–5872.

[35] W. Ma, Y. Han, W. Ma, H. Han, H. Zhu, C. Xu, K. Li, D. Wang, Enhanced nitrogen removal from coal gasification wastewater by simultaneous nitrification and denitrification (SND) in an oxygen-limited aeration sequencing batch biofilm reactor, *Bioresour. Technol.* 244 (2017) 84–91.

[36] A.A.L. Zinatizadeh, E. Ghaytooli, Simultaneous nitrogen and carbon removal from wastewater at different operating conditions in a moving bed biofilm reactor (MBBR): process modeling and optimization, *J. Taiwan Inst. Chem. Eng.* 53 (2015) 98–111.

[37] M. Seifi, M.H. Fazaelipoor, Modeling simultaneous nitrification and denitrification (SND) in a fluidized bed biofilm reactor, *Appl. Math. Model.* 36 (2012) 5603–5613.

[38] R.L. Meyer, R.J. Zeng, V. Giugliano, L.L. Blackall, Challenges for simultaneous nitrification, denitrification, and phosphorus removal in microbial aggregates: mass transfer limitation and nitrous oxide production, *FEMS Microbiol.* Ecol. 52 (2005) 329–338.

[39] Y. Zhao, D. Liu, W. Huang, Y. Yang, M. Ji, L.D. Nghiem, Q.T. Trinh, N.H. Tran, Insights into biofilm carriers for biological wastewater treatment processes:

current state-of-the-art, challenges, and opportunities, *Bioresour. Technol.* 288 (2019) 121619.

[40] S. He, G. Xue, H. Kong, X. Li, Improving the performance of sequencing batch reactor (SBR) by the addition of zeolite powder, *J. Hazard. Mater*. 142 (2007) 493–499.

[41] L. Li, Y. Dong, G. Qian, X. Hu, L. Ye, Performance and microbial community analysis of bio-electrocoagulation on simultaneous nitrification and denitrification in submerged membrane bioreactor at limited dissolved oxygen, *Bioresour. Technol.* 258 (2018) 168–176.

[42] T. Liu, G. Jia, J. Xu, X. He, X. Quan, Simultaneous nitrification and denitrification in continuous flow MBBR with novel surface-modified carriers, *Environ. Technol.* (2020).

[43] R. Ferrentino, A. Ferraro, M.R. Mattei, G. Esposito, G. Andreottola, Process performance optimization and mathematical modelling of a SBR-MBBR treatment at low oxygen concentration, *Process Biochem.* 75 (2018) 230–239.

[44] R.B. Moura, M.H.R.Z. Damianovic, E. Foresti, Nitrogen and carbon removal from synthetic wastewater in a vertical structured-bed reactor under intermittent aeration, *J. Environ. Manage*. 98 (2012) 163–167.

[45] T. Liu, X. He, G. Jia, J. Xu, X. Quan, S. You, Simultaneous nitrification and denitrification process using novel surface-modified suspended carriers for the treatment of real domestic wastewater, *Chemosphere.* 247 (2020) 125831.

[46] D. Gao, L. Liu, H. Liang, W. Wu, Aerobic granular sludge: characterization, mechanism of granulation and application to wastewater treatment, *Crit. Rev. Biotechnol.* 31 (2011) 137–152.

[47] N. Puznava, M. Payraudeau, D. Thornberg, Simultaneous nitrification and denitrification in biofilters with real time aeration control, *Water Sci. Technol.* 43 (2001) 269–76.

[48] A.R. Massoompour, S.M. Borghei, M. Raie, Enhancement of biological nitrogen removal performance using novel carriers based on the recycling of waste materials, *Water Res*. 170 (2020) 115340.

[49] M. Layer, M. Garcia, A. Hernandez, E. Reynaert, E. Morgenroth, N. Derlon, Limited simultaneous nitrification-denitrification (SND) in aerobic granular

sludge systems treating municipal wastewater: mechanisms and practical implications, *Water Res. X.* 7 (2020) 100048.

[50] S. He, G. Xue, B. Wang, Factors affecting simultaneous nitrification and de-nitrification (SND) and its kinetics model in membrane bioreactor, *J. Hazard. Mater.* 168 (2009) 704–710.

[51] J. Wang, H. Rong, Y. Cao, C. Zhang, Factors affecting simultaneous nitrification and denitrification (SND) in a moving bed sequencing batch reactor (MBSBR) system as revealed by microbial community structures, *Bioprocess Biosyst. Eng.* 43 (2020) 1833–1846.

[52] J. Zhou, H. Yu, K. Ye, H. Wang, Y. Ruan, J. Yu, Optimized aeration strategies for nitrogen removal efficiency: application of end gas recirculation aeration in the fixed bed biofilm reactor, *Environ. Sci. Pollut. Res.* 26 (2019) 28216–28227.

[53] Y. Jia, M. Zhou, Y. Chen, Y. Hu, J. Luo, Insight into short-cut of simultaneous nitrification and denitrification process in moving bed biofilm reactor: effects of carbon to nitrogen ratio, *Chem. Eng. J.* 400 (2020) 125905.

[54] S. Bengtsson, M. De Blois, B. Wilén, D. Gustavsson, Treatment of municipal wastewater with aerobic granular sludge, *Crit. Rev. Environ. Sci. Technol.* 48 (2018) 119–166.

[55] L. Yan, M. Zhang, Y. Liu, C. Liu, Y. Zhang, S. Liu, L. Yu, Enhanced nitrogen removal in an aerobic granular sequencing batch reactor under low DO concentration: role of extracellular polymeric substances and microbial community structure, *Bioresour. Technol.* 289 (2019) 121651.

[56] Q. He, W. Zhang, S. Zhang, H. Wang, Enanced nitrogen removal in an aerobic granular sequencing batch reactor performing simultaneous nitrification, endogenous denitrification and phosphorus removal with low superficial gas velocity, *Chem. Eng. J.* 326 (2017) 1223–1231.

[57] Q. He, L. Chen, S. Zhang, R. Chen, H. Wang, Hydrodynamic shear force shaped the microbial community and function in the aerobic granular sequencing batch reactors for low carbon to nitrogen (C/N) municipal wastewater treatment, *Bioresour. Technol.* 271 (2019) 48–58.

[58] W. Chen, Y. Lu, Q. Jin, M. Zhang, J. Wu, A novel feedforward control strategy for simultaneous nitrification and denitrification (SND) in aerobic granular sludge sequential batch reactor, *J. Environ. Manage.* 260 (2020) 110103.

[59] Y.Q. Gu, T.T. Li, H.Q. Li, Biofilm formation monitored by confocal laser scanning microscopy during startup of MBBR operated under different intermittent aeration modes. *Process Biochem.,* 74 (2018) 132–140.

[60] H. Doan, A. Lohi, Intermittent aeration in biological treatment of wastewater, *Am. J. Eng. Appl. Sci.* 2 (2009) 260–267.

[61] H. Chai, Y. Xiang, R. Chen, Z. Shao, L. Gu, L. Li, Q. He, Enhanced simultaneous nitrification and denitrification in treating low carbon-to-nitrogen ratio wastewater: Treatment performance and nitrogen removal pathway, *Bioresour. Technol.* 280 (2019) 51–58.

[62] R. Campo, S. Sguanci, S. Caffaz, L. Mazzoli, C. Lubello, T. Lotti, Efficient carbon, nitrogen and phosphorus removal from low C/N real domestic wastewater with aerobic granular sludge, *Bioresour. Technol.* 305 (2020) 122961.

[63] F. Han, W. Ye, D. Wei, W. Xu, B. Du, Q. Wei, Simultaneous nitrification-denitrification and membrane fouling alleviation in a submerged biofilm membrane bioreactor with coupling of sponge and biodegradable PBS carrier, *Bioresour. Technol.* 270 (2018) 156–165.

[64] K.M. Wang, S.F. Jiang, Z.H. Zhang, Q.Q. Ye, Y.C. Zhang, J.H. Zhou, Q.K. Hong, J.M. Yu, H.Y. Wang, Impact of static biocarriers on the microbial community, nitrogen removal and membrane fouling in submerged membrane bioreactor at different COD:N ratios, *Bioresour. Technol.* 301 (2020) 122798.

[65] F. Wang, S. Lu, Y. Wei, M. Ji, Characteristics of aerobic granule and nitrogen and phosphorus removal in a SBR, *J. Hazard. Mater.* 164 (2009) 1223–1227.

[66] H. Wang, Q. Song, J. Wang, H. Zhang, Q. He, W. Zhang, J. Song, Simultaneous nitrification, denitrification and phosphorus removal in an aerobic granular sludge sequencing batch reactor with high dissolved oxygen: effects of carbon to nitrogen ratios, *Sci. Total Environ.* 642 (2018) 1145–1152.

[67] J. Wang, L. Chu, Biological nitrate removal from water and wastewater by solid-phase denitrification process, *Biotechnol. Adv.* 34 (2016) 1103–1112.

[68] S. Wang, L. Gai, L. Zhao, M. Fan, W. Gong, B. Gao, Y. Ma, Aerobic granules for low-strength wastewater treatment: formation, structure, and microbial community, *Chem. Technol. Biotechnol.* (2009) 1015–1020.

[69] J. Wagner, R. Helena, Aerobic granulation in a sequencing batch reactor using real domestic wastewater, *J. Environ. Eng.* 139 (2013) 1391–1396.

[70] L. Chu, J. Wang, Nitrogen removal using biodegradable polymers as carbon source and biofilm carriers in a moving bed biofilm reactor, *Chem. Eng. J.* 170 (2011) 220–225.

[71] L. Chu, J. Wang, Comparison of polyurethane foam and biodegradable polymer as carriers in moving bed biofilm reactor for treating wastewater with a low C/N ratio, *Chemosphere.* 83 (2011) 63–68.

[72] L. Feng, R. Jia, Z. Zeng, G. Yang, X. Xu, Simultaneous nitrification – denitrification and microbial community profile in an oxygen-limiting intermittent aeration SBBR with biodegradable carriers, *Biodegradation*. 29 (2018) 473–486.

[73] B. Fu, X. Liao, L. Ding, H. Ren, Characterization of microbial community in an aerobic moving bed biofilm reactor applied for simultaneous nitrification and denitrification, *World J. Microbiol. Biotechnol.* 26 (2010) 1981–1990.

[74] S. Yang, F. Yang, Nitrogen removal via short-cut simultaneous nitrification and denitrification in an intermittently aerated moving bed membrane bioreactor, J. *Hazard. Mater.* 195 (2011) 318–323.

[75] L. Zhang, C. Wei, K. Zhang, C. Zhang, Q. Fang, S. Li, Effects of temperature on simultaneous nitrification and denitrification via nitrite in a sequencing batch biofilm reactor, *Bioprocess Biosyst. Eng.* 32 (2009) 175–182.

[76] C. Tan, F. Ma, S. Qiu, Impact of carbon to nitrogen ratio on nitrogen removal at a low oxygen concentration in a sequencing batch biofilm reactor, *Water Sci. Technol.* 67 (2013) 612–618.

[77] Z. She, L. Wu, Q. Wang, M. Gao, C. Jin, Y. Zhao, L. Zhao, L. Guo, Salinity effect on simultaneous nitrification and denitrification, microbial characteristics in a hybrid sequencing batch biofilm reactor, *Bioprocess Biosyst. Eng*. 41 (2017) 67–75.

[78] L.M.C. Daniel, E. Pozzi, E. Foresti, F.A. Chinalia, Removal of ammonium via simultaneous nitrification – denitrification nitrite-shortcut in a single packed-bed batch reactor, *Bioresour. Technol.* 100 (2009) 1100–1107.

[79] S. Lochmatter, J. Maillard, C. Holliger, Nitrogen removal over nitrite by aeration control in aerobic granular sludge sequencing batch reactors, *Int. J. Enviromental Reaserch Public Heal*. 11 (2014) 6955–6978.

[80] P. Taylor, W. Zheng, Y. Zhang, L. Li, Y. Pen, S. Wang, Simultaneous nitritation and denitritation of domestic wastewater without addition of external carbon

sources at limited aeration and normal temperatures, *Desalin. Water Treat.* 21 (2010) 210–219.

[81] G. Liu, J. Wang, Long-term low DO enriches and shifts nitrifier community in activated sludge, *Environ. Sci. Technol.* 47 (2013) 5109–5117.

[82] P. Bao, S. Wang, B. Ma, Q. Zhang, Y. Peng, Achieving partial nitrification by inhibiting the activity of *Nitrospira*-like bacteria under high-DO conditions in an intermittent aeration reactor, *J. Environ. Sci.* 56 (2016) 71–78.

[83] H. Yoo, K. Ahn, H. Lee, K. Lee, Y. Kwak, K. Song, Nitrogen removal from synthetic wastewater by simultaneous nitrification and denitrification (SND) via nitrite in an intermittently-aerated reactor, *Water Res.* 33 (1999) 145–154.

[84] E.M. Gilbert, S. Agrawal, F. Brunner, T. Schwartz, H. Horn, S. Lackner, Response of different *Nitrospira* species to anoxic periods depends on operational DO, *Environ. Sci. Technol.* 48 (2014) 2934–2941.

[85] Z. Xia, Q. Wang, Z. She, M. Gao, Y. Zhao, L. Guo, C. Jin, Nitrogen removal pathway and dynamics of microbial community with the increase of salinity in simultaneous nitrification and denitrification process, *Sci. Total Environ.* 697 (2019) 134047.

[86] Q. He, H. Wang, L. Chen, S. Gao, W. Zhang, J. Song, J. Yu, Elevated salinity deteriorated enhanced biological phosphorus removal in an aerobic granular sludge sequencing batch reactor performing simultaneous nitrification, denitrification and phosphorus remova, *J. Hazard. Mater.* 390 (2019) 121782.

[87] J.T. Bunce, E. Ndam, I.D. Ofiteru, A. Moore, D.W. Graham, A review of phosphorus removal technologies and their applicability to small-scale domestic wastewater treatment systems, *Front. Environ. Sci.* 6 (2018).

[88] C. Pratt, S.A. Parsons, A. Soares, B.D. Martin, Biologically and chemically mediated adsorption and precipitation of phosphorus from wastewater, *Curr. Opin. Biotechnol.* 23 (2012) 890–896.

[89] P. Loganathan, P. Taylor, S. Vigneswaran, J. Kandasamy, S. Nanthi, Removal and recovery of phosphate from water using sorption, *Crit. Rev. Environ. Sci. Technol.* 44 (2014) 847–907.

[90] J.C. Leyva-Díaz, M.M. Muñío, J. González-López, J.M. Poyatos, Anaerobic/anoxic/oxic configuration in hybrid moving bed biofilm reactor-

membrane bioreactor for nutrient removal from municipal wastewater, *Ecol. Eng.* 91 (2016) 449–458.

[91] S. Salehi, K.Y. Cheng, A. Heitz, M.P. Ginige, Simultaneous nitrification, denitrification and phosphorus recovery (SNDPr) - an opportunity to facilitate full-scale recovery of phosphorus from municipal wastewater, *J. Environ. Manage.* 238 (2019) 41–48.

[92] E. Ashra, A.M. Zeinabad, S.M. Borghei, E. Torresi, J.M. Sierra, Optimising nutrient removal of a hybrid five-stage Bardenpho and moving bed biofilm reactor process using response surface methodology, *J. Environ. Chem. Eng.* 7 (2019) 102861.

[93] S.Y. Gebremariam, M.W. Beutel, D. Christian, T.F. Hess, Research advances and challenges in the microbiology of enhanced biological phosphorus removal — a critical review, *Water Environ. Res.* 83 (2011) 195–219.

[94] M. Pijuan, A. Guisasola, J.A. Baeza, J. Carrera, C. Casas, J. Lafuente, Net P-removal deterioration in enriched PAO sludge subjected to permanent aerobic conditions, *J. Biotechnol.* 123 (2006) 117–126.

[95] H. Ge, D.J. Batstone, J. Keller, Biological phosphorus removal from abattoir wastewater at very short sludge ages mediated by novel PAO clade *Comamonadaceae*, *Water Res.* 69 (2014) 173–182.

[96] D. Yadav, N. Kumar, V. Pruthi, P. Kumar, Ensuring sustainability of conventional aerobic wastewater treatment system via bio-augmentation of aerobic bacterial consortium: an enhanced biological phosphorus removal approach, *J. Clean. Prod.* 262 (2020) 121328.

[97] D. Yadav, V. Pruthi, P. Kumar, Enhanced biological phosphorus removal in aerated stirred tank reactor using aerobic bacterial consortium, *J. Water Process Eng.* 13 (2016) 61–69.

[98] C.M. López-Vázquez, C.M. Hooijmans, D. Brdjanovic, H.J. Gijzen, M.C.M. van Loosdrecht, Factors affecting the microbial populations at full-scale enhanced biological phosphorus removal (EBPR) wastewater treatment plants in The Netherlands, *Water Res.* 42 (2009) 2349–2360.

[99] J. Yin, P. Zhang, F. Li, G. Li, B. Hai, Simultaneous biological nitrogen and phosphorus removal with a sequencing batch reactor-biofilm system, *Int. Biodeterior. Biodegradation.* (2015) 1–6.

[100] Q. He, Q. Song, S. Zhang, W. Zhang, H. Wang, Simultaneous nitrification, denitrification and phosphorus removal in an aerobic granular sequencing batch reactor with mixed carbon sources: reactor performance, extracellular polymeric substances and microbial successions, *Chem. Eng. J.* 331 (2017) 841–849.

[101] R. Khanongnuch, F. Di Capua, A.-M. Lakaniemi, E.R. Rene, P.N.L. Lens, Long-term performance evaluation of an anoxic sulfur oxidizing moving bed biofilm reactor under nitrate limited conditions, *Environ. Sci. Water Res. Technol.* 5 (2019) 1072–1081.

[102] C. Suarez, M. Piculell, O. Modin, S. Langenheder, F. Persson, M. Hermansson, Thickness determines microbial community structure and function in nitrifying biofilms via deterministic assembly, *Sci. Rep.* 9 (2019) 5110.

[103] X. Zhang, X. Chen, C. Zhang, H. Wen, W. Guo, H.H. Ngo, Effect of filling fraction on the performance of sponge-based moving bed biofilm reactor, *Bioresour. Technol.* 219 (2016) 762–767.

[104] T.T. Nguyen, H.H. Ngo, W. Guo, A. Johnston, A. Listowski, Effects of sponge size and type on the performance of an up-flow sponge bioreactor in primary treated sewage effluent treatment, *Bioresour. Technol.* 101 (2010) 1416–1420.

[105] M. Sandip, V. Kalyanraman, Enhanced simultaneous nitri-denitrification in aerobic moving bed biofilm reactor containing polyurethane foam-based carrier media, *Water Sci. Technol.* 79 (2019) 510–517.

[106] J. Lim, C. Seng, P. Lim, S. Ng, A.A. Sujari, Nitrogen removal in moving bed sequencing batch reactor using polyurethane foam cubes of various sizes as carrier materials, *Bioresour. Technol.* 102 (2011) 9876–9883.

[107] X. Zhang, Z. Song, W. Guo, Y. Lu, L. Qi, H. Wen, H. Hao, Behavior of nitrogen removal in an aerobic sponge based moving bed biofilm reactor, *Bioresour. Technol.* 245 (2017) 1282–1285.

[108] F. Quan, W. Yuxiao, W. Tianmin, Z. Hao, C. Libing, Z. Chong, C. Hongzhang, K. Xiuqin, X. Xin-hui, Effects of packing rates of cubic-shaped polyurethane foam carriers on the microbial community and the removal of organics and nitrogen in moving bed biofilm reactors, *Bioresour. Technol*. 117 (2012) 201–207.

[109] Y.-X. Wei, Y.-F. Li, Z.-F. Ye, Enhancement of removal efficiency of ammonia nitrogen in sequencing batch reactor using natural zeolite, *Environ. Earth Sci.* 60 (2010) 1407–1413.

[110] T. Liu, G. Jia, X. Quan, Accelerated start-up and microbial community structures of simultaneous nitrification and denitrification by using novel suspended carriers, *Chem. Technol. Biotechnol.* 93 (2018) 577–584.

[111] H. Chen, A. Li, Q. Wang, D. Cui, C. Cui, F. Ma, Nitrogen removal performance and microbial community of an enhanced multistage A/O biofilm reactor treating low- strength domestic wastewater, *Biodegradation.* 29 (2018) 285–299.

[112] G. Ge, J. Zhao, X. Li, X. Ding, A. Chen, Y. Chen, B. Hu, S. Wang, Effects of influent COD/N ratios on nitrous oxide emission in a sequencing biofilm batch reactor for simultaneous nitrogen and phosphorus removal, *Sci. Rep.* 7 (2017).

[113] J. Lim, P. Lim, C. Seng, Enhancement of nitrogen removal in moving bed sequencing batch reactor with intermittent aeration during REACT period, *Chem. Eng. J.* 197 (2012) 199–203.

[114] I.W. Lo, K.V. Lo, D.S. Mavinic, D. Shiskowski, W. Ramey, Contributions of biofilm and suspended sludge to nitrogen transformation and nitrous oxide emission in hybrid sequencing batch system, *J. Environ. Sci.* 22 (2010) 953–960.

[115] Y. Mao, X. Quan, H. Zhao, Y. Zhang, S. Chen, T. Liu, W. Quan, Accelerated startup of moving bed biofilm process with novel electrophilic suspended biofilm carriers, *Chem. Eng. J.* 315 (2017) 364–372.

[116] H. Sun, H. Liu, M. Zhang, Y. Liu, A novel single-stage ceramic membrane moving bed bio fi lm reactor coupled with reverse osmosis for reclamation of municipal wastewater to NEWater-like product water, *Chemosphere.* 2 (2020) 128836.

[117] H. Ødegaard, Innovations in wastewater treatment: the moving bed biofilm process, *Water Sci. Technol.* 53 (9) (2006) 17–33.

[118] S. Yang, F. Yang, Z. Fu, T. Wang, R. Lei, Simultaneous nitrogen and phosphorus removal by a novel sequencing batch moving bed membrane bioreactor for wastewater treatment, *J. Hazard. Mater.* 175 (2010) 551–557.

[119] F. Di Capua, S. Papirio, P.N.L. Lens, G. Esposito, Chemolithotrophic denitrification in biofilm reactors, *Chem. Eng. J.* 280 (2015) 643–657.

[120] L. Deng, W. Guo, H.H. Ngo, X. Zhang, X.C. Wang, Q. Zhang, R. Chen, New functional biocarriers for enhancing the performance of a hybrid moving bed biofilm reactor-membrane bioreactor system, *Bioresour. Technol.* 208 (2016) 87–93.

[121] I. Kocaturk, T.H. Erguder, Influent COD/TAN ratio affects the carbon and nitrogen removal efficiency and stability of aerobic granules, *Ecol. Eng.* 90 (2016) 12–24.

[122] S. Yang, F. Yang, Z. Fu, R. Lei, Comparison between a moving bed membrane bioreactor and a conventional membrane bioreactor on organic carbon and nitrogen removal, *Bioresour. Technol.* 100 (2009) 2369–2374.

[123] F. Meng, S. Chae, A. Drews, M. Kraume, H. Shin, Recent advances in membrane bioreactors (MBRs): membrane fouling and membrane material, *Water Res.* 43 (2009) 1489–1512.

[124] F. Sun, Y. Lu, J. Wu, Comparison of operational strategies for nitrogen removal in aerobic granule sludge sequential batch reactor (AGS-SBR): a model-based evaluation, *J. Environ. Chem. Eng.* 7 (2019) 103314.

[125] S.J. Sarma, J. Tay, Carbon, nitrogen and phosphorus removal mechanisms of aerobic granules, *Crit. Rev. Biotechnol.* 38 (2018) 1077–1088.

[126] A. Chyi, E. We, A. Aris, N. Azimah, M. Zain, A review of the treatment of low–medium strength domestic wastewater using aerobic granulation technology, Environ. *Sci. Water Res. Technol.* 6 (2020) 464–490.

[127] S.L. de S. Rollemberg, A.R.M. Barros, P.I.M. Firmino, A.B. d. Santos, Aerobic granular sludge: cultivation parameters and removal mechanisms, *Bioresour. Technol.* 270 (2018) 678–688.

[128] M. Layer, A. Adler, E. Reynaert, A. Hernandez, M. Pagni, E. Morgenroth, Organic substrate diffusibility governs microbial community composition, nutrient removal performance and kinetics of granulation of aerobic granular sludge, *Water Res. X.* 4 (2019) 100033.

[129] R. Pishgar, J.A. Dominic, Z. Sheng, J.H. Tay, Influence of operation mode and wastewater strength on aerobic granulation at pilot scale: startup period, granular sludge characteristics, and effluent quality, *Water Res.* 160 (2019) 81–96.

[130] L.S. de S. Rollemberg, Q.L. De Oliveira, A.R.M. Barros, V.M.M. Melo, P.I.M. Firmino, A.B. do. Santos, Effects of carbon source on the formation, stability, bioactivity and biodiversity of the aerobic granule sludge, *Bioresour. Technol.* 278 (2019) 195–204..

[131] Ś. Piotr, A. Cydzik-kwiatkowska, Performance and microbial characteristics of biomass in a full-scale aerobic granular sludge wastewater treatment plant, *Environ. Sci. Pollut. Res.* 25 (2018) 1655–1669.

[132] Q. He, S. Zhang, Z. Zou, L. Zheng, H. Wang, Unraveling characteristics of simultaneous nitrification, denitrification and phosphorus removal (SNDPR) in an aerobic granular sequencing batch reactor, *Bioresour. Technol.* 220 (2016) 651–655.

[133] Q. He, H. Wang, X. Yang, J. Zhou, Y. Ye, D. Chen, Culture of denitrifying phosphorus removal granules with different influent wastewater, *Desalin. Water Treat.* 57 (2016) 17247–17254.

[134] Q. He, J. Zhou, H. Wang, J. Zhang, L. Wei, Microbial population dynamics during sludge granulation in an A/O/A sequencing batch reactor, *Bioresour. Technol*. 214 (2016) 1–8.

[135] Y. Lu, H. Wang, T.A. Kotsopoulos, R.J. Zeng, Advanced phosphorus recovery using a novel SBR system with granular sludge in simultaneous nitrification, denitrification and phosphorus removal process, *Appl. Microbiol. Biotechnol.* 100 (2016) 4367–4374.

[136] L. Yan, S. Zhang, G. Hao, X. Zhang, Y. Ren, Y. Wen, Y. Guo, Simultaneous nitrification and denitrification by EPSs in aerobic granular sludge enhanced nitrogen removal of ammonium-nitrogen-rich wastewater, *Bioresour. Technol.* 202 (2016) 101–106.

[137] J. Wagner, L.B. Guimarães, T.R. V Akaboci, R.H.R. Costa, Aerobic granular sludge technology and nitrogen removal for domestic wastewater treatment, *Water Sci. Technol.* 71 (2015) 1040–1047.

[138] M. Pronk, M.K. De Kreuk, B. De Bruin, P. Kamminga, R. Kleerebezem, M.C.M. Van Loosdrecht, Full scale performance of the aerobic granular sludge process for sewage treatment, *Water Res.* 84 (2015) 207–217.

[139] G. Di Bella, M. Torregrossa, Simultaneous nitrogen and organic carbon removal in aerobic granular sludge reactors operated with high dissolved oxygen concentration, *Bioresour. Technol.* 142 (2013) 706–713.

[140] S. Lochmatter, G. Gonzalez-gil, C. Holliger, Optimized aeration strategies for nitrogen and phosphorus removal with aerobic granular sludge, *Water Res.* 47 (2013) 6187–6197.

[141] M. Coma, M. Verawaty, M. Pijuan, Z. Yuan, P.L. Bond, Enhancing aerobic granulation for biological nutrient removal from domestic wastewater, *Bioresour. Technol.* 103 (2012) 101–108.

[142] E. Isanta, M.E. Suárez-ojeda, Á. Val, N. Morales, J. Pérez, J. Carrera, Long term operation of a granular sequencing batch reactor at pilot scale treating a low-strength wastewater, *Chem. Eng. J.* 198–199 (2012) 163–170.

[143] F. Chen, Y. Liu, J. Tay, P. Ning, Operational strategies for nitrogen removal in granular sequencing batch reactor, *J. Hazard. Mater.* 189 (2011) 342–348.

[144] Y. Liu, B. Moy, Y. Kong, J. Tay, Formation, physical characteristics and microbial community structure of aerobic granules in a pilot-scale sequencing batch reactor for real wastewater treatment, *Enzyme Microb. Technol.* 46 (2010) 520–525.

[145] N. Kishida, S. Tsuneda, Y. Sakakibara, J.H. Kim, R. Sudo, Real-time control strategy for simultaneous nitrogen and phosphorus removal using aerobic granular sludge, *Water Sci. Technol.* 58 (2008) 445–450.

[146] N. Kishida, J. Kim, S. Tsuneda, R. Sudo, Anaerobic/oxic/anoxic granular sludge process as an effective nutrient removal process utilizing denitrifying polyphosphate-accumulating organisms, *Water Res.* 40 (2006) 2303–2310.

[147] A. Mosquera-corral, M.K. De Kreuk, J.J. Heijnen, M.C.M. Van Loosdrecht, Effects of oxygen concentration on N-removal in an aerobic granular sludge reactor, *Water Res.* 39 (2005) 2676–2686.

[148] S. Yang, J. Tay, Y. Liu, A novel granular sludge sequencing batch reactor for removal of organic and nitrogen from wastewater, *J. Biotechnol.* 106 (2003) 77–86.

[149] M.K. De de Kreuk, J.J. Heijnen, M.C.M. van Loosdrecht, Simultaneous COD , Nitrogen, and phosphate removal by aerobic granular sludge, (2005).

[150] N. Derlon, J. Wagner, R. Helena, E. Morgenroth, Formation of aerobic granules for the treatment of real and low-strength municipal wastewater using a sequencing batch reactor operated at constant volume, *Water Res.* 105 (2016) 341–350.

[151] L. Campos, A. Magrı, M. Sepu, Moving forward in the use of aerobic granular sludge for municipal wastewater treatment: an overview, *Rev. Environ. Sci. Bio/Technology* Vol. 18 (2019) 741–769.

[152] Y. V Nancharaiah, G.K.K. Reddy, Aerobic granular sludge technology: mechanisms of granulation and biotechnological applications, *Bioresour. Technol.* 247 (2017) 1128–1143.

[153] C. Zhang, H. Zhang, F. Yang, Diameter control and stability maintenance of aerobic granular sludge in an A/O/A SBR, *Sep. Purif. Technol.* 149 (2015) 362–369.

[154] T.R. Devlin, A. Biase, M. Kowalski, J.A. Oleszkiewicz, Granulation of activated sludge under low hydrodynamic shear and different wastewater characteristics, *Bioresour. Technol.* 224 (2016) 229–235.

[155] B. Ozkaya, A.H. Kaksonen, E. Sahinkaya, J.A. Puhakka, Fluidized bed bioreactor for multiple environmental engineering solutions, *Water Res.* 150 (2019) 452–465.

[156] Q. Wen, Z. Chen, H. Shi, T-RFLP detection of nitrifying bacteria in a fluidized bed reactor of achieving simultaneous nitrification – denitrification, *Chemosphere.* 71 (2008) 1683–1692.

CHAPTER 3.

Effect of carbon-to-nitrogen ratio on simultaneous nitrification denitrification in a microaerobic moving bed biofilm reactor

Part of the content of this chapter has been published as:

Iannacone, F., Di Capua, F., Granata, F., Gargano, R., Pirozzi, F., Esposito, G., 2019. Effect of carbon-to-nitrogen ratio on simultaneous nitrification denitrification and phosphorus removal in a microaerobic moving bed biofilm reactor. *J. Environ. Manage.* 250, 109518.

Abstract

In this study, long-term simultaneous nitrification denitrification (SND) and phosphorous removal were investigated in a continuous-flow microaerobic MBBR (mMBBR) operated at a dissolved oxygen (DO) concentration of 1.0 (±0.2) mg L^{-1}. MBBR performance was evaluated at different feed carbon-to-nitrogen (C/N) ratios (2.7, 4.2 and 5.6) and HRTs (2 days and 1 day). Stable long-term MBBR operation and chemical oxygen demand (COD), total inorganic nitrogen (TIN) and phosphorous (P-PO_4^{3-}) removal efficiencies up to 100%, 68% and 72%, respectively, were observed at a feed C/N ratio of 4.2. Lower TIN removal efficiency and unstable performance were observed at feed C/N ratios of 2.7 and 5.6, respectively. HRT decrease from 2 days to 1 day resulted in transient NH_4^+ accumulation and higher NO_2^-/NO_3^- ratio in the effluent. Batch activity tests showed that biofilm cultivation at a feed C/N ratio of 4.2 resulted in the highest denitrifying activity (189 mg N $gVSS^{-1}$ d^{-1}), whereas the highest nitrifying activity (316 mg N $gVSS^{-1}$ d^{-1}) was observed after cultivation at a feed C/N ratio of 2.7. Thermodynamic modeling with Visual MINTEQ and stoichiometric evaluations revealed that P removal was mainly biological and can be attributed to the P-accumulating capacity of denitrifying bacteria.

Keywords

Microaerobic operation; moving bed biofilm reactor; nutrient removal; phosphorous removal; simultaneous nitrification denitrification.

Graphical Abstract

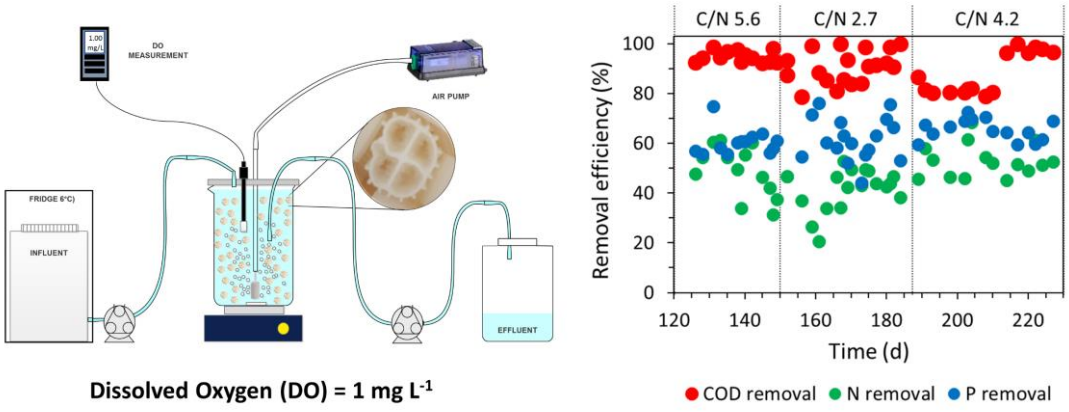

3.

3.1 Introduction

The exponential growth of urbanization, industrial production and household consumption in the last decades has inevitably led to an increase in the production of

nutrient-rich wastewater [1]. Excess nutrient discharge in water bodies results in unbalanced ecosystems and leads to eutrophication. The main source of nitrogen pollution is the run-off from agricultural land, whereas phosphorus pollution comes primarily from households and industry [2,3]. The removal of nitrogenous compounds, i.e. NH_4^+ and NO_3^-, in municipal wastewater treatment plants (MWWTPs) is conventionally accomplished with a combination of two separate biological processes, i.e. nitrification (**Eq. 3.1**), performed by ammonium and nitrite oxidizing bacteria (AOB and NOB, respectively) consuming oxygen and alkalinity, and denitrification (**Eq. 3.2**), performed by heterotrophic denitrifying bacteria (HDB) under anoxic conditions [4].

$$NH_4^+ + 1.82\ O_2 + 0.13\ CO_2 \rightarrow 0.03\ C_5H_7O_2N + 0.97\ NO_3^- + 0.92\ H_2O + 1.97\ H^+ \quad (3.1)$$

$$NO_3^- + 0.87\ CH_3COO^- + H^+ \rightarrow 0.46\ N_2 + 0.08\ C_5H_7O_2N + 0.44\ CO_2 + 1.07\ H_2O + 0.87\ HCO_3^- \quad (3.2)$$

Organic carbon, usually measured in terms of chemical oxygen demand (COD), is removed via aerobic and anoxic oxidation by heterotrophic aerobic bacteria (HAB) and HDB, respectively. Phosphorus is removed either chemically via precipitation with Fe^{3+}, Al^{3+} or Ca^{2+} salts or biologically with the alternation of anaerobic, anoxic and aerobic phases [5].

Simultaneous nitrification and denitrification (SND) offers several advantages over distinct nitrogen removal processes: (1) SND is performed in a single aerated basin, reducing plant footprint and investment costs, 2) carbon demand and sludge production are reduced by over 30% [6], (3) alkalinity supply by denitrification (**Eq. 3.2**) helps to maintain a circumneutral pH, (4) there is no need of NO_3^- recirculation and 5) less energy for aeration is required. In contrast, SND usually results in a lower nitrogen removal efficiency (RE) compared to separate denitrification and nitrification and significant accumulation of nitrous oxide (N_2O), a powerful greenhouse gas [7].

Biofilm reactors have been widely applied for nutrient removal from wastewater, being robust and high-performance systems with extremely high solid retention time (SRT) [8–11]. Moving bed biofilm reactors (MBBRs) enable the formation of a stratified biofilm on mobile carriers with a bacterial community depending on the wastewater composition [12]. Substrates are transported into the biofilm via diffusion mechanisms, which enable the formation of aerobic, anoxic and anaerobic layers. Concentration gradients depend on biofilm density and thickness as well as bulk concentrations of the substrates [13]. As a result, the MBBR is a more suitable technology for SND than conventional activated sludge (CAS) systems due to low density and size of CAS flocs [14]. Dissolved oxygen (DO) concentrations ≥ 2 mg L^{-1} are often used to support SND in MBBR (**Table 3.1**) in

order to ensure oxygen diffusion through the aerobic layer and sustain nitrification. Maintaining high DO levels in the reactor is expensive and may reduce denitrification efficiency, while excess organic carbon in the influent wastewater may result in HAB overgrowth and suppression of the nitrification process [15]. As a result, a strict control of the feed carbon-to-nitrogen (C/N) ratio is necessary to maintain the efficiency and stability of the SND process.

MBBRs have been often operated in sequencing batch mode alternating anaerobic and aerobic (or anoxic) conditions to simultaneously remove nitrogen and phosphorous, while fewer studies on continuous-flow MBBR operation for N and P removal are reported in literature (**Table 3.1**). Additionally, the optimal C/N ratios and DO concentrations reported for the SND process in MBBR reveal a large variability, which can be attributed to the different biofilm composition and/or uncontrolled growth of HAB resulting in significant $N\text{-}NH_4^+$ uptake for biomass synthesis. Literature lacks a long-term evaluation of SND stability in continuous-flow MBBR at microaerobic conditions ($DO \leq 1$ mg L^{-1}) [16,17], being crucial to assess the reliability of a process based on a delicate equilibrium among different microbial groups.

The application of machine learning algorithms can be an effective solution for modeling non-linear processes. Generally, biological processes exhibit a high non-linear characteristic influenced by different parameters [18]. Khanongnuch et al. [10] applied artificial neural network (ANN) in order to predict thiosulfate $(S_2O_3^{2})^-$ and NO_3^- removal efficiencies and SO_4^{2-} production in a fluidized bed reactor (FBR) for anoxic $S_2O_3^{2-}$ oxidation trough autotrophic denitrification. The ANN model was able to successfully predict the output parameters, achieving a determination coefficient (R^2) of 0.90. Other application of ANNs model have been carried out to evaluate the performance of biological waste-gas systems [19,20]. Recently, Multilayer Perceptron (MLP) and Random Forest (RF) algorithms have shown good performances modeling complex and highly non-linear processes (e.g. evapotranspiration phenomenon in wetlands) [21].

Table 3.1 - Comparative analysis of the SND performance of different bioreactors.

Reactor type	Operational time (days)	Carrier type	HRT (h)	DO (mg L^{-1})	Influent composition (mg L^{-1})	Feed C/N	COD removal (%)	TIN removal (%)	TP removal (%)	Reference
MBBR	37	Bio-carriers	8	n.a.	TIN 51 TP 5.7 COD 315	2.4	< 90	≤ 30	≤ 30	[17]
MBBR	12–16	Polyethylene carriers	10	3.0–4.0	N-NH_4^+ 100 COD 500-1500	4.5–13.4	91–96	40–60	n.a.	[22]
MBBR	n.a.	Kaldnes-3 – Ring R2	4–12	2.0–4.0	COD:N:P 100:20:3	n.a.	50–88	26–51	0–38	[23]
MBBR	85	Cupic-shaped polyurethane sponges	12	5.0–6.5	TIN 13-18 TOC 100-118 TP 2.7-3.5	6.5–10	94–96[a]	77–87	n.a.	[24]
Sequencing batch MBBR	n.a.	KMT	n.a.	0–2.0	N-NH_4^+ 25 COD 75-300 TP 2-21	n.a.	60–80	20–80	50–98	[25]
Sequencing batch MBBR	450	Cascade-1A	n.a.	n.a.	TIN 35–69 COD 50–200 TP 15–22	n.a.	n.a.	6–20	20–23	[26]
Sequencing batch MBBR	141	HX9KL/ Biomaster BCN 012KLS	12–24	0.8–1	TIN 35-46 COD 270-291	6.0–8.3 [b]	88–92	47–75	n.a.	[27]
Activated sludge	240	n.a.	8–42	0.3–0.8	TIN 32-63 COD 118–335	2–10	73–96	8–67	n.a.	[14]
MBBR	227	Kaldnes K1	24–48	1.0 (±0.2)	TIN 29-71 COD 203-562 TP 9-17	2.7–5.6	74–100	21–68	22–79	This study

n.a. = not available.

[a] measured as total organic carbon (TOC).

[b] available as COD/TN

In this work, the simultaneous removal of organic carbon, nitrogen and phosphorous from a synthetic municipal wastewater was studied for 183 days in a continuous flow microaerobic MBBR (mMBBR) under different feed C/N ratios and HRTs (**Table 3.2**). Batch activity tests were conducted to assess the effect of microaerobic cultivation at different feed C/N ratios on the nitrifying and denitrifying activities of the MBBR biofilm. Finally, machine learning algorithms were applied to predict the effluent concentrations of TIN (i.e. RF and MLP).

3.2 Materials and methods

3.2.1 Synthetic municipal wastewater

The synthetic wastewater used as reactor influent in this study was prepared with tap water and composed of 0.532–1.064 g L^{-1} sodium acetate trihydrate ($CH_3COONa \cdot 3H_2O$) as organic carbon source, 0.123–0.246 g L^{-1} of ammonium chloride (NH_4Cl) as $N\text{-}NH_4^+$ source, 1 g L^{-1} of sodium bicarbonate ($NaHCO_3$) as inorganic carbon source and a nutrient solution as follows (mg L^{-1}): $MgCl_2 \cdot 6H_2O$ (150), KH_2PO_4 (50), $CaCl_2 \cdot H_2O$ (20), $MnCl_2 \cdot 6H_2O$ (1.75), $Na_2MoO_4 \cdot 2H_2O$ (0.1), $CoCl_2$ (0.05). The pH of the synthetic wastewater was 7.84 (±0.13). During the study, the influent tank was kept in the fridge at a temperature of 6 °C.

3.2.2 Bioreactor set-up and start-up

The MBBR used in this study (**Fig. 3.1**) was composed of a 2.2 L glass vessel and an acrylic lid with three openings. The vessel was filled up to 2 L with synthetic wastewater, inoculum (250 mL) and Kaldnes K1 carriers (Veolia, France) at a 40% carrier filling ratio. The inoculum was composed of 80% recycle sludge (3.0 ± 0.5 g TS L^{-1}, 2.5 ± 0.1 g VS L^{-1}) collected from the pre-denitrification system of the MWWTP of Cassino (Italy) and 20% suspended biomass from an aerobic lab-scale MBBR treating high-strength ammonium wastewater as described by Moreno Osorio et al. [28]. Air was delivered to the medium through a ceramic porous stone connected to the lid by a polystyrene tube, which was connected to an aquarium air pump by a flexible polymer tube. Mixing was provided by a magnetic stirrer (ARGO LAB M2-A) at 100 rpm (**Fig. 3.1**). The bioreactor was operated in batch mode for 8 days at room temperature (22 ± 2 °C) to allow bacterial colonization of the carriers. Half of the bioreactor solution was replaced with fresh synthetic wastewater as soon as the fed COD and/or NH_4^+ was consumed. The DO concentration in the bioreactor was not controlled in this phase and ranged between 0.5 and 4.6 mg L^{-1}. The pH and alkalinity varied from 7.69 to 8.88 and from 183 to 1250 mg

$CaCO_3$ L^{-1}, respectively. After 8 days, biofilm formation on the K1 carriers was observed and the reactor operation was switched to continuous mode.

An HRT of 2 days was initially used for continuous MBBR operation (start-up, **Table 3.2**). In preliminary experiments, nitrification was severely inhibited when microaerobic conditions were immediately applied at the beginning of continuous operation (data not shown). As a result, the DO concentration during start-up was gradually decreased from 4.09 to 1.95 mg L^{-1} to facilitate the adaptation of the nitrifying biomass to low oxygen conditions.

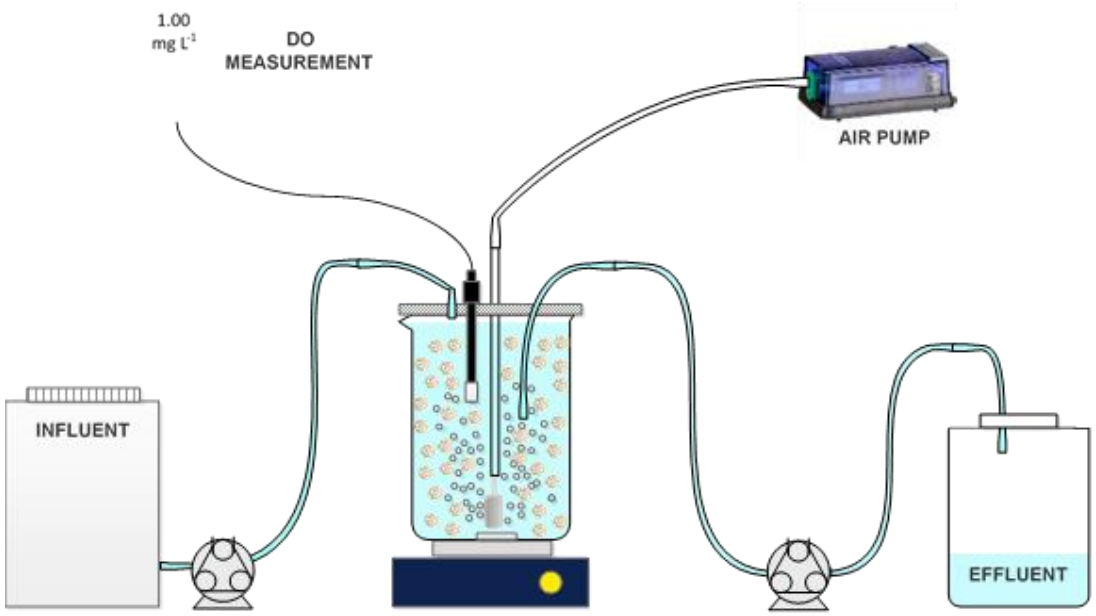

Figure 3.1 - Experimental set-up of the MBBR used in this study.

3.2.3 Experimental design

The MBBR was operated in continuous mode during five experimental periods (P1–P5, **Table 3.2**). Each experimental period was maintained for at least 4 weeks in order to evaluate the stability of the SND process. From the beginning of P1 (day 45) until the end of the study, the DO concentration in the MBBR was monitored three times day^{-1} and maintained at 1.0 (±0.2) mg L^{-1} by manually adjusting the air flow. A feed C/N ratio of 2.9 (±0.2) and an HRT of 2 days were maintained during the first period of continuous operation (P1, **Table 3.2**).

The HRT was decreased to 1 day at the beginning of P2 (day 86–124) and maintained until the end of the study. During P2, the feed C/N ratio was not changed (3.0 ± 0.2) maintaining the COD and TIN concentrations at 492 (±32) and 62 (±4) mg L^{-1}, respectively. In P3 (days 125–152) the C/N ratio was increased to 5.6 (±0.5) by decreasing the influent N-NH_4^+ concentration to 31 (±1) mg L^{-1} to avoid process inhibition due to

NO_2^- accumulation. During P1-P3 (days 45–152), the feed alkalinity was stable at 1174 (±30) mg $CaCO_3$ L^{-1}.

On day 153, the influent COD concentration was reduced from 471 (±35) mg L^{-1} (P3) to 231 (±18) mg L^{-1} (P4) to recover nitrification and the MBBR operated at a feed C/N ratio of 2.7 (±0.3). During P4 (days 153–187), the influent TIN was maintained at 31 (±2) mg L^{-1} and the influent alkalinity decreased to 1049 (±52) mg $CaCO_3$ L^{-1}. In P5 (days 188–227) the feed C/N ratio was increased to 4.2 (±0.3) by increasing the influent COD concentration to 373 (±15) mg L^{-1}. Alkalinity in the feed increased to 1132 (±22) mg $CaCO_3$ L^{-1}, while the influent TIN concentration was maintained at 33 (±2) mg L^{-1}. K1 carrier and suspended biomass samples were collected during the study for volatile suspended solid (VSS) analysis.

3.2.4 Batch activity tests

Three batch activity tests (**Table 3.3**) were performed at the end of P3, P4 and P5 to evaluate the nitrifying (ATN tests) and denitrifying (ATD tests) activities of the MBBR biofilm after cultivation at feed C/N ratios of 5.6 (P3), 2.7 (P4) and 4.2 (P5). The experiments were performed in duplicate at 22 (±2) °C by using 50 mL wide neck conical flasks and 100 mL glass serum flasks for the ATN and ATD tests, respectively. The flasks were inoculated with 12 K1 carriers collected from the MBBR and rinsed with ultrapure water. The medium added to the flasks for the ATN tests was as the MBBR influent during periods P3–P5 (**Table 3.2**) except for acetate not being added to the flasks. The medium used for the ATD tests was composed of NO_3^- (50 mg L^{-1}), sodium acetate (500 mg L^{-1}) and nutrients as in the MBBR influent. The ATD flasks were purged for 10 min with N_2 prior to inoculation and sealed with rubber septa and aluminum crimps to ensure anoxic conditions. Mixing was provided by a gyratory shaker at the speed of 150 rpm. During the experiments, the ATN flasks were monitored for NH_4^+, NO_3^- and NO_2^- concentrations, while only NO_3^- and NO_2^- concentrations were measured in the ATD flasks.

Table 3.2 - Experimental conditions during continuous MBBR operation.

Experimental period	**Time (d)**	**HRT (d)**	**Feed C/N ratio**	**Feed COD (mg L^{-1})**	**Feed N-NH_4^+ (mg L^{-1})**	**Organic loading rate (mg COD L^{-1} h^{-1})**	**Nitrogen loading rate (mg N-NH_4^+ L^{-1} h^{-1})**	**Feed alkalinity (mg $CaCO_3$ L^{-1})**
Start-up	10–44	2	3.0 (±0.2)	509 (±12)	63 (±3)	10.6 (±0.3)	1.3 (±0.1)	1143 (±39)
P1	45–85	2	2.9 (±0.2)	502 (±26)	64 (±3)	10.5 (±0.5)	1.3	1175 (±35)
P2	86–124	1	3.0 (±0.2)	492 (±32)	62 (±4)	20.5 (±1.3)	2.6 (±0.2)	1173 (±28)
P3	125–152	1	5.6 (±0.5)	471 (±35)	31 (±1)	19.6 (±1.5)	1.3 (±0.1)	1173 (±26)
P4	153–187	1	2.7 (±0.3)	231 (±18)	31 (±2)	9.6 (±0.7)	1.3 (±0.1)	1049 (±52)
P5	188–227	1	4.2 (±0.3)	373 (±15)	33 (±2)	15.6 (±0.6)	1.4 (±0.1)	1132 (±22)

3.2.5 Analytical methods

Liquid samples collected from the MBBR and batch flasks were filtered through 0.45 μm syringe filters with polypropylene membrane (VWR, USA) prior to analysis. NH_4^+ concentration was determined spectrophotometrically using the indophenol blue method [29]. COD and alkalinity concentrations were determined by closed reflux colorimetric method and potentiometric titration, respectively [30]. DO, pH and anionic concentrations (NO_3^-, NO_2^- and PO_4^{3-}) were measured as described by Di Capua et al. [31]. VS, TS and VSS concentrations were analyzed according to Standard Methods [30]. Prior to VSS analysis, the K1 carriers were added to a Falcon tube containing 10 mL of ultrapure water and the biofilm detached by sonication followed by manual shaking. The solution containing the detached biofilm was used for VSS determination. Chemical phosphorous precipitation during the study was predicted using the thermodynamic equilibrium modeling software Visual MINTEQ (http://vminteq.lwr.kth.se/). The average values of the effluent pH, alkalinity and monitored ionic concentrations were used as input data. The temperature was set to 22 ºC and the oversaturated solids were allowed to precipitate.

3.2.6 Machine learning application

Prior to model the biological process of TIN removal, the dataset has to be split into training and testing folds. The most used method is to split randomly the dataset into training and testing subsets with typical training test of data varying between 70–80% [20]. In this study, a K-fold cross-validation method was used to select the data for training and testing the model. The cross-validation method provides to randomly divide the dataset into K folds (K = 10), then K-1 folders are used for model training, while 1-fold for model testing. The cross-validation method is repeated K times in order to use each k fold as validation dataset. The overall model performance is estimated as average of performances obtain for each subset.

To evaluate the performances of model, R^2, mean absolute error (MAE), root mean square error (RMSE), and relative absolute error (RAE) were evaluated. R^2 indicates how well the model predicts the data (**Eq. 3.3**); MAE is the average of absolute difference between the predicted value and the experimental value, i.e. MAE is a measure of the average error between these values (**Eq. 3.4**); RMSE is evaluated as the square root of the average squared differences between predicted value and effective value and represents the standard deviation of the foretold differences (**Eq. 3.5**); RAE is the normalized total absolute error (**Eq. 3.6**).

$$R^2 = 1 - \frac{\sum_{I=1}^{m}(f_i - y_i)^2}{\sum_{I=1}^{m}(y_a - y_i)^2} \quad (3.3)$$

$$MAE = \frac{\sum_{I=1}^{m}|f_i - y_i|}{m} \quad (3.4)$$

$$RMSE = \sqrt{\frac{\sum_{I=1}^{m}(f_i - y_i)^2}{m}} \quad (3.5)$$

$$RAE = \frac{\sum_{I=1}^{m}|f_i - y_i|}{\sum_{I=1}^{m}|y_a - y_i|} \quad (3.6)$$

Where m is the total number of data, y_i is the experimental data, y_a the average value of the experimental data and f_i is the predicted value. The algorithms used are RF and MLP implemented in WEKA (University of Waikato, NZ). The algorithms are fully described by Granata et al. [21,32]. Briefly, RF is an Ensemble Model consisting of regression trees not correlated. Regression tree is characterized by a building process which consist in splits data into "branches". The input variables are grouped in a single partition and after are allocated in the first two branches. The model proceeds considering all the possible splits. In the case of a random forest, hyperparameters include the number of decision trees in the forest and the number of features considered by each tree when splitting a node. The random forest used counted 100 trees.

MLP is a system of interconnected nodes which belongs to the class of supervised feed forward networks. MLP is the most common type of ANN used for environmental problem [19,20]. The structure of MLP is composed by an input layer, one or more hidden layers and an output layer [33]. The optimal number of hidden layers can be obtained whit a trial-and-error process, nevertheless an insufficient number of hidden layers can determine an underfitting problem while a high number of hidden layers can determine an overfitting problem. In this study, backpropagation technique was used. The correlation between the input x_i, processed through the hidden layers, and output y_j can be expressed as follow (**Eq. 3.7**):

$$y_j = f\left(\sum_{i=1}^{n} w_{ij} x_i + b\right) \quad (3.7)$$

Where $f(x)$ is the transfer function, n the number of input variables, w_{ij} is the connection weight multiplied for the input of previous layer x_i. The weighted input is than summarized to bias value b. Each nodes or neurons use a non-linear activation function, except the input nodes. The neural networks were composed by 1 hidden layer, with 2 neurons. The activation function was the sigmoid function, while the learning rate and momentum rate were 0.3 and 0.2, respectively.

3.2.7 Statistical Analysis

The statistical analysis of the data was performed using the Data Analysis Tool of Excel 2016 (Microsoft Corporation, USA). The one-way analysis of variance (ANOVA) method was conducted in order to determine the statistical differences in the performance parameters, i.e. COD, TIN and TP removal, during each period of mMBBR operation. The significant difference was set at 95% ($p < 0.05$).

3.3 Results

3.3.1 MBBR performance

The temporal profiles of the influent and effluent DO, COD, NH_4^+, NO_3^-, NO_2^- and alkalinity concentrations and pH during continuous MBBR operation are shown in **Fig. 3.2**. On day 42 (start-up), the effluent COD decreased from 134 (±20) mg L^{-1} (days 10–40) to 19 mg L^{-1} and remained stable until the end of P1. Similarly, alkalinity and NH_4^+ concentration in the effluent remained stable during P1, while fluctuations in NO_3^- and NO_2^- concentrations were observed until the end of the period.

The decrease of HRT from 2 days (P1) to 1 day (P2) resulted in COD and N-NH_4^+ breakthrough in the effluent up to 130 and 49 mg L^{-1}, respectively. The effluent alkalinity increased up to 1300 mg $CaCO_3$ L^{-1}, higher than that observed in the feed. Conversely, the effluent NO_3^- concentration decreased sharply to below the detection limit on day 89. The VSS concentration of the suspended biomass at the end of P1 (day 85) and P2 (day 124) was 91 and 107 mg L^{-1}, respectively. From day 98 onward, as the effluent NH_4^+ started to decrease, the N-NO_2^- and TIN concentrations in the effluent progressively increased up to 29 and 41 mg L^{-1} (day 120), respectively. As the feed NH_4^+ concentration was reduced to 32.5 mg N-NH_4^+ L^{-1} (P3) to avoid NO_2^- inhibition, NO_2^- concentration in the effluent decreased to 9 mg N-NO_2^- L^{-1} (day 126) and remained below this value for the whole period, except on day 139 (14 mg N-NO_2^- L^{-1}) due to a peak in DO concentration (1.5 mg L^{-1}). During days 126–142 (P3), the effluent TIN concentration was 16 (±3) mg L^{-1}, resulting in a TIN RE of 52 (±9) % (**Fig. 3.3**). However, a sudden increase of the effluent NH_4^+ concentration up to 17 mg N-NH_4^+ L^{-1} was observed between days 140 and 145. Similarly, the effluent alkalinity increased from 1135 (day 140) to 1303 (day 145) mg $CaCO_3$ L^{-1}, being above the influent value. As a result, the TIN RE sharply decreased from 60% on day 142 to 32% on day 148 (**Fig. 3.3**). The VSS concentrations of the carrier-attached and suspended biomass at the end of P3 (day 152) were 2.0 mg $carrier^{-1}$ and 150 mg L^{-1}, respectively.

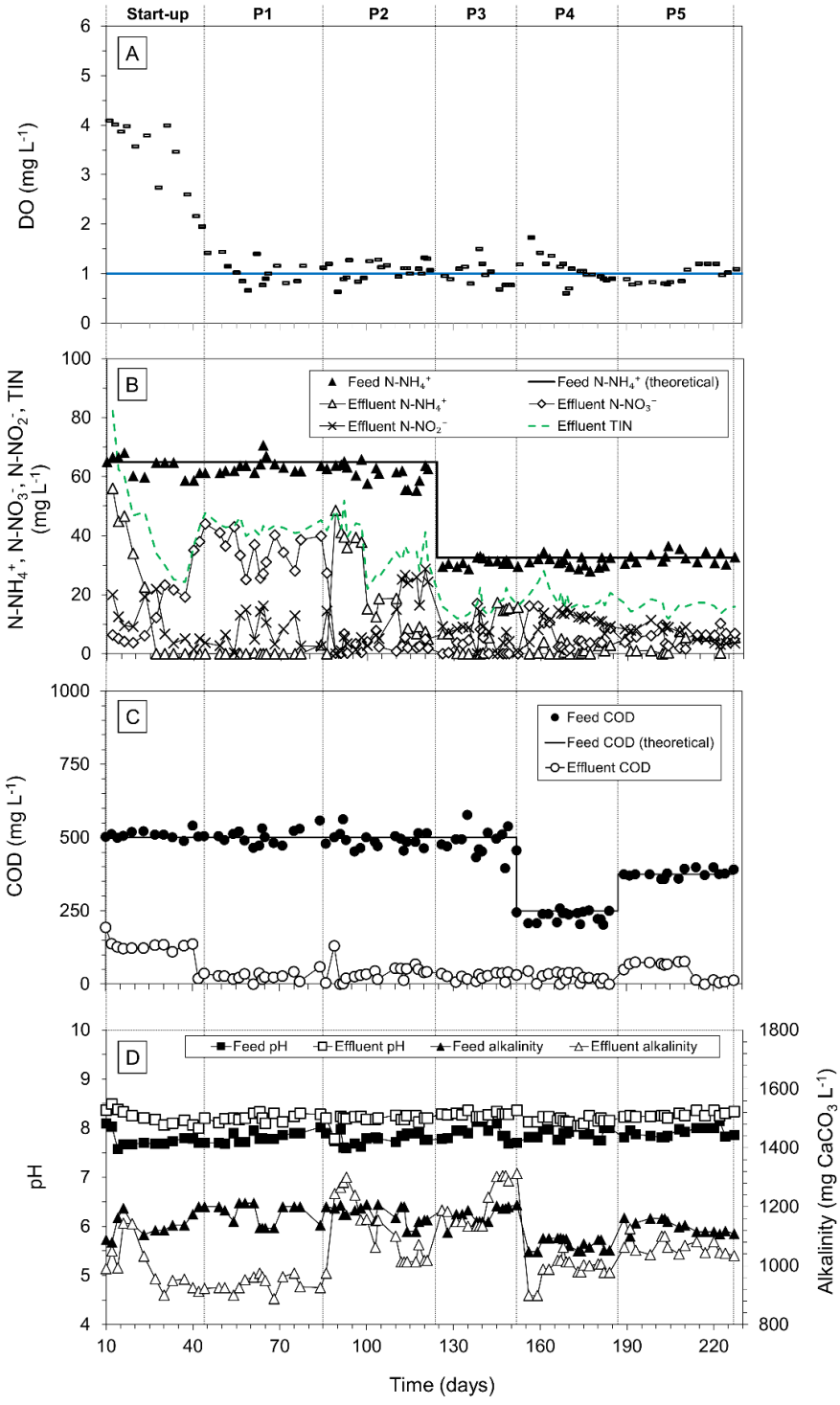

Figure 3.2 - Time course of DO and influent and effluent N-NH_4^+, N-NO_3^-, N-NO_2^-, TIN, COD, pH and alkalinity concentrations during continuous MBBR operation.

As the C/N ratio was decreased to 2.7 (±0.3), the effluent NH_4^+ concentration decreased to below the detection limit in 4 days and did not exceed 5 mg N-NH_4^+ L^{-1} until

the end of P4. NH_4^+ depletion resulted in a decrease of the effluent alkalinity to 899 mg $CaCO_3$ L^{-1} and in a breakthrough of both NO_3^- and NO_2^- concentrations up to 16 mg N L^{-1}. The concentrations of the carrier-attached and suspended biomass (1.5 mg $carrier^{-1}$ and 50 mg L^{-1}, respectively) measured on day 187 (P4) were lower than those observed at the end of P3. The MBBR experienced high TIN levels at the beginning of P4, which gradually decreased with the effluent NO_3^- and NO_2^- concentrations during the period. As a result, the TIN RE increased to an average value of 46 (±4) % between days 168 and 184 (**Fig. 3.3**). At the beginning of P4, the COD RE temporarily dropped from 93% (day 152) to 79% (day 156). Nevertheless, the effluent COD concentration during P3 and P4 remained below 45 mg L^{-1}. At the end of P4 (day 187), the VSS concentrations of the carrier-attached and suspended biomass were 1.5 mg $carrier^{-1}$ and 50 mg L^{-1}, respectively.

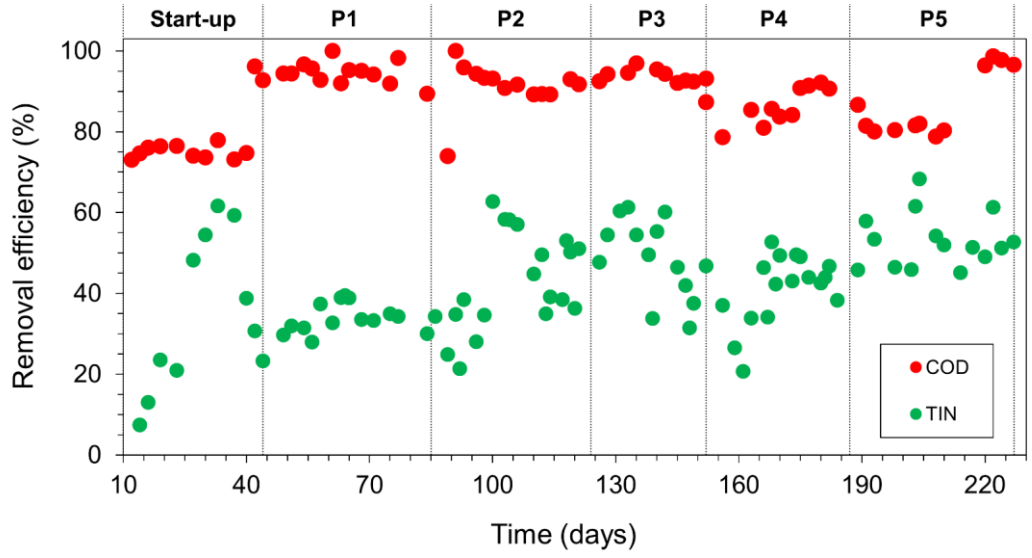

Figure 3.3 - TIN and COD REs profiles during continuous MBBR operation.

An increase of the COD levels in the effluent was observed at the beginning of P5 in response to the increase of the feed C/N ratio from 2.7 to 4.2. The effluent COD concentration during days 191–210 was 72 (±4) mg L^{-1} prior to decrease to below 15 mg L^{-1}. As a result, the COD RE increased from 81 (±2) % (days 189-210) to 98 (±1) % (days 214–227). The effluent TIN concentration remained below 19 mg L^{-1} throughout the entire period, resulting in TIN REs up to 68%. The carrier-attached and suspended biomass concentrations at the end of P5 (day 227) were 1.7 mg $carrier^{-1}$ and 139 mg L^{-1}, respectively.

During P1–P5, $P\text{-}PO_4^{3-}$ concentration in the influent was 14 (±2) mg L^{-1} (**Fig. 3.4**) and stable $P\text{-}PO_4^{3-}$ levels (5 ± 2 mg L^{-1}) were observed in the effluent. The highest $P\text{-}PO_4^{3-}$ RE was observed during P5, being 66 (±4) %, with a peak of 72% on day 203. Thermodynamic modeling with Visual MINTEQ revealed that phosphorous precipitation

accounted for less than 1 mg L^{-1} and indicated $MnHPO_4$ as the main phosphorous precipitate.

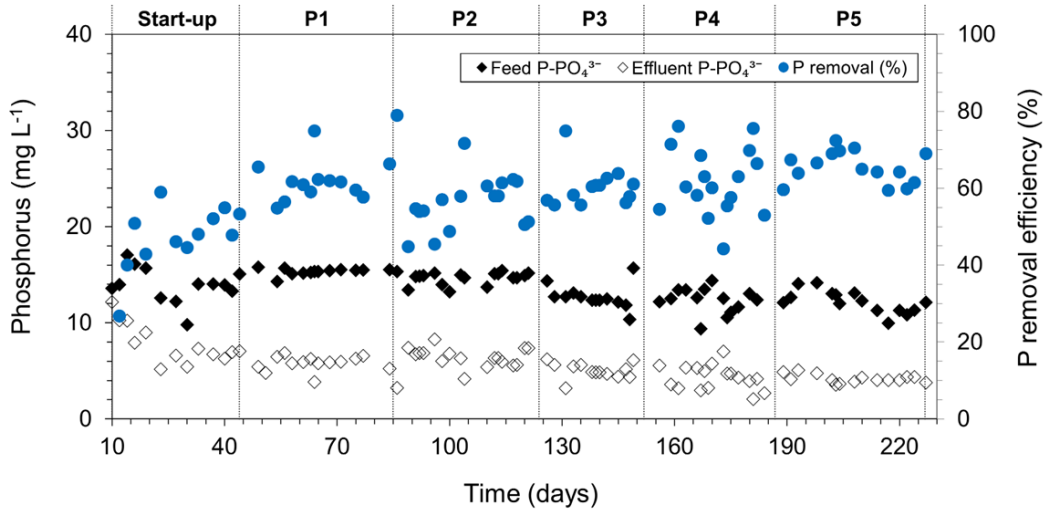

Figure 3.4 - Temporal profiles of feed and effluent $P\text{-}PO_4^{3-}$ concentrations and P RE in the MBBR.

3.3.2 Nitrogen removal activities of the MBBR biofilm

The results of the batch activity tests performed with the MBBR carrier-attached biomass under aerobic (ATN tests) and anoxic (ATD tests) conditions are shown in **Fig. 3.5**.

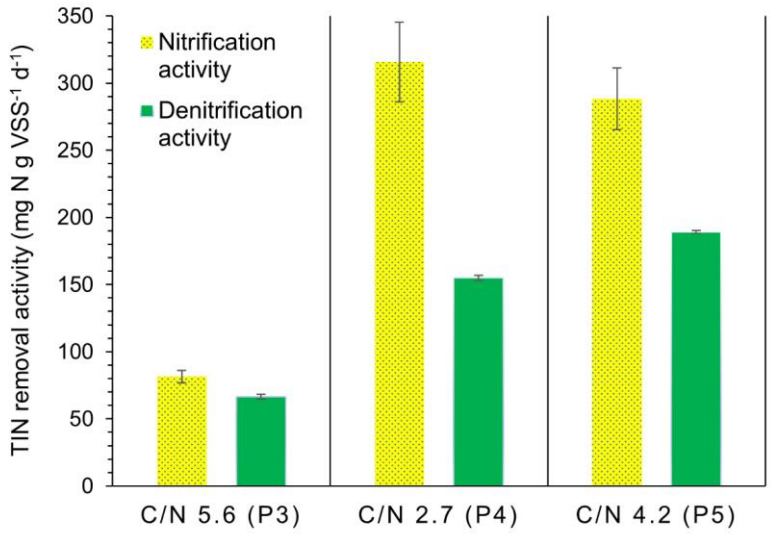

Figure 3.5 - Nitrogen removal activities of the MBBR biofilm at the different feed C/N ratios tested.

The nitrifying and denitrifying activities of the MBBR biofilm at the end of P3 (day 152) were 81 (±5) and 66 (±2) mg N g VSS^{-1} d^{-1}, respectively. MBBR operation at a feed C/N ratio of 2.7 resulted in 3.9 and 2.3 fold higher nitrifying and denitrifying activities, respectively (**Table 3.3**). The activity tests run at the end of the study (P5, day 227)

showed that the nitrifying activity of the MBBR biofilm slightly decreased during reactor operation at a feed C/N ratio of 4.2 compared to that observed at the end of P4 (**Table 3.3**). In contrast, the denitrifying activity of the MBBR biofilm increased by 22%. NO_2^- accumulated up to 3 mg N-NO_2^- L^{-1} during the ATD tests, whereas no NO_2^- accumulation was observed during the ATN tests (**Table 3.3**).

Table 3.3 - Activity test performed with the carrier-attached MBBR biomass under aerobic (ATN) and anaerobic (ATN) conditions.

Period	**Day**	**Feed C/N ratio**	**Biomass concentration (mg carrier^{-1})**	**Experiment**	**TIN removal activity (mg N g VSS^{-1} d^{-1})**	**NO_2^- accumulation (mg N L^{-1})**
P3	152	5.6	2.0	ATN1	82 (±5)	n.d.
				ATD1	66 (±2)	0.5
P4	187	2.7	1.5	ATN2	316 (±30)	n.d.
				ATD2	155 (±2)	3.2
P5	227	4.2	1.7	ATN3	288 (±23)	n.d.
				ATD3	189 (±1)	2.9

n.d. = not detected

3.3.3 Nitrogen prediction

The input variables for the prediction of TIN RE in the mMBBR were evaluated by means of trial-and-error process. The observed and predicted TIN effluent concentrations are plotted in **Fig. 3.6**. A further comparison between MLP and RF performances prediction is represented by relative errors. The relative errors were evaluated as the ratio between the measured and predicted values difference and the measured value [34]. **Fig. 3.6** shows that 70% of the values predicted by RF were affected by an error less than 20% in absolute value (**Fig. 3.6a**), while less than 60% of the values predicted by MLP were affected by an error less than 20% (**Fig. 3.6b**).

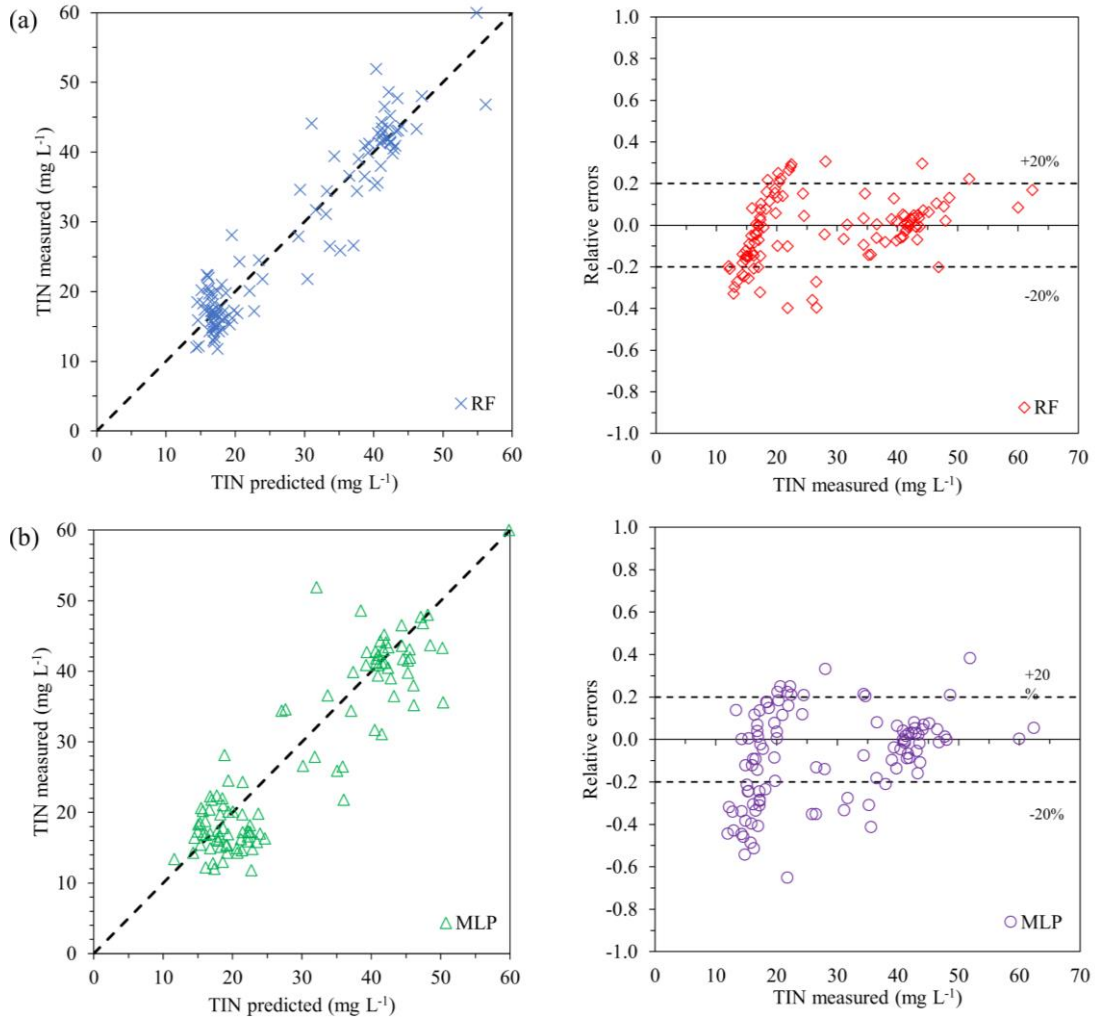

Figure 3.6 - Nitrogen prediction: in the left column, measured versus predicted values, in the right column, relative errors versus measured values.

Positive relative error results in an overestimation of TIN effluent concentrations, while negative error corresponds to an underestimation of predicted values [34]. The

combination of input variables with best prediction performances (R^2, MAE, RMSE and RAE) are shown in **Table 3.4**.

Table 3.4 - Model comparison - summary of the results

Input variables	Measure units	Algorithm	R^2	MAE	RMSE	RAE
HRT	[d]					
DO	[mg/l]	RF	0.90	3.0	4.0	25.7%
COD	[mg/l]	MLP	0.84	4.1	5.4	35.3%
TIN	[mg/l]					

3.4 Discussion

3.4.1 Feasibility of long-term SND in a MBBR under microaerobic conditions

The MBBR exhibited good carbon and nitrogen removal at the microaerobic conditions applied during the study (**Fig. 3.3**), demonstrating the feasibility of long-term SND in a MBBR at DO concentrations as low as 1.0 (±0.2) mg L^{-1}. COD RE during P1-P5 was always above 80% ($F = 2.42$, $DF = 67$, $p > 0.05$) except at the beginning of P3, while lower values were observed during days 10–40 ($F = 15.72$, $DF = 95$, $p < 0.05$). The low COD RE observed during the start-up period can be attributed to the inactivity of the denitrifying bacteria due to the high DO concentrations in the reactor (**Fig. 3.2A**). This is supported by the sudden increase of the COD RE during days 42–44, being concomitant with the decrease in the effluent DO values to approximately 2 mg L^{-1}. The activation of the nitrifying biomass in the start-up phase was demonstrated by the rapid decrease of the NH_4^+ (**Fig. 3.2B**) and alkalinity (**Fig. 3.2D**) concentrations in the effluent. Biological nitrification consumes almost 7.1 mg $CaCO_3$ L^{-1} of alkalinity for each mg of N-NH_4^+ oxidized due to release of H^+ during the process [35]. Supporting nitrification during the initial phase of mMBBR operation is of paramount importance for the SND process. The development of a robust nitrifying layer allows the establishment of an oxygen gradient within the biofilm and favors the activation of the denitrifying bacteria on a deeper layer [36–38]. As a result of bacterial adaptation, NH_4^+ was never detected in the effluent during P1, while significant NO_3^- and NO_2^- fluctuations were observed (**Fig. 3.2B**). Long-term observation during each experimental phase was crucial to ascertain the reactor

response to the applied conditions and for a correct assessment of SND feasibility at the low DO levels tested.

3.4.2 Impact of feed C/N ratio and HRT on SND in the mMBBR

Changes in operational conditions, i.e. HRT and feed C/N ratio, were shown to produce short- and long-term effects on the SND performance of the MBBR. The HRT decrease from 2 days to 1 day severely affected the nitrification activity at the beginning of P2 as NH_4^+ and alkalinity concentrations rapidly increased up to 48.6 mg N-NH_4^+ L^{-1} and 1313 mg $CaCO_3$ L^{-1}, respectively. Despite the gradual recovery of the nitrification process (**Fig. 3.2B**), the effluent NO_2^- concentration during P2 (days 112–121) reached potential inhibitory levels (up to 28.7 mg N-NO_2^- L^{-1}) for the nitrifying biomass [39]. TIN REs (**Fig. 3.3**) observed during periods P1 (HRT = 2 days) and P4 (HRT = 1 day) were statistically different **(**$F = 9.36$, $DF = 31$, $p < 0.05$**)**, despite similar feed C/N ratios **(Table 3.2)**. During P4, NO_2^- levels were constantly higher than those of NO_3^-, while the opposite was observed in P1. The lower HRT in P4 likely favored AOB activity over that of NOB as AOB grow faster than NOB [40]. In this condition, both the nitrification and denitrification are shortened as the NO_2^- produced by AOB is directly reduced to N_2 via the denitrification pathway. Short-cut nitrification denitrification can reduce the operational costs as it consumes less oxygen and results in lower sludge production [41,42].

The effect of three different feed C/N ratios on microaerobic SND was investigated during P3–P5. ANOVA indicated that TIN REs during P3-P5 were statistically different ($F = 7.743$, $DF = 47$, $p < 0.05$). MBBR operation at a feed C/N ratio of 5.6 (±0.5) resulted in a stable COD RE (95 ± 2%) (**Fig. 3.3**), while nitrification was severely inhibited after 16 days as confirmed by the high effluent N-NH_4^+ and alkalinity concentrations (**Fig. 3.2**) and by the low nitrifying (and denitrifying) activity of the carrier-attached MBBR biomass at the end of P3 (**Fig. 3.5**). Nitrification efficiency was limited by the excess growth of HAB as suggested by the high carrier-attached and suspended biomass concentrations (2.0 mg VSS $carrier^{-1}$ and 150 mg L^{-1}, respectively) observed at the end of P3. HAB grow faster than autotrophic nitrifiers and can outcompete them, suppressing nitrification in multiple strata biofilms, especially when the available DO is limited as they compete for O_2 and NH_4^+ [15]. This study shows that long-term SND in a mMBBR was not feasible at a feed C/N ratio as high as 5.6 and an HRT of 1 day.

The drop in the feed C/N ratio from 5.6 (P3) to 2.7 (P4) resulted in an immediate recovery of the nitrification process, as confirmed by the rapid decrease of $N\text{-}NH_4^+$ and alkalinity levels and increase in NO_3^- concentration in the effluent (**Fig. 3.2**). Activity tests revealed that biofilm cultivation in the MBBR at a feed C/N ratio of 2.7 (±0.3) resulted in a higher nitrification activity compared to those observed at the higher C/N ratios tested (**Fig. 3.5**). Denitrifying activity at the end of P4 was 2.3-fold higher than those observed in P3, being sustained by the higher availability of oxidized nitrogen species. Nevertheless, NO_2^- significantly accumulated in the effluent throughout P4 probably due to carbon limitation for denitrifiers, resulting in a 7% lower TIN RE compared to the initial phase of P3. The feed C/N ratio of 4.2 (±0.3) maintained during P5 resulted in lower NO_2^- accumulation and stable TIN REs, being the highest observed in this study (up to 68%) (**Fig. 3.3**). MBBR operation at a feed C/N ratio of 4.2 (±0.3) increased the activity of denitrifying bacteria compared to P4, while nitrifying activity slightly decreased (**Fig. 3.5**). COD levels in the effluent were higher than those observed during P3 and P4 likely due to the decrease in the population of attached- and suspended-growth HAB during previous low-carbon operation. Despite the increase of COD REs to 97 (±1) % at the end of P5 (days 220–227), the mMBBR maintained stable TIN RE until the end of the study (**Fig. 3.3**).

3.4.3 Possible pathways for phosphorus removal under microaerobic conditions

During periods P1–P5, between 8 and 10 mg $P\text{-}PO_4^{3-}$ L^{-1} (on average) was removed from the system, resulting in similar $P\text{-}PO_4^{3-}$ REs ($F = 2.35$, $DF = 78$, $p > 0.05$) (**Fig. 4**). According to Visual MINTEQ prediction, maximum 3 mg PO_4^{3-} L^{-1} could precipitate in the MBBR at all operational periods. As a result, biological phosphorus removal accounted for at least 85% of the $P\text{-}PO_4^{3-}$ removed from the MBBR during the study. Phosphorus requirement for bacterial synthesis can be estimated considering a required COD:P mass ratio for bacterial growth ranging between 100 and 500 [43]. Based on these values, between 2% and 23% of the phosphorous biologically removed from the MBBR could be used for biomass growth. This means that a significant biological P uptake occurred due to a different mechanism.

Enhanced biological phosphorus removal (EBPR) is commonly achieved through an alternation of anaerobic and aerobic (or anoxic) stages to allow a net phosphorus uptake by phosphorous accumulating organisms (PAO) [44]. Anaerobic, anoxic and aerobic layers can coexist in the biofilm structure if oxygen and NO_3^- only penetrate to a certain

depth [36]. However, in this study the DO concentration was maintained at 1.0 (±0.2) mg L^{-1} and alternation of anaerobic and aerobic (or anoxic) stages in the biofilm did not occur. Besides PAO metabolism, polyphosphate synthesis can occur under anoxic/aerobic conditions without the need of an anaerobic phase, being a widespread mechanism among denitrifiers [45]. Denitrifying P-accumulating bacteria (DPB), e.g. some members of the genus *Paracoccus*, are capable of polyphosphate accumulation beyond metabolic needs by using O_2 and/or NO_3^- as the electron acceptors and acetate as external carbon source [46,47]. All these components were present in the MBBR and microaerobic operation guaranteed both aerobic and anoxic zones in the biofilm. Moreover, the highest P-PO_4^{3-} RE (66 ± 4%) was concomitant with the highest denitrifying activity (**Table 3**) by the mMBBR biofilm during P5. As a result, biological P-PO_4^{3-} removal in the mMBBR was likely driven by denitrifying bacteria, resulting in a substantial withdrawal of phosphorus during the entire operation.

3.4.4 Random Forest and Multilayer Perceptron modeling

A trial and error method was used to identify the most influential input parameters, i.e. HRT, DO, COD and TIN (**Table 3.4**). According to the evolution of TIN removal trough the SND process, the change of these input parameters could have a significant impact on the bioreactor performances [17,23,35]. RF algorithm showed the best accuracy (R^2 = 0.90, MAE = 3.02, RMSE=4.0, RAE = 25.7%) (**Fig. 3.6a**), while the higher R^2 value obtained with RF algorithm compared with MLP (i.e. 0.84) confirmed a highly accuracy in predicting the experimental data (**Table 3.4**) [21]. It is interesting to note that MLP showed a tendency to underestimate actual TIN concentrations in the effluent, resulting in the prediction of higher TIN REs **(Fig. 3.6b**).

3.4.5 Practical implications and future perspectives

The results of this study allow to identify which C/N ratio is more suitable to support long-term SND in a single-stage continuous-flow MBBR under microaerobic conditions. C/N ratios higher than 4.2 may result in excess growth of HAB and reduce the efficiency of both nitrification and denitrification processes. Based on the obtained nutrient removal efficiency, microaerobic MBBR operation would be a suitable and convenient choice for the treatment of medium- and low-strength wastewater from small communities or to be discharged in non-sensitive areas where less stringent standards are applied. However, further studies should investigate the P removal performance of the mMBBR treating real wastewater, as the presence of slow-biodegradable and recalcitrant organic matter may significantly affect the process efficiency [48].

Performing SND in a continuous-flow MBBR at DO levels as low as 1 mg L^{-1} would considerably reduce the aeration costs and CO_2 emissions of the plant. Additionally, the use of MBBR results in lower reactor volumes and eliminates the sludge recycle typical of CAS systems, resulting in a further decrease of investment and operational costs. Microaerobic SND in suspended-growth systems has been shown to produce a conspicuous amount of N_2O, being higher than that observed during the conventional nitrification and denitrification processes [49]. The same might apply to biofilm systems performing SND, with the N_2O being produced by denitrifying bacteria [50]. In this case, controlling of COD oxidation and biofilm thickness might help scavenging N_2O [37]. Further research should assess whether continuous-flow mMBBR operation can attenuate N_2O emissions and investigate the effect of operational conditions, e.g. C/N ratio, HRT, DO concentration and aeration strategy, on N_2O production.

In full scale application, WWTPs could be controlled by online monitoring, using programmable sensors integrated with artificial intelligence that can suggest appropriate changes in operating conditions when poor N removal occurs. It should be noted that the measured data were collected within a very short period (10 months). A large dataset is recommended for a recalibration and revalidation of the models proposed.

3.5 Conclusion

Long-term and stable mMBBR operation was feasible at feed C/N ratio 4.2. Lower nitrogen REs occurred at feed C/N ratio 2.7, whereas feed C/N ratio 5.6 led to uncontrolled growth of HAB and unstable performance. Biomass cultivation at feed C/N ratios 2.7 and 4.2 resulted in the highest nitrifying and denitrifying activities, respectively. Phosphorous removal significantly occurred in the mMBBR and can be attributed to phosphorous accumulation by DPB growing on acetate. The use of mMBBR is recommended in MWWTPs serving small communities and treating low- and medium-strength wastewaters, as it results in lower costs compared to CAS.

3.6 Acknowledgements

This study was supported by Programma di Sviluppo Rurale (PSR) Campania 2014/2020 - METAGRO Project and Programma Operativo Nazionale (PON) 2014/2020 – BIOFEEDSTOCK Project.

3.7 References

[1] EEA, EEA signals 2018 - Water is life, Copenhagen, Denmark, 2018.

[2] P.J.T.M. van Puijenbroek, A.H.W. Beusen, A.F. Bouwman, Global nitrogen and phosphorus in urban waste water based on the Shared Socio-economic pathways, *J. Environ. Manage.* 231 (2019) 446–456.

[3] F. Di Capua, F. Pirozzi, P.N.L. Lens, G. Esposito, Electron donors for autotrophic denitrification, *Chem. Eng. J.* 362 (2019) 922–937.

[4] B.E. Rittmann, P.L. McCarty, Environmental biotechnology: principles and applications, McGraw Hill Education, 2012.

[5] J.L. Nielsen, P.H. Nielsen, Microbial nitrate-dependent oxidation of ferrous iron in activated sludge, *Environ. Sci. Technol.* 32 (1998) 3556–3561.

[6] Y.Z. Li, Y.L. He, D.G. Ohandja, J. Ji, J.F. Li, T. Zhou, Simultaneous nitrification–denitrification achieved by an innovative internal-loop airlift MBR: comparative study, *Bioresour. Technol.* 99 (2008) 5867–5872.

[7] R.L. Meyer, R.J. Zeng, V. Giugliano, L.L. Blackall, Challenges for simultaneous nitrification, denitrification, and phosphorus removal in microbial aggregates: mass transfer limitation and nitrous oxide production, *FEMS Microbiol. Ecol.* 52 (2005) 329–338.

[8] F. Di Capua, I. Milone, A.-M. Lakaniemi, E.D.V. Hullebusch, P.N.L. Lens, G. Esposito, Effects of different nickel species on autotrophic denitrification driven by thiosulfate in batch tests and a fluidized-bed reactor, *Bioresour. Technol.* 238 (2017) 534–541.

[9] R. Khanongnuch, F. Di Capua, A.-M. Lakaniemi, E.R. Rene, P.N.L. Lens, Effect of N/S ratio on anoxic thiosulfate oxidation in a fluidized bed reactor: experimental and artificial neural network model analysis, *Process Biochem.* 68 (2018) 171–181.

[10] R. Khanongnuch, F. Di Capua, A.-M. Lakaniemi, E.R. Rene, P.N.L. Lens, H_2S removal and microbial community composition in an anoxic biotrickling filter under autotrophic and mixotrophic conditions, *J. Hazard. Mater.* 367 (2019) 397–406.

[11] F. Di Capua, S. Papirio, P.N.L. Lens, G. Esposito, Chemolithotrophic denitrification in biofilm reactors, *Chem. Eng. J.* 280 (2015) 643–657.

[12] R. Khanongnuch, F. Di Capua, A.M. Lakaniemi, E.R. Rene, P.N.L. Lens, Long-term performance evaluation of an anoxic sulfur oxidizing moving bed biofilm reactor under nitrate limited conditions, *Environ. Sci. Water Res. Technol.* 5 (2019) 1072–1081.

[13] C. Suarez, M. Piculell, O. Modin, S. Langenheder, F. Persson, M. Hermansson, Thickness determines microbial community structure and function in nitrifying biofilms via deterministic assembly, *Sci. Rep.* 9 (2019) 5110.

[14] P. Zhang, Z. Qi, Simultaneous nitrification and denitrification in activated sludge system under low oxygen concentration, *Front. Environ. Sci. Eng. China.* 1 (2007) 49–52.

[15] S. Zhu, S. Chen, Effects of organic carbon on nitrification rate in fixed film biofilters, *Aquac. Eng.* 25 (2001) 1–11.

[16] B. Fu, X. Liao, L. Ding, H. Ren, Characterization of microbial community in an aerobic moving bed biofilm reactor applied for simultaneous nitrification and denitrification, *Process Biochem.* (2010) 1981–1990.

[17] Y.Q. Gu, T.T. Li, H.Q. Li, Biofilm formation monitored by confocal laser scanning microscopy during startup of MBBR operated under different intermittent aeration modes, *Process Biochem.* 74 (2018) 132–140.

[18] H. Guo, K. Jeong, J. Lim, J. Jo, Y.M. Kim, J. Park, J.H. Kim, K.H. Cho, Prediction of effluent concentration in a wastewater treatment plant using machine learning models, *J. Environ. Sci.* 32 (2015) 90–101.

[19] E.R. Rene, M. Estefanı, M. Veiga, C. Kennes, Neural network models for biological waste-gas treatment systems, *N. Biotechnol.* 29 (2011) 56–73..

[20] M. Asadi, H. Guo, K. Mcphedran, Biogas production estimation using data-driven approaches for cold region municipal wastewater anaerobic digestion, *J. Environ. Manage.* 253 (2020) 109708.

[21] F. Granata, R. Gargano, G. De Marinis, Artificial intelligence based approaches to evaluate actual evapotranspiration in wetlands, *Sci. Total Environ*. 703 (2019) 135653..

[22] B. Fu, X. Liao, L. Ding, H. Ren, Characterization of microbial community in an aerobic moving bed biofilm reactor applied for simultaneous nitrification and denitrification, *World J. Microbiol. Biotechnol.* 26 (2010) 1981–1990.

[23] A.A.L. Zinatizadeh, E. Ghaytooli, Simultaneous nitrogen and carbon removal from wastewater at different operating conditions in a moving bed biofilm reactor (MBBR): process modeling and optimization, *J. Taiwan Inst. Chem. Eng.* 53 (2015) 98–111.

[24] X. Zhang, X. Chen, C. Zhang, H. Wen, W. Guo, H.H. Ngo, Effect of filling fraction on the performance of sponge-based moving bed biofilm reactor, *Bioresour. Technol*. 219 (2016) 762–767.

[25] H. Helness, H. Ødegaard, Biological phosphorus removal in a sequencing batch moving bed biofilm reactor, *Water Sci. Technol.* 40 (1999) 161–168.

[26] B. Vallet, M.A. Labelle, L. Rieger, S. Bigras, S. Parent, P. Juteau, R. Villemur, Y. Comeau, Inhibition of biological phosphorus removal in a sequencing moving bed biofilm reactor in seawater, *Water Sci. Technol.* 59 (2009) 1101–1110.

[27] R. Ferrentino, A. Ferraro, M.R. Mattei, G. Esposito, G. Andreottola, Process performance optimization and mathematical modelling of a SBR-MBBR treatment at low oxygen concentration, *Process Biochem.* 75 (2018) 230–239.

[28] J.H. Moreno Osorio, V. Luongo, A. Del Mondo, G. Pinto, A. Pollio, L. Frunzo, P.N.L. Lens, G. Esposito, Nutrient removal from high strength nitrate containing industrial wastewater using *Chlorella sp.* strain *ACUF_802*, *Ann. Microbiol.* 68 (2018) 899–913.

[29] APAT ISRA-CNR, Analytical Methods for Water, Agenzia per la protezione dell'ambiente e per i servizi tecnici (APAT) Istituto di Ricerca sulle Acque - Consiglio Nazionale delle Ricerche (ISRA-CNR), 2003.

[30] APHA, Standard Methods for the Examination of Water and Wastewater, 2005.

[31] F. Di Capua, S.H. Ahoranta, S. Papirio, P.N.L. Lens, G. Esposito, Impacts of sulfur source and temperature on sulfur-driven denitrification by pure and mixed cultures of *Thiobacillus*, *Process Biochem*. 51 (2016) 1576–1584.

[32] F. Granata, S. Papirio, G. Esposito, R. Gargano, G. De Marinis, Machine learning algorithms for the forecasting of wastewater quality indicators, (2017) 1–12.

[33] H.R. Maier, G.C. Dandt, Neural network based modelling of environmental variables: a systematic approach, *Math. Comput. Model.* 33 (2001) 669–682.

[34] F. Di Nunno, F. Granata, Groundwater level prediction in Apulia region (Southern Italy) using NARX neural network, *Environ. Res.* 190 (2020) 110062.

[35] C.Z. Correa, K.V.M.C. Prates, E.F. de Oliveira, D.D. Lopes, A.C. Barana, Nitrification/denitrification of real municipal wastewater in an intermittently aerated structured bed reactor, *J. Water Process Eng.* 23 (2018) 134–141.

[36] F. Sabba, C. Picioreanu, R. Nerenberg, Mechanisms of nitrous oxide (N_2O) formation and reduction in denitrifying biofilms, *Biotechnol. Bioeng.* 114 (2017) 2753–2761.

[37] F. Sabba, A. Terada, G. Wells, B.F. Smets, R. Nerenberg, Nitrous oxide emissions from biofilm processes for wastewater treatment, *Appl. Microbiol. Biotechnol.* 102 (2018) 9815–9829.

[38] M. Seifi, M.H. Fazaelipoor, Modeling simultaneous nitrification and denitrification (SND) in a fluidized bed biofilm reactor, *Appl. Math. Model.* 36 (2012) 5603–5613.

[39] L.Y. Stein, D.J. Arp, Loss of ammonia monooxygenase activity in *Nitrosomonas europaea* upon exposure to nitrite, *Appl. Environ. Microbiol.* 64 (1998) 4098–4102.

[40] F. Fang, B.J. Ni, X.Y. Li, G.P. Sheng, H.Q. Yu, Kinetic analysis on the two-step processes of AOB and NOB in aerobic nitrifying granules, *Appl. Microbiol. Biotechnol.* 83 (2009) 1159–1169.

[41] F. Jaramillo, M. Orchard, C. Muñoz, M. Zamorano, C. Antileo, Advanced strategies to improve nitrification process in sequencing batch reactors - a review, *J. Environ. Manage*. 218 (2018) 154–164.

[42] M. Capodici, S.F. Corsino, M. Torregrossa, G. Viviani, Shortcut nitrification-denitrification by means of autochthonous halophilic biomass in an SBR treating fish-canning wastewater, *J. Environ. Manage.* 208 (2018) 142–148.

[43] L.J. Thompson, V. Gray, D. Lindsay, A. Von Holy, Carbon:nitrogen:phosphorus ratios influence biofilm formation by *Enterobacter cloacae* and *Citrobacter freundii*, *J. Appl. Microbiol.* 101 (2006) 1105–1113.

[44] S. Salehi, K.Y. Cheng, A. Heitz, M.P. Ginige, Simultaneous nitrification, denitrification and phosphorus recovery (SNDPr) - an opportunity to facilitate full-scale recovery of phosphorus from municipal wastewater, *J. Environ. Manage.* 238 (2019) 41–48.

[45] H.P. Shi, C.M. Lee, Combining anoxic denitrifying ability with aerobic-anoxic phosphorus-removal examinations to screen denitrifying phosphorus-removing bacteria, *Int. Biodeterior. Biodegrad.* 57 (2006) 121–128.

[46] Y. Barak, J. Van Rijn, Atypical polyphosphate accumulation by the denitrifying bacterium *Paracoccus* denitrificans, *Appl. Environ. Microbiol.* 66 (2000) 1209–1212.

[47] H.W. Lee, Y.K. Park, Characterizations of denitrifying polyphosphate-accumulating bacterium *Paracoccus sp.* strain *YKP-9*, *J. Microbiol. Biotechnol.* 18 (2008) 1958–1965.

[48] J. Drewnowski, J. Makinia, The role of colloidal and particulate organic compounds in denitrification and EBPR occurring in a full-scale activated sludge system, *Water Sci. Technol.* 11 (2011) 1973–1988.

[49] Y. Yan, S. Liang, H.H. Ngo, W. Guo, W. Jia, J. Zhang, Y. Zou, Nitrous oxide emission in low-oxygen simultaneous nitrification and denitrification process: Sources and mechanisms, *Bioresour. Technol.* 136 (2013) 444–451.

[50] G. Mannina, M. Capodici, A. Cosenza, D. Di Trapani, V. Armando, H. Ødegaard, Nitrous oxide from moving bed based integrated fixedfilm activated sludge membrane bioreactors, *J. Environ. Manage.* 187 (2017) 96–102.

CHAPTER 4.

Simultaneous nitrification, denitrification and phosphorus removal in a continuous-flow moving bed biofilm reactor alternating microaerobic and aerobic conditions

This Chapter has been published as:

Iannacone, F., Di Capua, F., Granata, F., Gargano, R., Esposito, G., 2020. Simultaneous nitrification, denitrification and phosphorus removal in a continuous-flow moving bed biofilm reactor alternating microaerobic and aerobic conditions. *Bioresour. Technol.* 123453

Abstract

A continuous-flow intermittent aeration moving bed biofilm reactor (IAMBBR) alternating microaerobic and aerobic conditions was used to remove carbon, nitrogen and phosphorus through simultaneous nitrification and denitrification coupled to phosphorus removal (SNDPR). The IAMBBR was operated under different dissolved oxygen (DO) ranges (0.2–2, 0.2–3 and 0.2–4 mg L^{-1}) and feed C/N ratios (2.8, 3.6 and 4.2) at HRT of 1 day. At a DO range of 0.2–3 mg L^{-1} and feed C/N ratio of 3.6, the IAMBBR achieved simultaneous removal of dissolved organic carbon (DOC), total inorganic nitrogen (TIN) and P-PO43- with average efficiencies of 100%, 62% and 75%, respectively. Illumina sequencing revealed the coexistence of nitrifiers and denitrifiers with P-accumulating ability (*Hydrogenophaga* and *Dokdonella*) in the IAMBBR biofilm. Batch activity tests showed that phosphorus uptake did not occur under stable anaerobic or anoxic conditions, nor under aerobic conditions in absence of nitrate.

Keywords

Intermittent aeration; MBBR; microaerobic-aerobic cycle; phosphorus removal; simultaneous nitrification denitrification.

Graphical abstract

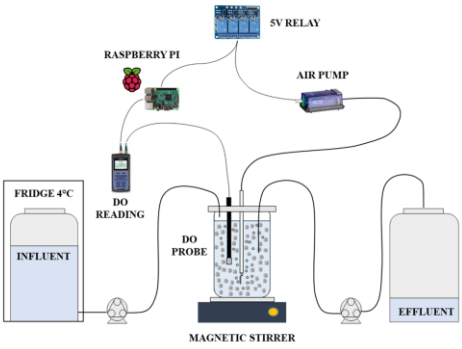

Intermittent aeration moving bed biofilm reactor (IAMBBR)

- Simultaneous nitrification denitrification and phosphorous removal (SNDPR) was studied in a continuous-flow IAMBBR.
- DOC and TIN removals were 100% and 62% at feed C/N 3.6 and DO range 0.2 – 3 mg L^{-1}.
- The microaerobic-aerobic cycle determined a P-PO_4^{3-} removal up to 81%.
- Nitrifiers and P-accumulating denitrifiers coexisted in the MBBR biofilm.
- *Hydrogenophaga* and *Dokdonella* could carry out P removal under aerobic conditions.

4.

4.1 Introduction

Due to environmental problems connected with nutrient discharge in aquatic environments and phosphorus resource depletion, nitrogen removal and phosphorus recovery from municipal wastewater have become nowadays key challenges [1,2]. Municipal wastewater commonly features low C/N ratios which limit denitrification efficiency [3]. Phosphorus concentration is typically in the range of 6–8 mg L^{-1}, although concentrations exceeding 10 mg L^{-1} are often observed at the treatment sites [4,5].

The removal of nitrogenous compounds in municipal wastewater treatment plants (MWWTPs) is conventionally carried out by separate nitrification and denitrification processes. Nitrification is carried out by ammonia oxidizing bacteria (AOB) and nitrite oxidizing bacteria (NOB) able to convert ammonia (NH_4^+) to nitrate (NO_3^-) and results in alkalinity consumption (7.1 g $CaCO_3$ are consumed for each g N-NH_4^+ oxidized) [6]. NO_3^- is reduced to dinitrogen gas (N_2) under anoxic conditions by heterotrophic denitrifying bacteria (DNB) producing alkalinity. Phosphorus removal can be achieved by means of physical, chemical or biological methods [7]. Physical methods, including ion exchange and osmosis, are often inefficient and expensive [8]. Chemical phosphorus removal can be accomplished by precipitation and adsorption. Precipitation involves the use of metal (Fe, Al and Ca) salts and results in the production of chemical-rich sludge that may limit its biological conversion to biogas [1,7]. Adsorption is rarely used in MWWTPs due to the high costs of the adsorbent and regeneration process [9].

Enhanced biological phosphorus removal (EPBR) is conventionally achieved by enriching polyphosphate (poly-P) accumulating organism (PAOs), able to store more phosphorus than that needed for growth when exposed to alternating anaerobic and aerobic/anoxic conditions [10]. Under anaerobic conditions, PAOs store soluble organic carbon (e.g. acetate) as poly-β-hydroxybutyrate (PHB), poly-β-hydroxyvalerate (PHV) or poly- hydroxyalkanoate (PHA) and phosphorus is released as soluble poly-P to produce the energy required for PHB/PHV/PHA storage [11]. During the aerobic phase, the stored organic carbon is oxidized to produce energy for growth and phosphorus uptake. Denitrifying PAOs (DNPAOs) are capable of using nitrate as electron acceptor instead of oxygen, coupling denitrification to phosphorus accumulation under the alternation of anaerobic and anoxic conditions [12]. EBPR is commonly carried out in multistage systems combining anaerobic, anoxic and aerobic stages through sludge and liquor recycling. This results in complex operation, large space requirement and investment and operational costs hardly sustainable by small MWWTPs [7]. Jena et al. [13] showed that the combined removal of COD (72%), NO_3^- (98%) and PO_4^{3-} (86%) could be achieved in an aerobic-anoxic sequencing batch reactor (SBR) without an anaerobic phase. In the aerobic-anoxic cycle, phosphorus accumulation is carried out by DNPAOs during the anoxic phase by coupling poly-P uptake to complete nitrate reduction via direct acetate oxidation. In contrast, the absence of a suitable electron acceptor for DNPAOs during the aerobic phase induces a metabolic stress promoting phosphorous release. Nevertheless, the aerobic phase provides an essential fasting condition to sustain the dominance of DNPAOs over heterotrophic DNB, being DNPAOs able to use the internal phosphorous storage to supply the energy required for cell maintenance [13]. In an earlier study, Satoh

et al. [14] demonstrated that applying a microaerobic/aerobic cycle in SBR was effective for the enrichment of PHA-accumulating microorganisms. The microaerobic/aerobic cycle is a modification of the conventional anaerobic-aerobic/anoxic process in which anaerobic conditions are replaced by a microaerobic phase.

SBRs have been widely used for the simultaneous removal of nitrogen and phosphorus as they easily allow to establish and alternate anaerobic and aerobic/anoxic conditions [10,15–17]. Although satisfactory phosphorus removal can be achieved with SBRs, batch systems are mainly used to treat industrial wastewaters being discontinuously produced during industrial processing. Additionally, SBR application in MWWTPs requires a large number of treatment, timing and control units as well as a higher level of maintenance compared to conventional systems [18,19]. This may result in unbearable capital and operational costs for wastewater treatment in small communities and rural areas.

The moving bed biofilm reactor (MBBR) represents a compact and cost-effective solution for municipal wastewater treatment and has been recently proposed as a valid continuous-flow alternative to the SBR for the combined removal of carbon, nitrogen and phosphorus [20,21]. The MBBR technology is also a valuable option for small decentralized facilities due to compact footprint and high-performance in carbon and nitrogen removal [22]. The formation of a stratified biofilm on the moving supports enables the simultaneous removal of carbon and nutrients, while the high biomass concentration in the reactor basin allows to reduce the plant footprint. In a recent work, Iannacone et al. [21] showed that a simultaneous removal of COD, total inorganic nitrogen (TIN) and $P\text{-}PO_4^{3-}$ up to 100%, 68% and 72%, respectively, could be obtained in a continuous-flow MBBR under stable microaerobic conditions. Changes in dissolved oxygen (DO) regime may improve the MBBR performance by providing more suitable conditions for the different microbial groups composing the biofilm. Up to date, the alternation of microaerobic and aerobic conditions for the simultaneous removal of carbon, nitrogen and phosphorus in continuous-flow bioreactors has not been applied yet and deserves investigation.

In this work, a continuous-flow intermittent-aeration MBBR (IAMBBR) was operated for 173 days under microaerobic-aerobic conditions. The main objectives of the study were to: (1) determine the IAMBBR performance in terms of TIN, $P\text{-}PO_4^{3-}$ and dissolved organic carbon (DOC) removal efficiency (RE) under different DO regimes; (2) evaluate the influence of the feed C/N ratio on IAMBBR performance; (3) investigate the dominant bacteria responsible for carbon, nitrogen and phosphorus removal at the different DO regimes tested; (4) evaluate the metabolic activities of the IAMBBR biofilm under anaerobic, anoxic and aerobic conditions.

4.2 Materials and methods

4.2.1 Cultivation of denitrifying and nitrifying biomass

Activated sludge (3.3 g TS L^{-1}, 2.5 g VS L^{-1}) was collected from the pre-denitrification system of a local MWWTP (Cassino, Italy) and used as microbial source for cultivating denitrifying and nitrifying bacteria. Denitrifying biomass was cultivated in fed-batch mode in a glass vessel sealed with a plastic plug (D1). The bioreactor was filled up to 1.8 L with cultivation medium, inoculum (200 mL) and Kaldness K1 carriers (Veolia, France) at 50 % filling ratio. The cultivation medium was composed of distilled water, 0.469 g L^{-1} of potassium nitrate (KNO_3), 0.798 g L^{-1} of sodium acetate trihydrate ($CH_3COONa \cdot 3H_2O$) and nutrients as follows (mg L^{-1}): $MgCl_2 \cdot 6H_2O$ (150), KH_2PO_4 (50), $CaCl_2 \cdot H_2O$ (20), $MnCl_2 \cdot 6H_2O$ (1.75), $Na_2MoO_4 \cdot 2H_2O$ (0.1), $CoCl_2$ (0.05). A feed COD/N ratio > 5.0 was chosen to sustain the denitrification process [23]. Mixing was provided by a magnetic stirrer at 120 rpm. NO_3^-, NO_2^-, and COD concentrations were monitored daily and half of the reactor solution was replaced with fresh medium as soon as the fed COD or N-NO_3^- was consumed. The bioreactor was purged with N_2 for 15 min after inoculation and each medium refresh to ensure anoxic conditions. Cultivation of denitrifying biomass was carried out for 100 days until denitrifying activity and biofilm growth in the bioreactor were verified.

Nitrifying biomass was cultivated in a glass bioreactor (N1) filled with 400 mL of cultivation medium and 100 mL of inoculum. The cultivation medium was composed of distilled water, 0.246 g L^{-1} of NH_4Cl, 1 g L^{-1} of $NaHCO_3$ and nutrients as described in **Section 4.2.1**. Half of the bioreactor solution was replaced with fresh medium as soon as the fed NH_4^+ was consumed. DO concentration in the medium was maintained above 5 mg L^{-1} by means of an aeration pump and a porous stone. Mixing was provided by a magnetic stirrer at 70 rpm. The bioreactor was operated for almost 100 days and NO_3^-, NO_2^- and NH_4^+ concentrations were measured daily to assess the nitrifying activity

4.2.2 Experimental set-up

The IAMBBR used in this study was a laboratory-scale (2 L) glass vessel sealed by a plexiglass lid with six openings for influent and effluent tubes, DO probe, air injection, liquid sampling and gas outlet. A peristaltic pump (Watson-Marlow, UK) was used for influent feeding and effluent suction. Mixing conditions were provided using a magnetic stirrer at 110 rpm. Air was delivered to the IAMBBR at a flow rate of 0.9 L min^{-1} using an aquarium air pump and solubilized into the reactor medium through a porous stone.

DO was continuously monitored using a FDO 925 optical probe (WTW, Germany) connected to an OXI 3410 portable meter (WTW, Germany). A Raspberry PI 3 Model B+ single-board computer (Raspberry Pi Foundation, UK) coupled with Python software 3.0 (Python Software Foundation, USA) was used to control and automate aeration in the reactor. The portable DO meter was connected via USB port to the Raspberry PI, which was programmed to switch on and off a 5V relay connected to the air pump at selected DO values.

4.2.3 Bioreactor start-up and influent composition

The start-up of the IAMBBR was carried out by transferring all carriers from D1, 250 mL of nitrifying biomass from N1 and synthetic municipal wastewater in the reactor vessel up to 1.5 L. Synthetic wastewater (pH 8.0 ± 0.1) was used in order to select for different feed C/N ratios to test during the study and was prepared using tap water, 0.552–1.064 g L^{-1} of $CH_3COONa \cdot 3H_2O$, 0.246 g L^{-1} of NH_4Cl, 1 g L^{-1} of $NaHCO_3$ and nutrients as described in **Section 4.2.1**. KNO_3 (1 g L^{-1}) was added only during the start-up period (**Table 4.1**) to sustain the denitrification process. During the study, the synthetic wastewater was maintained in the fridge at 4°C.

The IAMBBR was operated for 1 week in batch mode. Half of the solution was replaced with fresh synthetic wastewater as soon as DOC or NH_4^+ was consumed. The DO concentration was not controlled in this phase and ranged between 0.5 and 3 mg L^{-1}. Subsequently, the IAMBBR was operated in continuous mode at a 2-day HRT for 35 days to allow the establishment of a multilayer microbial biofilm on the carriers (Start-up, **Table 4.1**). The DO concentration was controlled by the Raspberry platform and maintained between 0.2 and 2 mg L^{-1}.

Table 4.1 - Experimental conditions and feed composition during IAMBBR operation.

Experimental period	**Time (day)**	**HRT (day)**	**DO range (mg L^{-1})**	**C/N ratio**	**DOC (mg L^{-1})**	**N-NH_4^+ (mg L^{-1})**	**TIN (mg L^{-1})**	**Alkalinity (mg $CaCO_3$ L^{-1})**	**TP (mg L^{-1})**
Start-up	0–35	2	0.2–2	2.0 (±0.1)	134 (±17)	33 (±2)	66 (±5)	942 (±102)	11 (±1)
P1	36–49	1	0.2–2	4.2 (±0.3)	131 (±17)	33 (±1)	33 (±1)	985 (±133)	11 (±1)
P2	50–66	1	0.2–2	2.8 (±0.5)	94 (±4)	34 (±1)	34 (±1)	1064 (±32)	10 (±1)
P3	67–91	1	0.2–3	2.9 (±0.3)	96 (±8)	33 (±1)	33 (±1)	1035 (±37)	11 (±1)
P4	92–109	1	0.2–4	2.8 (±0.1)	94 (±1)	33 (±1)	33 (±1)	931 (±158)	10 (±1)
P5	110–122	1	0.2–3	2.8 (±0.1)	94 (±3)	33 (±1)	33 (±1)	1036 (±46)	10 (±1)
P6	123–173	1	0.2–3	3.6 (±0.4)	116(±10)	33 (±0)	33 (±0)	1050 (±36)	10 (±1)

4.2.4 IAMBBR operation

The IAMBBR was operated at a HRT of 1 day under 6 different experimental periods (**Table 1**). During P1 (days 36–49), the DO range was maintained at 0.2–2 mg L^{-1}, while a feed C/N ratio of 4.2 was chosen being the optimal value observed in a previous study for sustaining SNDPR under microaerobic conditions (Iannacone et al., 2019). At the beginning of P2 (days 50–66), the feed C/N ratio was decreased from 4.2 to 2.8 by reducing the influent DOC concentration from 131 (±17) to 94 (±4) mg L^{-1}, as overgrowth of suspended biomass was disturbing the DO monitoring. During P3-P5 (days 67–122), the DO range was maintained at 0.2–3 mg L^{-1} (P3 and P5) and 0.2–4 mg L^{-1} (P4), while the influent concentrations were not changed. At the beginning of P6 (day 123), the influent DOC concentration was increased from 94 (±12) mg L^{-1} (P2–P5) to 116 (±10) mg L^{-1} (resulting in a feed C/N ratio of 3.6) to study the effect of DOC concentration on phosphorus removal. The average duration of each cycle during P3–P6 ranged between 65 and 90 min, almost equally divided between aerobic and microaerobic conditions. During P1-P6, the feed pH and alkalinity concentration were stable at 7.9 (±0.1) and 1052 (±40) mg $CaCO_3$ L^{-1}, respectively.

4.2.5 Batch activity tests

Batch activity tests were conducted at the end of P6 to evaluate the nitrifying, denitrifying and P-PO_4^{3-} removal activities of the IAMBBR biofilm under stable aerobic (ATN tests), anoxic (ATD tests) and anaerobic (ATDC tests) conditions. All batch tests were performed in duplicate for 24 h at 22 (±2) °C. The medium solution for all bioassays was composed of 244 mg DOC L^{-1} as $CH_3COONa{\cdot}3H_2O$, 32.5 mg N-NH_4^+ L^{-1} as NH_4Cl, 1 g $NaHCO_3$ L^{-1} and nutrients as for the IAMBBR operation. NO_3^- (100 mg L^{-1}) was added only to ATD flasks. DOC concentration was doubled compared to that of the IAMBBR influent in P6 to ensure DOC availability to denitrifying bacteria during the entire tests.

ATD and ATDC tests were conducted in 100 mL glass serum flasks with a working volume of 50 mL. The flasks were purged with N_2 for 5 min and sealed with rubber septa and aluminum crimps to ensure anoxic conditions. ATN tests were conducted using 70 mL wide neck conical flasks with a working volume of 50 mL. All flasks were inoculated with 10 biofilm-coatd K1 carriers collected from the IAMBBR and rinsed with ultrapure water prior to inoculation. Afterwards, flasks were placed on a horizontal shaker at a speed of 150 rpm. This speed allowed to maintain a DO concentration of 2.5 (±0.5) mg L^{-1} in the ATN flasks during the experiment. Samples

were collected 12 times to measure the concentrations of NH_4^+, NO_3^-, NO_2^-, PO_4^{3-} and DOC in the flasks.

4.2.6 Microbial community analysis

Microbial community analysis was performed on carrier-attached biomass collected from the IAMBBR at the end of each experimental period except P1. DNA extraction was carried out by using a Quick-DNA Fungal/Bacterial Kit (Zymo Research, USA). Final yield and quality of the extracted DNA were determined by using a Qubit 1.0 fluorometer with a dsDNA HS Assay Kit (Invitrogen, USA). PCR amplification, library quantification, Illumina sequencing, sequence filtering and taxonomic classification were performed as described by Ucar et al. [24].

4.2.7 Sample collection and analysis

Liquid samples were collected daily (weekends and holidays excepted) from the IAMBBR at the end of both the aerobic and microaerobic phases of a single cycle and from the influent tank. Gas samples were collected periodically from the IAMBBR by connecting a 1 L gas bag to the gas outlet until it was filled. At the end of each experimental period, K1 carriers and suspended biomass were collected for volatile suspended solid (VSS) analyses. COD, pH, alkalinity and the concentrations of NO_3^-, NO_2^- and PO_4^{3-} in liquid samples were analyzed as described by Iannacone et al. (2019). DOC concentration was measured using a TOC L CSH/CSN analyzer (Shimadzu, Japan). Samples were filtered through 0.45 μm syringe filters (VWR, USA) prior to IC and DOC analyses. N_2O in the gas phase was measured using a Varian Star 3400 gas chromatograph equipped with a ShinCarbon ST 80/100 column and an electron capture detector. VSS concentration was analyzed according to Classen et al. (2013). Prior to VSS analysis, the K1 carriers were added to a Falcon tube containing 10 mL of ultrapure water and the biofilm detached by sonication (10 min, 45 Hz) followed by manual shaking. The solution containing the detached biofilm was used for VSS determination.

4.2.8 Statistical data analysis

A one-way analysis of variance (ANOVA) was performed for data analysis using the Data Analysis Tool of Excel 2016 (Microsoft Corporation, USA). The ANOVA was conducted in order to determine the statistical differences in the performance parameters, i.e. DOC, TIN and TP removal. The significant difference was set at 95 % ($p < 0.05$).

4.3 Results and discussion

Effluent concentrations are expressed as averages between the values measured at the end of the aerobic and microaerobic phases of a single cycle, as no significant difference was observed between the microaerobic and aerobic profiles of each parameter ($p > 0.05$).

4.3.1 Nitrogen removal in the IAMBBR

The decrease of HRT from 2 days to 1 day and the increase of feed C/N ratio from 2.0 to 4.2 at the beginning of P1 determined a transient accumulation of $N\text{-}NH_4^+$ up to 15 mg L^{-1} (day 39), followed by an increase of the effluent $N\text{-}NO_2^-$ concentration (up to 15 mg L^{-1}) until the end of the period (**Fig. 4.1**). Despite TIN RE at the end of P1 reached 61%, being the highest observed until P6, the feed C/N ratio was reduced from 4.2 (P1) to 2.8 (P2) as excess growth of suspended biomass led to DO probe malfunctioning and hampered DO control in the bioreactor. Previous studies reported that overgrowth of heterotrophic aerobic bacteria (HAB) can occur at high feed C/N ratios and suppress nitrification in SND systems [21,26]. The increase of feed C/N ratio and the subsequent HAB overgrowth likely affected nitrification activity during P1, contributing to $N\text{-}NH_4^+$ and $N\text{-}NO_2^-$ accumulation.

During P2–P5 (days 50–122), the IAMBBR was operated at a feed C/N ratio of 2.8 and showed a stable TIN RE around 40% (**Fig. 4.2**). Nevertheless, the different DO regimes tested significantly influenced the nitrifying and denitrifying activity of the IAMBBR biofilm, resulting in dynamic trends of $N\text{-}NH_4^+$, $N\text{-}NO_3^-$ and $N\text{-}NO_2^-$ concentrations in the effluent (**Fig. 4.1**). The effluent $N\text{-}NH_4^+$ concentration during P2 increased up to 9 mg L^{-1} (day 56) following the decrease of the feed C/N ratio from 4.2 (P1) to 2.8 (P2). The low relative abundances (< 2%) of nitrifying bacteria observed at the end of P2 (**Table 4.2**) were likely responsible for the high $N\text{-}NH_4^+$ levels occurring in the IAMBBR effluent (**Fig. 4.1**), resulting in a 12% lower TIN RE compared to that observed at the end of P1 (days 42–49, **Fig. 4.2**). The decrease of the feed C/N ratio reduced assimilative $N\text{-}NH_4^+$ uptake by HAB and contributed to increase $N\text{-}NH_4^+$ levels in the IAMBBR. $N\text{-}NO_2^-$ concentration in the effluent during P2 remained stable at 11 (±2) mg L^{-1}, while fluctuations in $N\text{-}NO_3^-$ concentration were observed until the end of the period (**Fig. 4.1**).

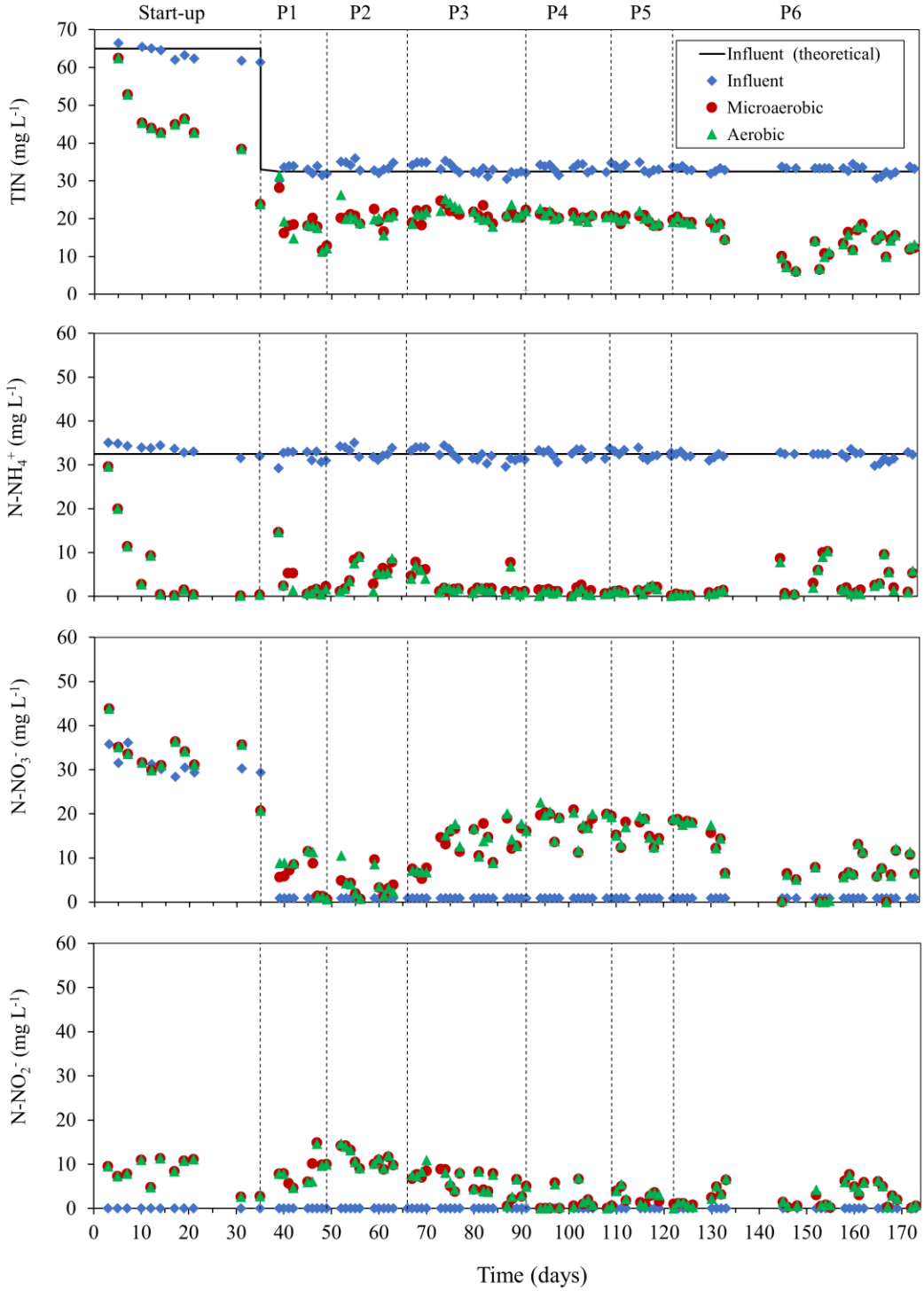

Figure 4.1 - Temporal profiles of the influent and effluent TIN, N-NH_4^+, N-NO_3^- and N-NO_2^- concentrations during continuous IAMBBR operation.

The modification of DO regime (0.2–3 mg L^{-1}) at the beginning of P3 determined an increase of *Nitrosomonas* abundance from 1.0% to 4.8% (**Table 4.2**), resulting in an immediate recovery of nitrification efficiency. N-NH_4^+ concentration in the effluent

rapidly decreased to 2 mg L^{-1} (day 74) and remained below this value until the end of P5, except on day 88 (7 mg L^{-1}). Similarly, N-NO_2^- concentrations in the effluent progressively decreased, while the concentration of N-NO_3^- rapidly increased and remained stable at 16 (±3) mg L^{-1} until the end of P4 (**Fig. 4.1**). Interestingly, the increase of DO concentrations at the beginning of P4 had a negative effect on *Nitrosomonas* abundance, which decreased from 4.8% (P3) to 2.5% (P4) (**Table 4.2**). This may be related to increased competition with HAB for N-NH_4^+, which was almost completely depleted during P4 (**Fig. 4.1**). During P1–P5, the combined nitrification and denitrification process allowed to maintain the effluent pH at 8.0 (±0.1), being optimal for both nitrifying and denitrifying bacteria [27]. Similarly, alkalinity concentration in the effluent was stable at 939 (±37) mg $CaCO_3$ L^{-1}. The concentrations of carrier-attached biomass during P1–P5 remained also stable, being 1.1 (±0.2) mg VSS $carrier^{-1}$, while the concentration of suspended biomass varied between 57 mg VSS L^{-1} (P3) and 104 mg VSS L^{-1} (P5), respectively.

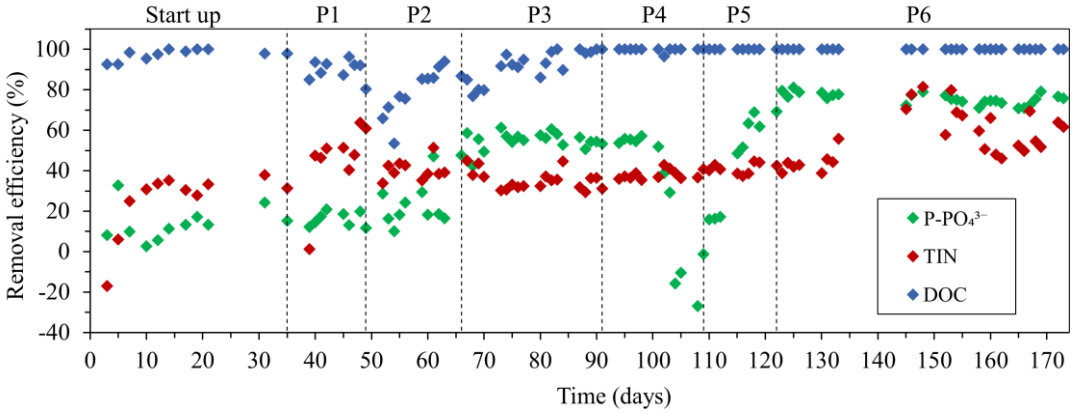

Figure 4.2 - TIN, P-PO_4^{3-} and DOC RE profiles during continuous IAMBBR operation.

Increasing the feed C/N ratio from 2.8 (P3–P5) to 3.6 (P6) was beneficial for TIN RE ($p < 0.05$). The decrease of the effluent N-NO_3^- concentration from 19 mg L^{-1} (day 122) to below the detection limit during P6 resulted in TIN REs up to 82% (62% on average) (**Fig. 4.2**), proving that denitrification efficiency was limited by the low DOC availability in previous periods. Improvement of denitrification efficiency in P6 was also indicated by the higher abundance of DNB in the IAMBBR biofilm (**Table 4.2**) and the increased pH (8.3 ± 0.1) and alkalinity concentration (1076 ± 37 mg $CaCO_3$ L^{-1}) in the IAMBBR effluent. The concentration of carrier-attached biomass during P6 increased by 2.4 times compared to the average value of previous periods, whereas the concentration of suspended biomass remained similar to that observed in P5. The increased abundance of NOB (*Devosia* and *Nitrospira*) in the IAMBBR biofilm

allowed to maintain the effluent $N\text{-}NO_2^-$ concentrations ≤ 8 mg L^{-1}. A possible explanation to the increased relative abundance of NOB during P6 is that the concomitant increase of denitrifying activity (**Fig. 4.1**) and relative abundance of DNB (**Table 4.2**) provided additional NO_2^- for NOB growth (a mechanism also known as nitrite-loop), increasing the ratio between NOB and AOB. Moreover, long-term low DO operation can significantly increase the oxygen affinity of NOB, which makes NOB better competitors for DO compared to AOB [28]. The decreased relative abundance of AOB during P6 (**Table 4.2**) can be attributed to the competition with HAB and NOB for DO, which was likely responsible for the lower $N\text{-}NH_4^+$ RE efficiency compared to P3–P5 (**Fig. 4.1**).

N_2O concentration in the gas phase remained below the detection limit during the entire IAMBBR operation. According to Sabba et al. [29], N_2O in combined nitrification and denitrification systems is produced by both nitrifiers and denitrifiers and reduced by denitrifiers. The authors explain that in aerated bioreactors with co-diffusional multilayered biofilms (as the IAMBBR), there is a greater N_2O mass transfer towards the aerated bulk rather than towards the anoxic zone where it can be reduced. In this study, intermittent aeration operation and highly enriched denitrifying community of the IAMBBR biofilm were effective in limiting N_2O emission at all tested conditions.

Table 4.2 - Identification of key functional group, bacterial genus, relative abundance and phylogenetic affiliation of carrier-attached IAMBBR bacteria. Only genera with relative abundance above 4 % are listed.

Key functional group	Genus	Phylum/family	Relative abundance [%]				
			P2	**P3**	**P4**	**P5**	**P6**
DNB	*Hydrogenophaga*	*Proteobacteria/Burkholderiaceae*	10.9	9.5	6.8	7.3	7.7
	SWB02	*Proteobacteria/Hyphomonadaceae*	8.1	11.4	8.2	9.6	3.2
	unidentified	*Proteobacteria/Rhizobiaceae*	4.0	0.9	4.1	1.6	3.7
	Dokdonella	*Proteobacteria/Rhodanobacteraceae*	n.d.	n.d.	n.d.	n.d.	4.4
	Arenimonas	*Proteobacteria/Xanthomonadaceae*	0.2	0.1	n.d.	n.d.	4.1
	Thauera	*Proteobacteria/Rhodocyclaceae*	5.7	1.0	0.3	0.2	0.6
	Planctopirus	*Planctomycetes/Schlesneriaceae*	0.8	3.5	4.2	4.1	4.1
	Rhizobium	*Proteobacteria/Rhizobiaceae*	7.3	2.3	0.1	0	0.9
	Rhodobacter	*Proteobacteria/Rhodobacteraceae*	n.d.	0.8	4.3	0.9	n.d.
	Flavobacterium	*Bacteroidetes/Flavobacteriaceae*	5.2	1.3	n.d.	n.d.	n.d.
	Pseudomonas	*Proteobacteria/ Pseudomonadaceae*	6.1	0.2	0.1	n.d.	0.2
HAB	*OLB12*	*Bacteroidetes/Microscillaceae*	1.6	5.8	4.7	11.9	1.6
	Pseudofulvimonas	*Proteobacteria/Rhodanobacteraceae*	4.8	7.2	4.1	3.0	0.2
	Chryseobacterium	*Proteobacteria/Weeksellaceae*	n.d.	n.d.	n.d.	n.d.	7.0
	unidentified	*Proteobacteria/Stappiaceae*	n.d.	n.d.	n.d.	n.d.	8.9
	Chryseolinea	*Bacteroidetes/Microscillaceae*	1.4	6.4	9.0	5.9	0.9
AOB	*Nitrosomonas*	*Proteobacteria/Nitrosomonadaceae*	1.0	4.8	2.5	6.3	2.4
NOB	*Nitrospira*	*Nitrospirae/Nitrospiraceae*	n.d.	n.d.	n.d.	0.2	5.0

n.d. not detected

4.3.2 Phosphorus removal in the IAMBBR

Effluent P-PO4^{3-} concentrations in the IAMBBR during P1 and P2 were 10 (±1) and 8 (±1) mg L^{-1}, resulting in P-PO_4^{3-} REs of 16 (±3) % and 25 (±4) %, respectively (**Fig. 4.3**). The low P-PO_4^{3-} REs observed in these periods can be attributed to the high levels of N-NO_2^- in the effluent (**Fig. 4.1**), which increased up to 15 mg L^{-1} (day 47). Previous studies reported considerable inhibition of aerobic phosphate uptake due to NO_2^-. Jabari et al. [30] observed increasing inhibition of aerobic phosphate uptake by attached and suspended biomass collected from an integrated fixed film sludge (IFAS) system at N-NO_2^- concentrations exceeding 10 mg L^{-1}. According to Saito et al. [31], inhibitory effects on aerobic phosphate uptake can be observed already at 2 mg N-NO_2^- L^{-1}, while 6 mg N-NO_2^- L^{-1} can lead to complete inhibition. The authors concluded that aerobic phosphate uptake is more sensitive to NO_2^- than anoxic phosphate uptake.

Change in DO range to 0.2–3 mg L^{-1} at the beginning of P3 resulted in an immediate increase of P-PO_4^{3-} RE, which remained at 55 (±4) % during the entire period (**Fig. 4.2**). In contrast, the change of DO range to 0.2–4 mg L^{-1} in P4 determined a dramatic increase of the effluent P-PO_4^{3-} concentrations above the influent values (**Fig. 4.3**), which indicates that P-PO_4^{3-} was released from the IAMBBR biofilm to the bulk liquid in this phase. Phosphorus release by microorganisms was probably induced by shortage and competition with HAB for the available DOC, being the effluent DOC levels below the detection limit during the entire P4 (expect on days 101–102) (**Fig. 4.3).** In a study conducted by Barak and Van Rijn [32], the authors observed phosphate release by DNB under aerobic conditions after all acetate was depleted, while phosphate was assimilated again upon acetate addition. As a result, DOC availability seems crucial to support P-PO_4^{3-} assimilation by DNB under aerobic conditions. The higher DO values (up to 4 mg L^{-1}) experienced by the IAMBBR biofilm during P4 triggered the proliferation of HAB such as *Chryseolinea* (**Table 4.2**) and the competition with DNB for organic carbon, which led to the inhibition of P-PO_4^{3-} uptake.

Change in DO regime to 0.2–3 mg L^{-1} at beginning of P5 immediately increased the P-PO_4^{3-} RE until a stable value of 66 (±4) % (days 117–122), 11% higher than that observed during P3 under similar operational conditions ($p < 0.05$). The higher P-PO_4^{3-} RE observed during P5 may be linked to the higher concentration of suspended biomass and the lower NO_2^- levels in the IAMBBR effluent compared to P3. While the concentration of attached-growth biomass in the two periods remained stable, the concentration of suspended biomass almost doubled. Effluent N-NO_2^- concentrations during P5 did not exceed 5 mg L^{-1}, while up to 10 mg L^{-1} was observed during P3 (**Fig.**

4.1), which could be linked to the higher relative abundance of NOB in P5 (1.7%) compared to P3 (1.2%). The slight variation of microbial community composition between P3 and P5 (**Table 4.2**, **Fig. 4.4**) may have also influenced $P\text{-}PO_4^{3-}$ RE, but the information obtained from microbial community analysis does not provide a clear explanation for this.

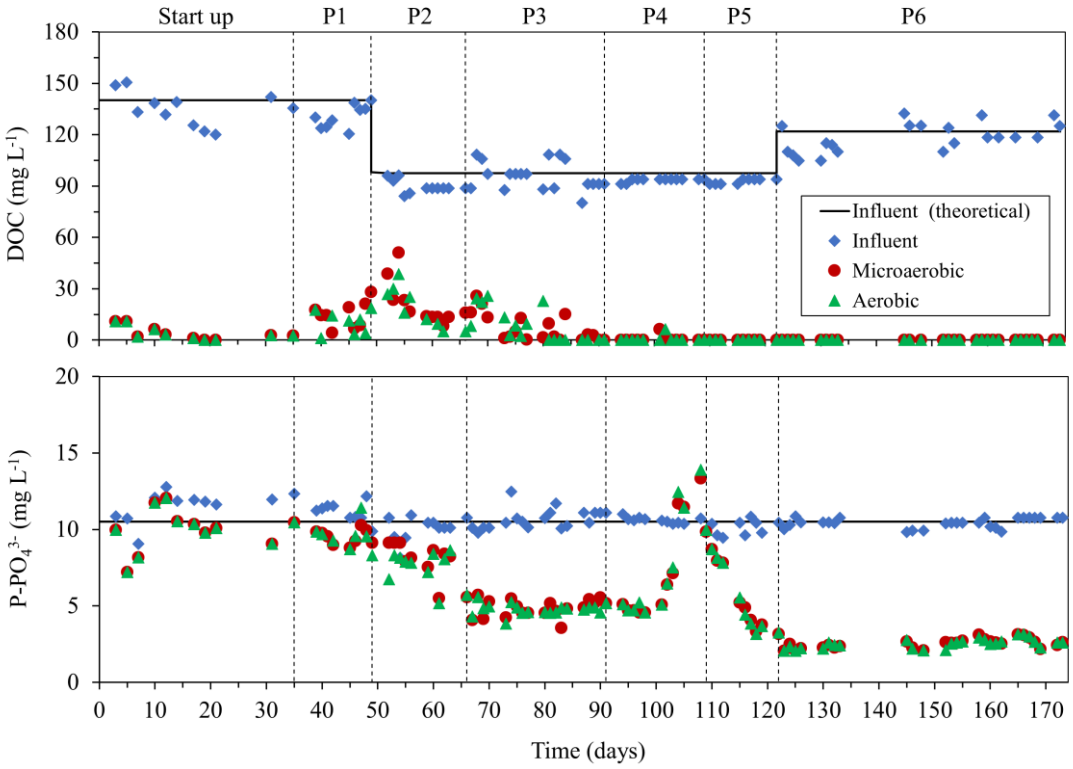

Figure 4.3 - Temporal profiles of influent and effluent DOC and $P\text{-}PO_4^{3-}$ concentrations in the IAMBBR.

The increase of feed C/N ratio to 3.6 at the beginning of P6 greatly enhanced $P\text{-}PO_4^{3-}$ RE, which increased by nearly 10% compared to the end of P5 (days 117–122) and 20% compared to P3 ($p < 0.05$), resulting in an average $P\text{-}PO_4^{3-}$ RE of 75% (**Fig. 4.2).** Despite the increase in the feed C/N ratio, DOC concentration in the effluent remained below the detection limit (**Fig. 4.3**), which means that DOC surplus was completely consumed by the IAMBBR biomass. The effluent $N\text{-}NO_3^-$ concentrations in P6 were significantly lower compared to P5 (**Fig. 4.1**) despite the considerable increase of NOB abundance (**Table 4.2**), which indicates that acetate addition stimulated the growth of DNB. The concomitant increase of $P\text{-}PO_4^{3-}$ RE indicates that DNB may have played a major role in phosphorus uptake under microaerobic/aerobic conditions.

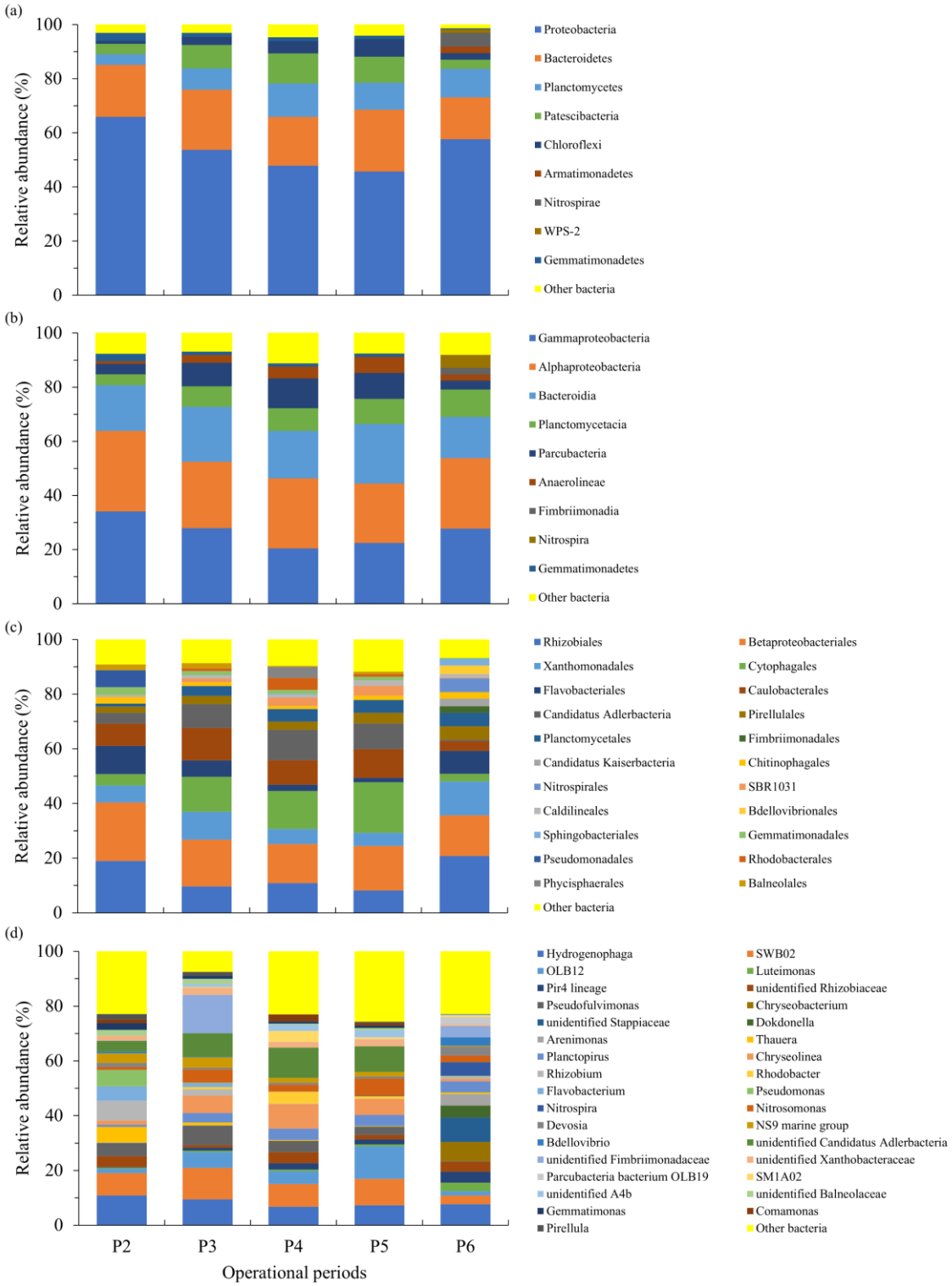

Figure 4.4 - Microbial community composition of the IAMBBR biofilm at (a) phylum level, (b) class level, (c) order level and (d) genus level.

4.3.3 Mechanisms for phosphorus removal within the microaerobic/aerobic cycle

During P3, P5 (days 117–122) and P6, between 4.1 and 8.8 mg $P\text{-}PO_4^{3-}$ L^{-1} was removed from the feed, resulting in a $P\text{-}PO_4^{3-}$ RE between 42% and 81%. $P\text{-}PO_4^{3-}$ uptake for cell growth, evaluated based on a C:N:P ratio of 100:5:1 [33], was between 12% and 19%, revealing that $P\text{-}PO_4^{3-}$ removal can be mainly considered as luxury biological uptake. Batch activity tests performed at the end of the study showed that $P\text{-}PO_4^{3-}$ uptake did not occur under stable anoxic and anaerobic conditions, nor under aerobic conditions in absence of NO_3^-. Based on these results, both microaerobic/aerobic conditions and NO_3^- are necessary to trigger luxury phosphorus uptake and achieve a satisfactory $P\text{-}PO_4^{3-}$ RE in the IAMBBR.

The alternation of microaerobic and aerobic conditions was firstly experimented by Satoh et al. [14] with the objective to promote PHA accumulation in the activated sludge. The authors showed that the microaerobic-aerobic cycle can double the PHA accumulating potential of the system compared to that obtained under the alternation of anaerobic and aerobic conditions. Under microaerobic conditions, microorganisms can take up and accumulate organic carbon as PHA, while organic carbon oxidation under aerobic conditions provides energy for assimilative activity. The microaerobic-aerobic cycle overcomes the energy limitation for PHA synthesis of the anaerobic-aerobic cycle, which is represented by the amount of stored poly-P and glycogen. By providing a limited oxygen supply during the microaerobic conditions, microorganisms can use the oxidative energy gained from acetate oxidation exclusively for PHA accumulation. In this condition, the breakage of poly-P molecules for PHA storage is not necessary, while the energy gained under aerobic conditions via PHA oxidation could still serve to generate poly-P granules, resulting in a net phosphorus accumulation.

Although the microaerobic-aerobic cycle does not specifically select for P-accumulating bacteria, it is known that poly-P synthesis is a distinctive trait of many PHA accumulators and DNB [32]. Jørgensen and Pauli [34] showed that genera belonging to *Hydrogenophaga*, *Pseudomonas*, *Flavobacterium* and *Comamonas*, which were all detected at the end of P2 (**Fig. 4d**), can accumulate $P\text{-}PO_4^{3-}$ under aerobic conditions. In particular, *Hydrogenophaga* was among the true DNB (bacteria able to convert more than 80% NO_3^- to N_2O) cultivated on acetate capable of synthesizing poly-P granules under aerobic conditions and showed an aerobic phosphorus uptake rate of approximately 6 mg P $g\ VSS^{-1}\ h^{-1}$ (considering a VSS/TS ratio of 0.5), being comparable to the rates observed for biomass collected from full-scale EBPR systems [35]. *Hydrogenophaga* was a

dominant genus in the IAMBBR throughout the entire study (**Table 4.2**) and seems to have played a major role in phosphorus removal.

4.3.4 Microbial community structure and evolution in the IAMBBR

Fig. 4.4 shows the bacterial community structure (relative abundance > 2%) in the IAMBBR biofilm during the study at phylum, class, order and genus levels. Proteobacteria (45.7–65.9%) was the dominant phylum during the entire IAMBBR operation, followed by *Bacteroidetes* (15.4–22.9%), *Planctomycetes* (4.0–12.3%), *Patescibacteria* (3.3–11.1%) and *Chloroflexi* (1.1–6.5%) (**Fig. 4.4a**). *Proteobacteria* and *Bacteroidetes* are commonly involved in nitrogen and phosphorus removal [36]. *Chloroflexi* can couple the degradation of a broad range of organic compounds to nitrogen removal [37]. *Gammaproteobacteria* (20.5–34.1%), *Alphaproteobacteria* (21.9–29.8%) and *Bacteroidia* (15.2–22.0%) were the dominant classes, followed by *Planctomycetacia* (4.0–10.2%), *Parcubacteria* (3.3–11.0%) and *Anaerolineae* (0.9–6.0%) (**Fig. 4.4b**). At order level, *Rhizobiales*, *Betaproteobacteriales*, *Xanthomonadales* and *Cytophagales* were the most abundant in the IAMBBR biofilm during the study (**Fig. 4.4c**).

Table 4.2 lists the most abundant bacterial genera (> 4 %) in the microbial community of the IAMBBR biofilm. *Hydrogenophaga* and *Hyphomonadaceae_SWB02* showed high relative abundances (3.2–11.4%) at all operational periods. Members of these two genera include heterotrophic and autotrophic DNB [38,39]. *Rhizobium* (7.3%), *Pseudomonas* (6.1%) and *Thauera* (5.7%) were also abundant in the IAMBBR biofilm at the end of P2 and have all been reported to possess denitrifying ability [38,40,41]. In contrast, low relative abundances (< 2%) were observed for nitrifying bacteria (**Fig. 4.4d**), i.e. *Nitrosomonas*, *Nitrospira* and *Devosia* [38,42,43].

At the end of P3, aerobic bacteria such as *Pseudofulvimonas* (7.2%), *Chryseolinea* (6.4%), *Microscillaceae OLB12* (5.8%) and *Nitrosomonas* (4.7%) showed increased abundance compared to the previous period. In contrast, the relative abundance of *Pseudomonas* (0.2%), *Thauera* (1.0%) and *Rhizobium* (2.3%) significantly decreased (**Table 4.2**, **Fig. 4.4d**). *Pseudofulvimonas* and *Chryseolinea* include HAB [44,45], while *Nitrosomonas* was the key functional group related to autotrophic ammonia oxidation in the IAMBBR.

The relative abundance of *Chryseolinea* further increased during P4, reaching 9.0% at the end of the period, whereas decrease in *Nitrosomonas* abundance from 4.8% to 2.5% was observed. *Rhodobacter*, classified as DNB by [46], were detected with an abundance

of 4.3% at the end of the period. At the end of P5, *Microscillaceae OLB12* (11.9%), *Hydrogenophaga* (7.3%), *Hyphomonadaceae_SWB02* (9.6%), *Nitrosomonas* (6.3%) and *Chryseolinea* (5.9%) were the dominant genera in the IAMBBR biofilm (**Table 4.2**).

Sequencing results at the end of P6 showed high relative abundances of previously undetected bacteria, such as unidentified *Stappiaceae* (8.9%), *Chryseobacterium* (7.0%) and *Dokdonella* (4.4%) (**Table 4.2**). In contrast, the relative abundance of *Hyphomonadaceae_SWB02*, *Microscillaceae OLB12* and *Nitrosomonas* was significantly lower compared to the previous period. *Chryseobacterium* and *Stappiaceae* are classified as HAB, although nitrate respiration is a widespread mechanism among members of the *Stappiaceae* family [47]. Similarly, members of the genus *Dokdonella* have been recognized as microorganisms involved in nitrogen removal [46,48]. Pishgar et al. (2019) reported a $P\text{-}PO_4^{3-}$ removal around 50% in *Dokdonella*-dominated aerobic systems coupled to both NO_3^- and NO_2^- reduction, which suggests that *Dokdonella* may also play a role in phosphorus accumulation. The relative abundance of *Acidovorax* (3.0%), *Arenimonas* (4.1%), *Luteimonas* (3.0%), *Bdellovibrio* (3.1%), *Nitrospira* (5.0%) and *Devosia* (3.3%) also increased significantly during P6 (**Table 4.2**). *Arenimonas* and *Luteimonas* genera belong to the *Xanthomonadaceae* family and have been reported as DNB [40,49]. Similarly, many *Acidovorax* members possess denitrification ability [10,38]. Interestingly, the increase of the NOB representatives *Devosia* and *Nitrospira* during P6 from 1.7% (P5) to 8.4% was accompanied by a decrease of AOB (*Nitrosomonas*) from 6.3% (P5) to 2.4%.

4.3.5 Practical applications and future research

Based on the results of this study, the IAMBBR can be considered as a novel and promising technology for the simultaneous removal of organic carbon, nitrogen and phosphorus from low- and medium-strength municipal wastewater. The highest REs could be obtained by maintaining the DO range at 0.2–3 mg L^{-1}, while higher DO levels were highly detrimental in terms of $P\text{-}PO_4^{3-}$ RE. In order to achieve satisfactory REs, oxygen dosing to the IAMBBR should be limited, which results in energy saving and reduced operational costs. In a previous study, Iannacone et al. [21] obtained COD, TIN and $P\text{-}PO_4^{3-}$ REs respectively up to 100%, 68% and 72% in a continuous-flow MBBR at a stable DO concentration of 1 mg L^{-1} and feed C/N ratio of 4.2. In the IAMBBR, higher REs were achieved at a lower feed C/N ratio of 3.6, whereas applying a feed C/N ratio of 4.2 resulted in overgrowth of suspended HAB and DO probe malfunctioning. Therefore, IAMBBR operation for SNDPR is recommended for wastewaters with C/N ratios < 4 to avoid disruption of the SNDPR process.

In Italy, more than 20% of untreated municipal wastewater is generated from towns and rural areas with less than 2000 population equivalent (PE) for which wastewater treatment is not economically feasible. The IAMBBR offers a compact solution for carbon and nutrient removal at a locally sustainable cost. Additionally, the Italian legislation has set less stringent limits for settlements with less than 10000 PE. Therefore, the discharge limits required for small communities can be easily met with the REs achieved by the IAMBBR.

Full- and pilot-scale studies are needed to evaluate the operational costs related to microaerobic and microaerobic/aerobic operation and the effects of scale-up on carbon and nutrient removal. Moreover, additional studies should investigate the $P\text{-}PO_4^{3-}$ removal performance of the IAMBBR with different organic compounds and when treating real wastewater containing a significant concentration of low-biodegradable and recalcitrant organic matter.

4.4 Conclusions

IAMBBR operation achieved DOC, TIN and P-PO43- REs up to 100%, 82% and 81%, respectively, at a DO range of 0.2–3 mg L^{-1}, feed C/N ratio of 3.6 and HRT of 1 day. The microaerobic-aerobic cycle allowed the coexistence of key species involved in nitrification, denitrification and phosphorus accumulation in the IAMBBR biofilm. Aerobic DNB, i.e. *Hydrogenophaga* and *Dokdonella*, were identified as potentially responsible for luxury P uptake. The IAMBBR is a compact and low-cost solution which can be successfully applied in small communities for the removal of organic carbon and nutrients from municipal wastewater.

4.5 Acknowledgements

This study was supported by Programma di Sviluppo Rurale (PSR) Campania 2014/2020 - METAGRO Project and Programma Operativo Nazionale (PON) 2014/2020 – BIOFEEDSTOCK Project. The authors would like to thank Ms. Giorgia Pinchera for her valuable support to laboratory work.

4.6 Supplementary materials

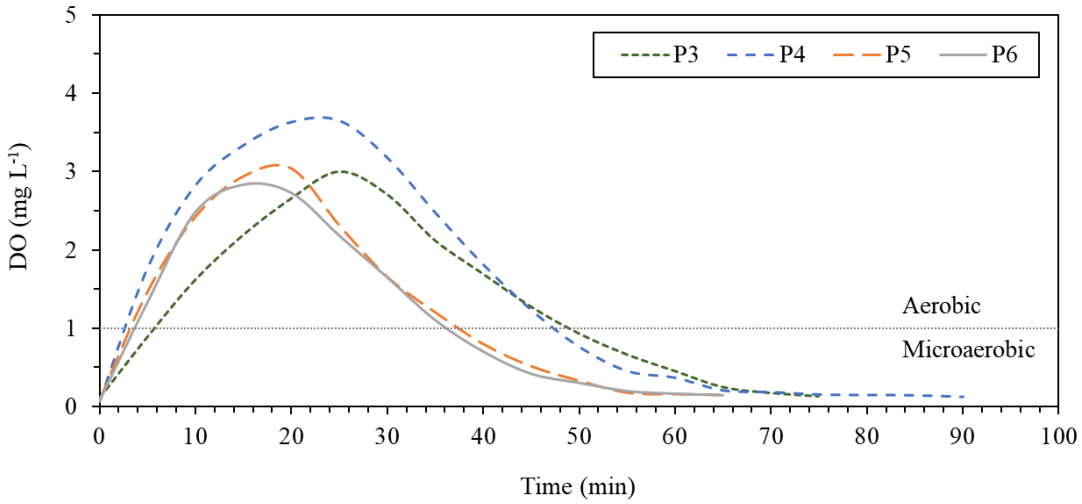

Figure S4.5 - DO profiles of the microaerobic-aerobic cycles applied during periods P3-P6 in the IAMBBR. Each DO profile shows the average values of 4-6 profiles automatically measured at 5-minute intervals in the respective period.

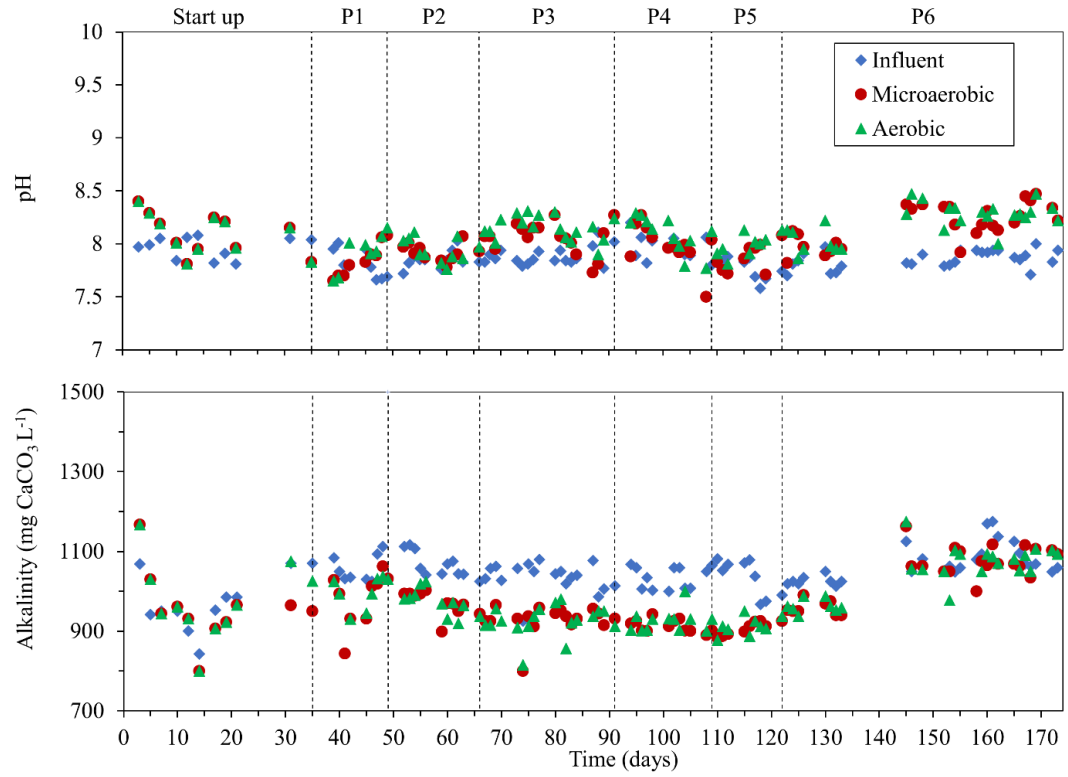

Figure S4.6 - Profiles of effluent pH and alkalinity concentration during IAMBBR operation.

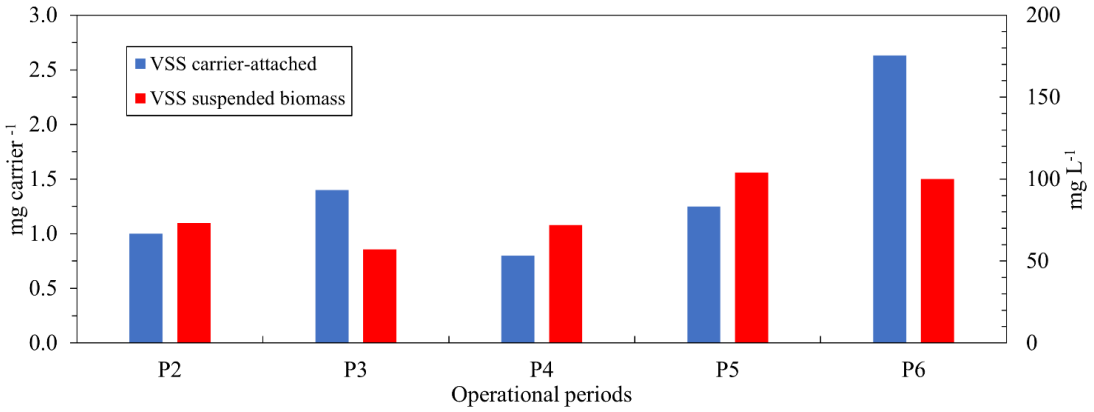

Figure S4.7 - Concentrations of carrier-attached and suspended biomass during IAMBBR operation.

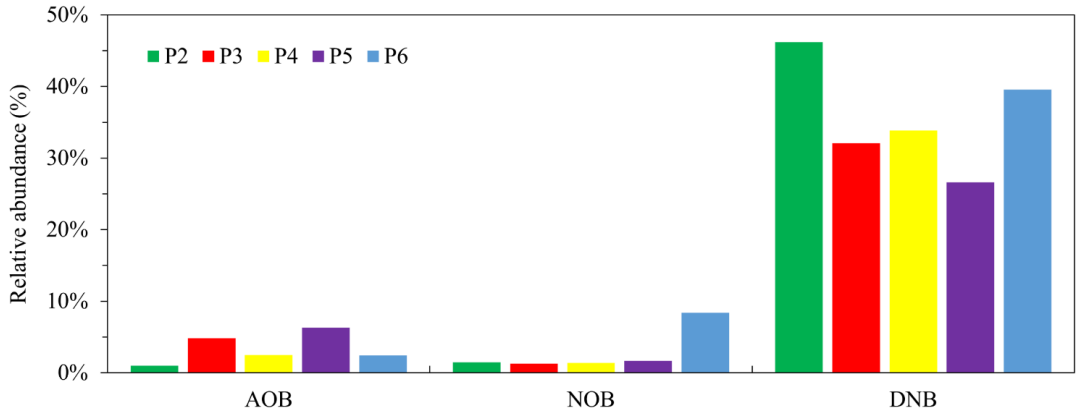

Figure S4.8 - Relative abundances of AOB, NOB and DNB in the IAMBBR biofilm during the study.

Table S4.3 - Activity tests performed with carrier-attached IAMBBR biomass under aerobic (ATN), anoxic (ATD) and anaerobic (ATDC) conditions.

Experiment	Biomass concentration (mg VSS carrier^{-1})	TIN removal activity (mg N g VSS^{-1} h^{-1})	NO_2^- accumulation (mg N L^{-1})	DOC removal activity (mg DOC g VSS^{-1} h^{-1})	P removal activity (mg P g VSS^{-1} h^{-1})
ATN	2.6	2.5	n.d.	15.4 (±1.3)	0.3
ATD	2.6	1.9 (±0.1)	n.d.	13.0 (±1.7)	0.1
ATDC	2.6	0.3	n.d.	6.7 (±0.3)	0.1

n.d. = not detected

4.7 References

[1] M.C. Chrispim, M. Scholz, M. Antunes, Phosphorus recovery from municipal wastewater treatment: critical review of challenges and opportunities for developing countries, *J. Environ. Manage.* 248 (2019) 109268.

[2] F. Jaramillo, M. Orchard, C. Muñoz, M. Zamorano, C. Antileo, Advanced strategies to improve nitrification process in sequencing batch reactors - a review, *J. Environ. Manage.* 218 (2018) 154–164.

[3] H. Chai, Y. Xiang, R. Chen, Z. Shao, L. Gu, L. Li, Q. He, Enhanced simultaneous nitrification and denitrification in treating low carbon-to-nitrogen ratio wastewater: Treatment performance and nitrogen removal pathway, *Bioresour. Technol.* 280 (2019) 51–58.

[4] S.A. Parsons, J.A. Smith, Phosphorus removal and recovery from municipal wastewaters, *Elements.* 4 (2008) 109–112.

[5] Y. Peng, S. Ge, Enhanced nutrient removal in three types of step feeding process from municipal wastewater, *Bioresour. Technol.* 102 (2011) 6405–6413.

[6] C.Z. Correa, K.V.M.C. Prates, E.F. de Oliveira, D.D. Lopes, A.C. Barana, Nitrification/denitrification of real municipal wastewater in an intermittently aerated structured bed reactor, *J. Water Process Eng.* 23 (2018) 134–141.

[7] J.T. Bunce, E. Ndam, I.D. Ofiteru, A. Moore, D.W. Graham, A review of phosphorus removal technologies and their applicability to small-scale domestic wastewater treatment systems, *Front. Environ. Sci.* 6 (2018).

[8] C. Pratt, S.A. Parsons, A. Soares, B.D. Martin, Biologically and chemically mediated adsorption and precipitation of phosphorus from wastewater, *Curr. Opin. Biotechnol.* 23 (2012) 890–896.

[9] P. Loganathan, P. Taylor, S. Vigneswaran, J. Kandasamy, S. Nanthi, Removal and recovery of phosphate from water using sorption, *Crit. Rev. Environ. Sci. Technol.* 44 (2014) 847–907.

[10] S. Salehi, K.Y. Cheng, A. Heitz, M.P. Ginige, Simultaneous nitrification, denitrification and phosphorus recovery (SNDPr) - an opportunity to facilitate full-scale recovery of phosphorus from municipal wastewater, *J. Environ. Manage.* 238 (2019) 41–48.

[11] Z. Yuan, S. Pratt, D.J. Batstone, Phosphorus recovery from wastewater through microbial processes, *Curr. Opin. Biotechnol.* 23 (2012) 878–883.

[12] B. Ma, S. Wang, G. Zhu, S. Ge, J. Wang, N. Ren, Y. Peng, Denitrification and

phosphorus uptake by DPAOs using nitrite as an electron acceptor by step-feed strategies, *Front. Environ. Sci. Eng.* 7 (2013) 267–272.

[13] J. Jena, R. Kumar, A. Dixit, T. Das, Anoxic – aerobic SBR system for nitrate, phosphate and COD removal from high-strength wastewater and diversity study of microbial communities, *Biochem. Eng. J.* 105 (2016) 80–89.

[14] H. Satoh, Y. Iwamoto, T. Mino, T. Matsuo, Activated sludge as a possible source of biodegradable plastic, *Water Sci. Technol.* 38 (1998) 103–109.

[15] R. Ferrentino, A. Ferraro, M.R. Mattei, G. Esposito, G. Andreottola, Process performance optimization and mathematical modelling of a SBR-MBBR treatment at low oxygen concentration, *Process Biochem.* 75 (2018) 230–239.

[16] P. Roots, F. Sabba, A.F. Rosenthal, Y. Wang, Q. Yuan, L. Rieger, F. Yang, J.A. Kozak, H. Zhang, G.F. Wells, Integrated shortcut nitrogen and biological wastewater: process operation and modeling, *Environ. Sci. Technol.* 6 (2019) 566–580.

[17] H. Wang, Q. Song, J. Wang, H. Zhang, Q. He, W. Zhang, J. Song, Simultaneous nitrification, denitrification and phosphorus removal in an aerobic granular sludge sequencing batch reactor with high dissolved oxygen: effects of carbon to nitrogen ratios, *Sci. Total Environ.* 642 (2018) 1145–1152.

[18] I.S. Arvanitoyannis, Waste management for the food industries, Elsevier Inc., 2008.

[19] S. Jafarinejad, Cost estimation and economical evaluation of three configurations of activated sludge process for a wastewater treatment plant (WWTP) using simulation, *Appl. Water Sci*. 7 (2017) 2513–2521.

[20] J.C. Leyva-díaz, A. Monteoliva-garcía, J. Martín-pascual, M.M. Munio, J.J. García-mesa, Moving bed biofilm reactor as an alternative wastewater treatment process for nutrient removal and recovery in the circular economy model, *Bioresour. Technol.* 299 (2020) 122631.

[21] F. Iannacone, F. Di Capua, F. Granata, R. Gargano, F. Pirozzi, G. Esposito, Effect of carbon-to-nitrogen ratio on simultaneous nitrification denitrification and phosphorus removal in a microaerobic moving bed biofilm reactor, *J. Environ. Manage.* 250 (2019) 109518.

[22] A. di Biase, M.S. Kowalski, T.R. Devlin, J.A. Oleszkiewicz, Moving bed biofilm reactor technology in municipal wastewater treatment: a review, *J. Environ. Manage.* 247 (2019) 849–866.

[23] Y. Peng, Y. MA, S. Wang, Denitrification potential enhancement by addition of external carbon sources in a pre-denitrification process, *J. Environ. Sci.* 19 (2007) 284–289.

[24] D. Ucar, T. Yilmaz, F. Di, G. Esposito, E. Sahinkaya, Comparison of biogenic and chemical sulfur as electron donors for autotrophic denitri fi cation in sulfur-fed membrane bioreactor (SMBR), *Bioresour. Technol.* 299 (2020) 122574.

[25] J.J. Classen, W.J. Chandler, R.S. Huie, J.A. Osborne, A centrifuge-based procedure for suspended solids measurements in Lagoon sludge, *Am. Soc. Agric. Biol. Eng.* 56 (2013) 747–752.

[26] G. Zajzon, D. Sándor, E. Fleit, A. Szabó, Investigation of simultaneous nitrification and denitrification process using biofilm formed on intelligent hydrogel micro-carriers, in: *Proc. 6th IWA Int. Young Water Prof. Conf.*, 2012: pp. 10–13.

[27] B.E. Rittmann, P.L. McCarty, Environmental biotechnology: principles and applications, McGraw Hill Education, 2012.

[28] G. Liu, J. Wang, Long-term low DO enriches and shifts nitrifier community in activated sludge, *Environ. Sci. Technol.* 47 (2013) 5109–5117.

[29] F. Sabba, A. Terada, G. Wells, B.F. Smets, R. Nerenberg, Nitrous oxide emissions from biofilm processes for wastewater treatment, *Appl. Microbiol. Biotechnol*. 102 (2018) 9815–9829.

[30] P. Jabari, G. Munz, Q. Yuan, J.A. Oleszkiewicz, Free nitrous acid inhibition of biological phosphorus removal in integrated fixed-film activated sludge (IFAS) system, *Chem. Eng. J.* 287 (2016) 38–46.

[31] T. Saito, D. Brdjanovic, M.C.M. Van Loosdrecht, Effect of nitrite on phosphate uptake by phosphate accumulating organisms, *Water Res.* 38 (2004) 3760–3768.

[32] Y. Barak, J. Van Rijn, Atypical polyphosphate accumulation by the denitrifying bacterium *Paracoccus* denitrificans, *Appl. Environ. Microbiol.* 66 (2000) 1209–1212.

[33] L.J. Thompson, V. Gray, D. Lindsay, A. Von Holy, Carbon:nitrogen:phosphorus ratios influence biofilm formation by *Enterobacter cloacae* and *Citrobacter freundii*, *J. Appl. Microbiol.* 101 (2006) 1105–1113.

[34] S.K. Jørgensen, A.S.L. Pauli, Polyphosphate accumulation among denitrifying bacteria in activated sludge, *Anaerobe.* 1 (1995) 161–168.

[35] C.M. López-Vázquez, C.M. Hooijmans, D. Brdjanovic, H.J. Gijzen, M.C.M. van Loosdrecht, Factors affecting the microbial populations at full-scale enhanced biological phosphorus removal (EBPR) wastewater treatment plants in The Netherlands, *Water Res.* 42 (2009) 2349–2360.

[36] J. Fu, Z. Lin, P. Zhao, Y. Wang, L. He, J. Zhou, Establishment and efficiency analysis of a single-stage denitrifying phosphorus removal system treating secondary effluent, *Bioresour. Technol.* 288 (2019) 121520.

[37] X. Zhang, Y. Liang, Y. Ma, J. Du, L. Pang, Ammonia removal and microbial characteristics of partial nitrification in biofilm and activated sludge treating low strength sewage at low temperature, *Ecol. Eng.* 93 (2016) 104–111.

[38] Y.Q. Gu, T.T. Li, H.Q. Li, Biofilm formation monitored by confocal laser scanning microscopy during startup of MBBR operated under different intermittent aeration modes, *Process Biochem.* 74 (2018) 132–140.

[39] A.R.M. Barros, S.L. de Sousa Rollemberg, C.D.A. de Carvalho, I.H.H. Moura, P.I.M. Firmino, A.B. dos Santos, Effect of calcium addition on the formation and maintenance of aerobic granular sludge (AGS) in simultaneous fill/draw mode sequencing batch reactors (SBRs), *J. Environ. Manage.* 255 (2020) 109850.

[40] L. Li, G. Qian, L. Ye, X. Hu, X. Yu, W. Lyu, Research on the enhancement of biological nitrogen removal at low temperatures from ammonium-rich wastewater by the bio-electrocoagulation technology in lab-scale systems, pilot-scale systems and a full-scale industrial wastewater treatment plant, *Water Res.* 140 (2018) 77–89.

[41] R. Pishgar, J.A. Dominic, Z. Sheng, J.H. Tay, Denitrification performance and microbial versatility in response to different selection pressures, *Bioresour. Technol.* 281 (2019) 72–83.

[42] S. Zhang, Z. Huang, S. Lu, J. Zheng, X. Zhang, Nutrients removal and bacterial community structure for low C/N municipal wastewater using a modified Anaerobic/Anoxic/Oxic (mA2/O) process at north areas of China, *Bioresour. Technol.* 243 (2017) 975–985.

[43] Z. Song, X. Zhang, H. Hao, W. Guo, P. Song, Y. Zhang, Zeolite powder based polyurethane sponges as biocarriers in moving bed biofilm reactor for improving nitrogen removal of municipal wastewater, *Sci. Total Environ.* 651 (2019) 1078–1086.

[44] P. Kämpfer, E. Martin, N. Lodders, S. Langer, P. Schumann, U. Ja, *Pseudofulvimonas gallinarii gen. nov., sp. nov.*, a new member of the family *Xanthomonadaceae*, *Int. J. Syst. Evol. Microbiol.* 60 (2010) 1427–1431.

[45] Z. Zhong, X. Wu, L. Gao, X. Lu, B. Zhang, Efficient and microbial communities for pollutant removal distributed-inflow biological reactor (DBR) for treating piggery wastewater, *RSC Adv.* 6 (2016) 95987–95998.

[46] Y.-Y. Qiu, L. Zhang, X. Mu, G. Li, X. Guan, J. Hong, F. Jiang, Overlooked

pathways of denitrification in a sulfur-based denitrification system with organic supplementation, *Water Res.* 169 (2020) 115084.

[47] C.F. Weber, G.M. King, Physiological, ecological, and phylogenetic characterization of *Stappia*, a marine co-oxidizing bacterial genus, *Appl. Environ. Microbiol.* 73 (2007) 1266–1276.

[48] Y. Luo, J. Yao, X. Wang, M. Zheng, D. Guo, Y. Chen, Efficient municipal wastewater treatment by oxidation ditch process at low temperature: bacterial community structure in activated sludge, *Sci. Total Environ.* 703 (2020) 135031.

[49] W. Xing, Y. Wang, T. Hao, Z. He, F. Jia, H. Yao, pH control and microbial community analysis with HCl or CO_2 addition in H_2 -based autotrophic denitrification, *Water Res.* 168 (2020) 115200.

CHAPTER 5.

Shortcut nitrification-denitrification and biological phosphorus removal in acetate- and ethanol-fed moving bed biofilm reactors under microaerobic/aerobic conditions

This Chapter has been published as:

Iannacone, F., Di Capua, F., Granata, F., Gargano, R., Esposito, G., 2021. Shortcut nitrification-denitrification and biological phosphorus removal in acetate-and ethanol-fed moving bed biofilm reactors under microaerobic/aerobic conditions. *Bioresour. Technol.* 124958.

Abstract

This study investigated the feasibility of coupling simultaneous partial nitrification and denitrification (SPND) to biological phosphorus removal in continuous-flow intermittently-aerated moving bed biofilm reactors (MBBRs) fed with different carbon sources, i.e. ethanol and acetate. Bacterial cultivation at pH 8.2 (±0.2), 26-28 °C and SRT of 4 day and microaerobic/aerobic MBBR operation allowed to achieve average dissolved organic carbon (DOC), total inorganic nitrogen (TIN) and P-PO_4^{3-} removal efficiencies (REs) of 100%, 81-88% and 83-86% at HRT of 1 day, dissolved oxygen (DO) range of 0.2–3 mg L^{-1} and feed C/N and C/P ratios of 3.6 and 11, respectively. Acetate supplementation favored a diversified microbial community, while overgrowth of heterotrophs was observed when increasing feed C/N ratio in ethanol-fed MBBR. Illumina sequencing displayed the presence of putative phosphorus accumulating organisms (PAOs) such as *Hydrogenophaga* and *Pseudomonas* in MBBR biofilm and suspended biomass, whereas no typical NOB was identified during the study.

Keywords

Intermittent aeration; MBBR; shortcut nitrification and denitrification; phosphorus removal; putative PAO.

Graphical abstract

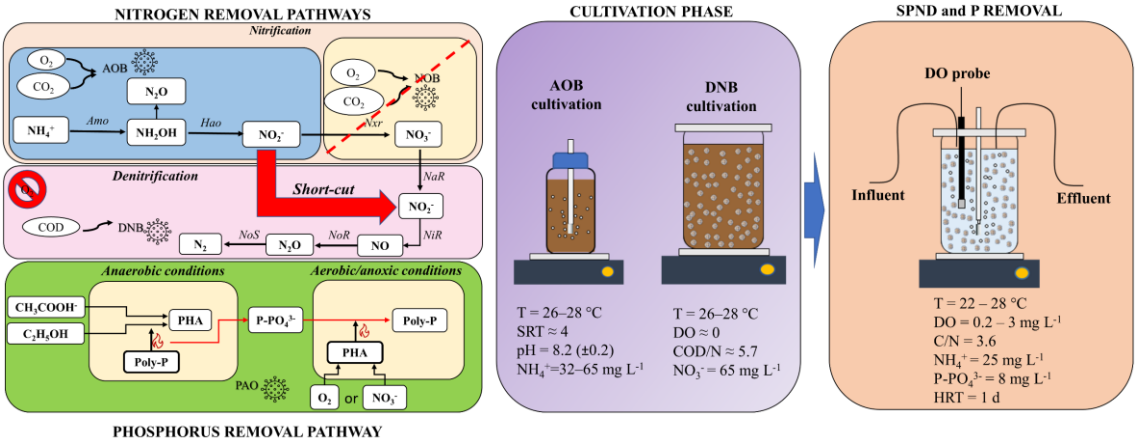

5.

5.1 Introduction

Groundwaters and surface waters are contaminated by nitrogen (N) and phosphorus (P) from different sources, e.g. industrial and intensive agricultural activities. An excessive discharge of nutrients in water bodies may have a serious environmental impact due to eutrophication [1]. In order to avoid this phenomenon, strict discharge limits have been enforced in many countries [2]. Hence, the removal and recovery of N and P from

wastewater effluents have become key challenges. In conventional activated sludge, biological nitrogen removal (BNR) from wastewater is achieved by means of two separated processes, i.e. nitrification and denitrification. Nitrification involves the oxidation of ammonia (NH_4^+) to nitrite (NO_2^-) (*nitritation*) by ammonia oxidizing bacteria (AOB) and then of NO_2^- to nitrate (NO_3^-) (*nitratation*) by nitrite oxidizing bacteria (NOB). During the denitrification process, denitrifying bacteria (DNB) reduce NO_3^- to NO_2^- (*denitratation*) and ultimately to N_2 through two intermediates, i.e. NO and N_2O. Since NO_2^- is produced during nitrification and then consumed during denitrification, NO_2^- oxidation by NOB becomes an unnecessary step. Hence, the concept of partial nitrification was born as an attractive alternative to full nitrification with the aim to reduce the consumption of oxygen and carbon [3].

Simultaneous nitrification and denitrification (SND) has gained increasing interest in the past years as an efficient and cost-effective process to treat wastewater with low carbon-to-nitrogen (C/N) ratios (< 5.0) [4–6] typical of municipal wastewater [7]. SND is carried out in a single bioreactor, thus reducing the number of basins, footprint and investment costs of conventional pre-denitrification [8]. If *nitratation* is inhibited, nitrogen removal takes place by shortcut SND, also known as simultaneous partial nitrification and denitrification (SPND).The SPND process offers several advantages compared to SND, including (1) 25% lower consumption of oxygen in aerobic phase [9], (2) 40% lower demand of electron donors in anoxic phase [10], (3) up to 2-fold faster NO_x reduction rates and (4) reduced CO_2 emissions [11]. Selective NOB inhibition can be accomplished by imposing several conditions, i.e. pH > 7.5 [12], temperature > 25 °C [4], solid retention time (SRT) < 5 day and dissolved oxygen (DO) between 1 and 2 mg L^{-1} [13], C/N ratios < 6, free ammonia (FA) in the range of 0.1–5 mg N L^{-1}, free nitrous acid (FNA) concentrations of 0.011-0.026 mg N L^{-1} and alternating anoxic and aerobic conditions [14,15]. Up to date, SPND has been mainly studied in sequencing batch reactor (SBR) [10,15,16], while only a few continuous-mode applications exist in the literature. Yang and Yang [9] were able to achieve N removal efficiency (RE) of 88% through SPND in an intermittent aeration (IA) continuous-flow moving bed membrane bioreactor with HRT of 16 h and COD/N ratios between 3.7 and 5.6, demonstrating that IA was an effective approach to achieve SPND, although fluorescence in situ hybridizations revealed the presence of NOB inside the system.

Combining biological nitrogen removal via SPND to P removal in a continuous-flow bioreactor represents a promising opportunity for achieving cost-effective nutrient removal from municipal wastewater. However, coupling the SPND process to P removal

might be challenging due to potential inhibitory effect of nitrite on phosphorus accumulating organisms (PAOs) [4]. Recently, Roots et al. [17] combined SPND and biological P removal by alternating anaerobic, anoxic and aerobic conditions in a sequencing batch reactor (SBR) treating real mainstream wastewater with influent N-NH_4^+ and P-PO_4^{3-} concentrations of 13.5–15.8 and 1.8–1.4 mg L^{-1}, respectively. The authors showed average COD, N and P REs of 70%, 83% and 81%, respectively. Up to date, no previous studies combined single-stage SPND and P removal in continuous-flow systems.

The key microorganisms involved in enhanced biological phosphorus removal (EBPR) include polyphosphate accumulating organisms (PAOs) and denitrifying PAOs (DPAOs) which are commonly cultivated under the alternation of anaerobic and aerobic (PAOs) or anoxic (DPAOs) conditions. Under anaerobic conditions PAOs uptake small organic carbon molecules such as short-chain volatile fatty acids (VFAs), glucose and ethanol and store them as polyhydroxyalkanoate (PHA) [18]. The energy is obtained from the breakage of internally-stored polyphosphate, which causes a release of orthophosphate into the bulk liquid [19]. During aerobic or anoxic conditions, PAOs or DPAOs oxidize the stored PHA through an available electron acceptor (DO or NO_x^-, respectively) and use the released energy for P uptake [20]. In particular, DPAOs can simultaneously remove nitrogen and phosphorus via NO_3^- and NO_2^- reduction [21]. Although an anaerobic phase is commonly foreseen for PAO and DPAO cultivation [17], biological P removal has been achieved also under continuous aerobic conditions when VFAs are provided externally [18,22,23]. Vargas et al. [22] reported net P removal in SBR during 46 days of aerobic operation with DO between 3.5 and 4.5 mg L^{-1} using propionate as carbon source. According to Pijuan et al. [23], PAO can uptake VFAs when fed under aerobic conditions in a similar way as under anaerobic conditions, while phosphate is released in the medium and glycogen is degraded (feast phase). Once VFAs are depleted, PAOs uptake phosphate and degrade PHA (famine phase) as in conventional EBPR.

Recently, Iannacone et al. [5] achieved combined SND and P removal in an acetate-fed MBBR alternating microaerobic and aerobic conditions with dissolved organic carbon (DOC), total inorganic nitrogen (TIN) and P-PO_4^{3-} REs > 80%, confirming that efficient biological N and P removal is possible under continuous microaerobic/aerobic conditions by maintaining the DO range at 0.2-3 mg L^{-1}. However, the study focused on the complete SND process with acetate as sole energy source. As a next step, the feasibility of combined SPND and P removal in single-stage MBBR under IA conditions should be investigated. Also, investigating the effect of different carbon sources is crucial, as carbon

source may exert a major impact on bioreactor operation and REs due to different COD requirement and microbial community development [24].

In the present study, SPND coupled to P removal was investigated in two continuous-flow MBBRs alternating microaerobic and aerobic conditions and fed with two different carbon sources, i.e. acetate and ethanol. The main objectives of the study were to (1) assess the feasibility to combine single-stage SPND and P removal in continuous-flow MBBRs, (2) determine the MBBR performances in terms of DOC, TIN and $P\text{-}PO_4^{3-}$ REs with two different organic carbon sources, (3) evaluate the influence of feed C/P ratio on MBBRs performance and (4) identify the dominant bacteria responsible for C, N and P removal in the two MBBRs.

5.2 Material and methods

5.2.1 Experimental set-up

Combined SPND and P removal was studied in two identical lab-scale MBBRs, one fed with acetate (MBBR-Ac) and one with ethanol (MBBR-Et) as organic substrate. The reactors were composed of a cylindrical glass vessel with working volume of 1.5 L sealed by a plexiglass lid with openings for probes and tubing. Each reactor was operated in continuous mode and a peristaltic pump was used for influent feeding and effluent suction (Watson-Marlow, UK) to maintain a constant level. The reactors were placed on a magnetic stirrer working at 120 rpm to maintain mixing conditions. Air was delivered to the reactors by an aquarium air pump and solubilized into the medium through a porous stone. The applied air flow rates were 120–130 mL min^{-1} for MBBR-Ac and 140–160 mL min^{-1} for MBBR-Et (**Table 1**). Differences in applied air flow rates for the two MBBRs were due to the higher COD of ethanol (COD/DOC = 4.0) compared to acetate (COD/DOC = 2.3). Automated DO control was carried out as described by Iannacone et al. [5].

5.2.2 Biomass cultivation

Recycle sludge with total solid (TS) and volatile solid (VS) concentrations of 3.0 and 2.1 g L^{-1}, respectively, was collected from the pre-denitrification system of the municipal wastewater treatment plant (WWTP) of Cassino (Italy) and used as inoculum for the cultivation of denitrifying and nitrifying biomass. Denitrifying bacteria were cultivated in batch mode as described by Iannacone et al. [5] for 40 days until denitrifying activity and biofilm growth in the bioreactor were verified. AOB were cultivated in a separate

glass bioreactor filled with 400 mL of cultivation medium and 100 mL of inoculum. The cultivation medium was composed of distilled water, 0.246 g L^{-1} of NH_4Cl, 1 g L^{-1} of $NaHCO_3$ and nutrients as described by Iannacone et al. [5]. pH was maintained at 8.2 (±0.2) by the addition of $NaHCO_3$ when necessary. Half of bioreactor mixed solution was replaced with fresh medium every 2 days (except the weekends), resulting in an average SRT of 4 days. AOB were sub-cultured 5 times before inoculating the two MBBRs. Samples from denitrifying and nitrifying bioreactors were collected before and after each refresh operation to monitor pH, total alkalinity and the concentrations of NH_4^+, NO_2^- and NO_3^-. During cultivation phase, temperature was in the range of 26–28°C.

5.2.3 Bioreactor start-up and influent composition

Bioreactor start-up was carried out by dividing biofilm-coated carriers, nitrifying biomass and synthetic wastewater into two reactor vessels up to 1.3 L. The carrier filling ratio in each MBBR was around 40%. Synthetic wastewater (pH 8.0±0.1) was used as influent to test different feed C/N and C/P ratios during the study and was prepared using tap water. Sodium acetate and ethanol (96% v/v) were used as carbon sources at theoretical DOC concentrations of 90–105 mg L^{-1}. Ammonium chloride (NH_4Cl) was added to obtain a theoretical N-NH_4^+ concentration of 25 mg L^{-1} (48 mg L^{-1} during start-up) and was the only nitrogen source in the medium except during start-up, when KNO_3 (0.23 g L^{-1} in the bulk liquid) was also supplemented to sustain denitrification (**Table 1**). Potassium phosphate monobasic (KH_2PO_4) was used as source of phosphorus to obtain theoretical P-PO_4^{3-} concentrations of 4.5 and 9 mg L^{-1} depending on the period (**Table 1**). Influent DOC, N-NH_4^+ and P-PO_4^{3-} concentrations were chosen based on a survey on the influent streams entering local WWTPs serving small communities. A trace element solution composed as described by Iannacone et al. [6] was also added to the feed. During the study, synthetic wastewater was maintained refrigerated at 5°C.

The two MBBRs were operated for 2 days in batch mode. Half of the mixed solution was replaced with fresh synthetic wastewater as soon as DOC or NH_4^+ was consumed. The DO concentration in this phase was set to alternate between 0.2 and 3 mg L^{-1}. Subsequently, the reactors were operated in continuous mode at a 1-day HRT for 1 week (**Table 1**) to allow the establishment of a multilayer microbial biofilm on the carriers.

5.2.4 MBBR operation

MBBR-Ac and MBBR-Et were operated at HRT of 1 day under five different experimental periods (P1–P5, **Table 5.1**).

Table 5.1 - Experimental conditions and feed composition during continuous MBBR-Ac and MBBR-Et operation.

Periods	Reactor	Time (day)	DO Range (mg L^{-1})	Air flow (mL min^{-1})	C/N Ratio	C/P ratio	N-NH_4^+ (mg L^{-1})	TIN (mg L^{-1})	P-PO_4^{3-} (mg L^{-1})
Start-up	MBBR-Ac	3–9	0.2–3.0	120	1.5 (±0.1)	10.1 (±1.5)	48 (±1)	65 (±1)	10 (±1)
	MBBR-Et		0.2–3.0	140	1.4 (±0.1)	10.0 (±0.4)	48 (±0)	66 (±1)	9 (±1)
P1	MBBR-Ac	10–51	0.2–3.0	120	3.5 (±0.3)	11.1 (±1.1)	26 (±1)	27 (±1)	8 (±1)
	MBBR-Et		0.2–3.0	140	3.6 (±0.3)	12.3 (±1.7)	26 (±1)	26 (±1)	8 (±1)
P2	MBBR-Ac	52–79	0.2–3.0	120	3.0 (±0.3)	19.9 (±2.0)	25 (±1)	26 (±1)	4 (±0)
	MBBR-Et		0.2–3.0	140	3.5 (±0.2)	21.9 (±3.0)	24 (±1)	25 (±1)	4 (±0)
P3	MBBR-Ac	80–93	0.2–2.0	120	3.4 (±0.1)	9.3 (±0.1)	26 (±0)	27 (±0)	9 (±1)
	MBBR-Et		0.2–2.0	140	3.4 (±0.3)	9.9 (±1.2)	25(±1)	26 (±1)	9 (±1)
P4	MBBR-Ac	94–105	0.2–3.0	120	3.3 (±0.1)	9.7 (±0.1)	25 (±0)	26 (±0)	8 (±0)
	MBBR-Et		0.2–3.0	140	3.5 (±0.2)	10.5 (±0.4)	24 (±0)	25 (±0)	8 (±0)
P5	MBBR-Ac	106–135	0.2–3.0	130	4.0 (±0.2)	13.1 (±0.8)	25 (±1)	26 (±1)	8 (±0)
	MBBR-Et		0.2–3.0	160	4.0 (±0.4)	13 (±0.9)	26 (±1)	27 (±1)	8 (±0)

During P1–P4 (days 10–105), the feed DOC concentrations were 89 (±9.1) mg L^{-1} for MBBR-Ac and 91 (±5.9) mg L^{-1} for MBBR-Et. During P1 (days 10–51), the DO range was maintained at 0.2–3 mg L^{-1} for both MBBRs and a feed C/N ratio of 3.6 was chosen being the optimal value observed in a previous study for sustaining combined SND and P removal in a microaerobic/aerobic MBBR [5]. Feed P–PO_4^{3-} concentration in the two MBBRs was 8 (±1) mg L^{-1}, resulting in feed C/P ratios of 11.1 (±1.1) for MBBR-Ac and 12.3 (±1.7) for MBBR-Et. At the beginning of P2, the feed C/P ratio was increased to 19.9 (±2.0) for MBBR-Ac and to 21.9 (±3.0) for MBBR-Et by decreasing the feed P-PO_4^{3-} concentrations to 4 mg L^{-1} (**Table 1**) to evaluate the impact of lower feed P-PO_4^{3-} concentrations on the process, being more representative of municipal wastewater. At the end of P2 (day 68), the DO range was set to 0.2–2 mg L^{-1} in both bioreactors with the objective to recover the SPND process after a malfunctioning of the DO control system. In order to evaluate the recovery of the SPND process, the C/P ratio was decreased to around 10 (P3) and the DO range was set to 0.2–3 mg L^{-1} (P4). At the beginning of P5 (day 106), the feed C/N ratio was increased to 4.0 for both MBBRs with the aim to support denitrification and enhance nitrogen removal.

Feed pH and alkalinity during the study were stable at 8.1 (±0.1) and 1011 (±39) mg $CaCO_3$ L^{-1} for MBBR-Et and at 8.1 (±0.2) and 1214 (±46) mg $CaCO_3$ L^{-1} for MBBR-Ac, respectively. Temperature was not controlled during the study and was in the range of 28–32°C during P1-P2 and 22–28°C during P3–P5. SRT was not controlled during continuous operation as no settling or recycling was provided.

5.2.5 Calculations

Total inorganic nitrogen (TIN), P-PO_4^{3-} and DOC REs as well as nitrification efficiency (N_{eff}) and denitrification efficiency (D_{eff}) were calculated as described by **Eqs. 5.1-5.5**:

$$\text{TIN RE (\%)} = \frac{\left([\text{N-NH}_{4,i}^{+}] + [\text{N-NO}_{3,i}^{-}] - [\text{N-NH}_{4,e}^{+}] - [\text{N-NO}_{3,e}^{-}] - [\text{N-NO}_{2,e}^{-}]\right)}{\left([\text{N-NH}_{4,i}^{+}] + [\text{N-NO}_{3,i}^{-}]\right)} \times 100 \quad (5.1)$$

$$\text{P-PO}_4^{3-}\ \text{RE (\%)} = \frac{\left([\text{P-PO}_{4,i}^{3-}] - [\text{P-PO}_{4,e}^{3-}]\right)}{\left([\text{P-PO}_{4,i}^{3-}]\right)} \times 100 \quad (5.2)$$

$$\text{DOC RE (\%)} = \frac{([\text{DOC}_i] - [\text{DOC}_e])}{([\text{DOC}_e])} \times 100 \quad (5.3)$$

$$N_{eff}\ (\%) = \frac{\left([\text{N-NH}_{4,i}^{+}] - [\text{N-NH}_{4,e}^{+}]\right)}{\left([\text{N-NH}_{4,i}^{+}]\right)} \times 100 \quad (5.4)$$

$$D_{eff}\ (\%) = \frac{\left([N\text{-}NH_{4,i}^{+}]\text{-}[N\text{-}NH_{4,e}^{+}]+[N\text{-}NO_{3,i}^{-}]\text{-}[N\text{-}NO_{3,e}^{-}]\text{-}[N\text{-}NO_{2,e}^{-}]\right)}{\left([N\text{-}NH_{4,i}^{+}]\text{-}[N\text{-}NH_{4,e}^{+}]+[N\text{-}NO_{3,i}^{-}]\right)} \text{ x } 100 \quad (5.5)$$

Where:

- $[N\text{-}NH_{4,i}^{+}]$ and $[N\text{-}NH_{4,e}^{+}]$ are the influent and effluent $N\text{-}NH_4^+$ concentrations, respectively;
- $[N\text{-}NO_{x,i}^{-}]$ and $[N\text{-}NO_{x,e}^{-}]$ are the influent and effluent $N\text{-}NO_x^-$concentrations, respectively;
- $[P\text{-}PO_{4,i}^{3-}]$ and $[P\text{-}PO_{4,e}^{3-}]$ are the influent and effluent $P\text{-}PO_4^{3-}$ concentrations, respectively;
- $[DOC_i]$ and $[DOC_e]$ are the influent and effluent DOC concentrations, respectively.

5.2.6 Microbial identification

The microbial communities of both biofilm and suspended biomass of the two MBBRs were analyzed at the end of P1 and P2. Samples were collected from the two MBBRs and stored at -20 °C before analysis. Biofilm was detached from the carriers by 5-min sonication at 45 Hz followed by manual shaking. DNA extraction and quantification were performed as described by Iannacone et al. [5]. PCR amplification, library quantification, Illumina sequencing, sequence filtering and taxonomic classification were performed as described by Ucar et al. [25].

5.2.7 Analytical methods

Liquid samples were collected 3–4 times/week from both bioreactors and influent tanks. At the end of each experimental period, carrier-attached and suspended biomass was collected for volatile suspended solid (VSS) analysis. The concentrations of DOC, NO_3^-, NO_2^- and PO_4^{3-} in liquid samples were measured immediately after sampling as described by Iannacone et al. [5] and upon filtration through 0.45 μm syringe filters (VWR, USA). pH and total alkalinity were analyzed in unfiltered samples as described by Di Capua et al. [26]. VSS was measured in duplicate according to Classen et al. [27].

5.2.8 Statistical data analysis

The statistical differences in the performance parameters (DOC, TIN and $P\text{-}PO_4^{3-}$ REs) between different periods were evaluated by one-way factor analysis of variance (ANOVA) using the Data Analysis Tool of Excel 2016 (Microsoft Corporation, USA). The significant difference was set at 95 % ($p < 0.05$).

5.3 Results and discussion

5.3.1 Inhibition of NOB activity during cultivation and MBBR operation

During cultivation phase, NOB growth was successfully inhibited by adopting the SRT, pH and temperature conditions described in Section 2.2. $N\text{-}NO_3^-$ concentration in the cultivation medium was stable at 11 (±1) mg L^{-1}, while $N\text{-}NO_2^-$ accumulation up to 91 mg L^{-1} was observed at each cycle due to $N\text{-}NH_4^+$ oxidation. In literature, pH values between 7.5 and 8.5 were reported to inhibit NOB activity due to direct effect on enzymatic mechanisms [4,12], while temperatures higher than 25°C expand the differences in specific growth rate between AOB and NOB. Due to lower maximum specific growth rate of NOB, these bacteria can only survive in reactors operated at long SRT [28].

NOB suppression during cultivation phase allowed to inoculate both MBBRs with a biomass pool devoid (or with negligible concentrations) of NOB, which resulted in successful SPND during the first 69 days of MBBR operation under IA (DO = 0.2-3 mg L^{-1}) and alkaline pH (≥ 8.2) conditions. Several studies demonstrated that IA can effectively induce NOB inhibition [9,28]. During the transition from microaerobic to aerobic conditions the lag time of AOB and NOB is the most important factor. NOB enzymes are deactivated under anoxic/microaerobic conditions and reactivated under aerobic conditions, but most importantly AOB recover faster than NOB under aerobic conditions resulting in NO_2^- accumulation. Inhibition of NOB was also confirmed by microbial identification of both MBBR biofilm and suspended biomass performed at the end of P1 and P2, as the relative abundance of NOB remained below detection limit (**Table 2, Figure 4**).

5.3.2 SPND performance of MBBR-Ac and MBBR-Et

The evolution of $N\text{-}NH_4^+$, $N\text{-}NO_2^-$ and $N\text{-}NO_3^-$ concentrations in MBBR-Ac and MBBR-Et effluents is described in **Fig. 1**, while TIN RE profiles are shown in **Fig. 2**. During P1 (days 10–51), MBBR-Ac and MBBR-Et showed stable TIN REs of 81 (±6) % and 86 (±6) %, respectively, with average $N\text{-}NH_4^+$ and $N\text{-}NO_2^-$ concentrations in the effluent below 5 mg L^{-1}. Effluent $N\text{-}NO_3^-$ concentration was below 1 mg L^{-1} (on average), indicating that satisfactory SPND was achieved. It is generally known that DO is the main limiting factor of NH_4^+ and NO_2^- oxidation during the SND process [10], also due to the electron acceptor competition between AOB and heterotrophic aerobic bacteria (HAB).

In this study, IA at DO levels between 0.2 and 3 mg L^{-1} was successful in inhibiting the growth of NOB during continuous MBBR operation.

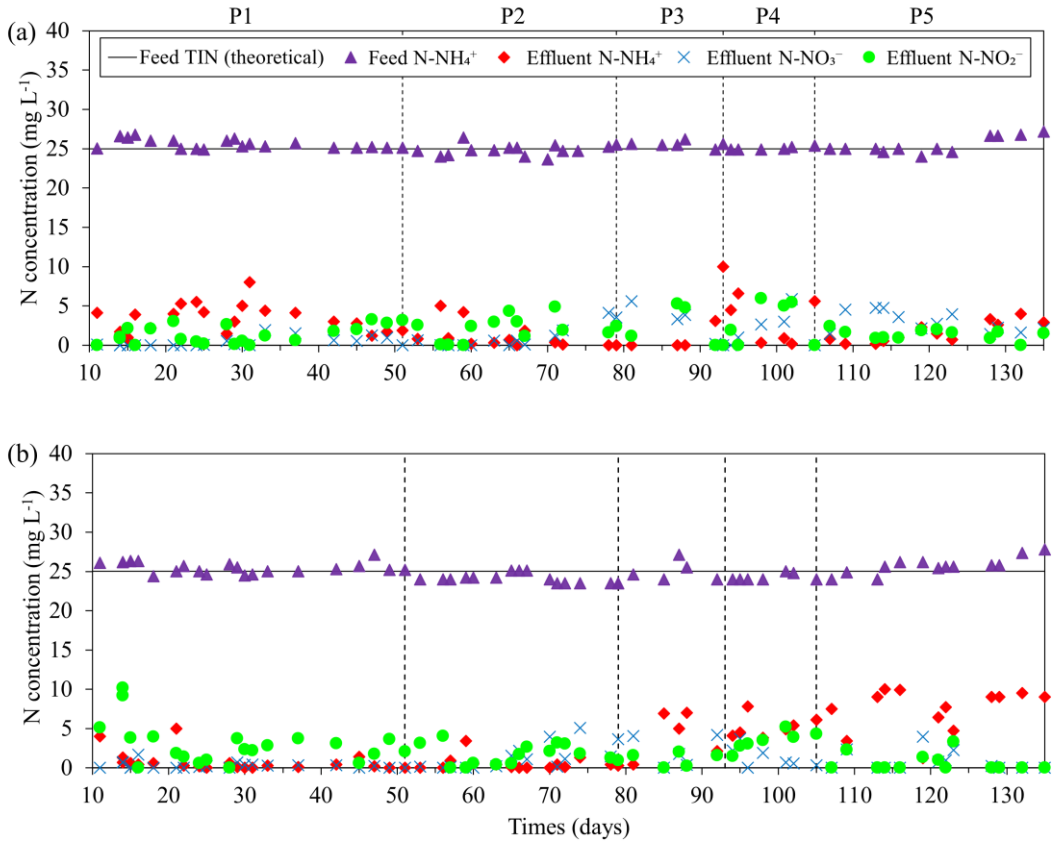

Figure 5.1 - Temporal profiles of the influent and effluent N-NH_4^+, N-NO_3^- and N-NO_2^- concentrations during continuous MBBR-Ac (a) and MBBR-Et (b) operation.

N_{eff} and D_{eff} of MBBR-Ac were 87 (±7) % and 93 (±6) %, respectively, with D_{eff} reaching 100% on day 16. MBBR-Et achieved N_{eff} of 100% (days 29–31), while D_{eff} remained at 88 (±8) %. During the entire experimental period, DOC in the two MBBRs remained below detection limit, being used from HAB and DNB activities, which means that DOC was the limiting factor for denitrification. Municipal wastewater often presents low C/N ratios and supplementation of additional organics can be required to achieve a satisfactory denitrification efficiency [29]. The SPND process demands less organic carbon for denitrification, which is advantageous for the treatment of low C/N wastewaters and leads to higher REs compared to SND. In a previous work, Iannacone et al. [5] achieved an average TIN RE of 62% by SND in a MBBR operated under similar feed C/N ratio and

IA conditions. In comparison, the SPND process established in this study improved average TIN RE in the MBBR by > 20%.

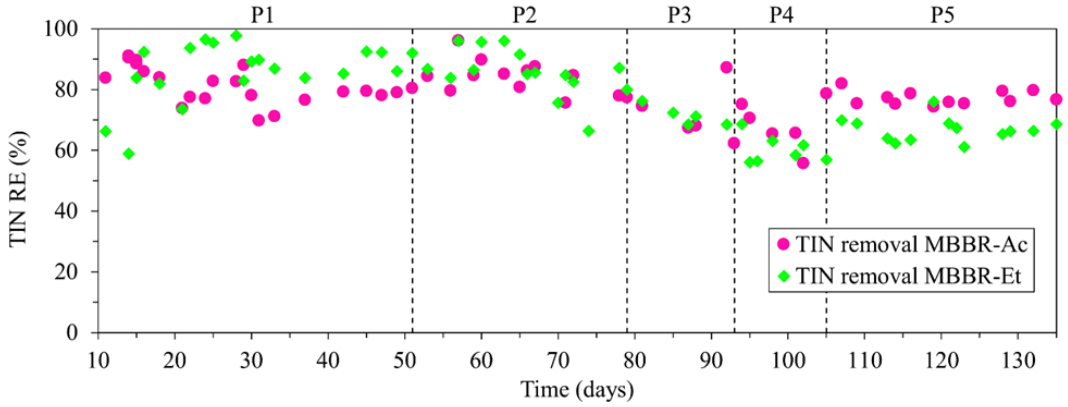

Figure 5.2 - TIN RE profiles during continuous MBBR-Ac and MBBR-Et operation.

The N_{eff} of MBBR-Et was higher than that of MBBR-Ac, despite the lower relative abundance of *Nitrosomonas* observed at the end of P1 in the biofilm of MBBR-Et compared to that of MBBR-Ac (**Table 2**). It could be possible that genera reported as potential heterotrophic nitrifiers (i.e. *Thauera* and *Pseudomonas*) or anammox bacteria (i.e. *OM190*), which were detected with higher abundance in MBBR-Et than in MBBR-Ac (**Table 2**), had a role in $N\text{-}NH_4^+$ removal. It should be highlighted that *Nitrosomonas* were detected only in the biofilm of the two MBBRs, indicating that suspended biomass was not responsible for *nitritation*.

During days 52–69 of P2, TIN RE of around 86% was observed for both MBBRs as average concentrations of $N\text{-}NH_4^+$, $N\text{-}NO_2^-$ and $N\text{-}NO_3^-$ did not exceed 2 mg L^{-1} (**Fig. 1**). N_{eff} reached 100% with an average value of 96 (±5) % for MBBR-Ac and 98 (±5) % for MBBR-Et. In particular, N_{eff} for MBBR-Et was around 10% higher than that observed during P1. This is consistent with the doubling of relative abundance of *Nitrosomonas* in the MBBR-Ac biofilm, which increased from 0.7% (P1) to 1.4% (P2) (**Table 2**). The average D_{eff} in MBBR-Et was 4% higher than that observed in P1 (which may be attributed to higher DOC availability due to the increase of feed C/P ratio in P2), while stable values were observed in MBBR-Ac. Carbon source was reported to affect the activity of the enzymes involved in nitrogen oxidation and reduction processes as well as microbial diversity [28]. In particular, acetate should favor bacterial diversity, while ethanol is one of the preferred organic substrate for heterotrophs and stimulates their growth [24]. This is congruent with sequencing results, showing a considerable increase in relative abundance of HAB such as *Neochlamydia* and *Bdellovibrio* in the suspended

microbial community of MBBR-Et during P2 and a lower relative abundance of *Nitrosomonas* in the MBBR-Et biofilm compared to MBBR-Ac (**Table 2**).

On day 69, a malfunctioning of the DO control system led to an increase of DO concentration to around 5 mg L^{-1} over the weekend. As a result, during days 70–79, NO_3^- was detected in the effluents of the two bioreactors at concentrations ranging from 1 to 5 mg L^{-1}. The presence of NO_3^- in the effluent indicates that NOB activity was ongoing, although Illumina sequencing of biofilm and suspended biomass did not detect typical NOB (**Fig. 4**). The increase of NO_3^- concentration at the end of P2 could be due to the activity of heterotrophic nitrifiers such as members of the genus *Flavobacterium* [8], which showed a strong increase of relative abundance in the microbial communities of both biofilm and suspended biomass compared to those observed in the previous period (**Table 2**).

The growth of NOB may be more restricted under low DO concentrations than that of AOB, as the latter have a higher affinity for oxygen. In the literature, the Monod oxygen saturation constant K_{DO} for AOB and NOB is reported to be equal to 0.3 and 1.1 mg L^{-1}, respectively [14]. Hence, during P3 (days 80–93) the objective was to recover shortcut SND by further limiting DO in the system. Therefore, DO regime was set to 0.2–2 mg L^{-1} to reduce NOB activity. In this way, effluent NO_3^- in MBBR-Ac could be depleted by the end of the period (**Fig. 1**). However, $N\text{-}NH_4^+$ concentration increased in both MBBRs up to 10 mg L^{-1} as a result of competition between AOB and HAB for the available DO (**Fig. 1**). $N\text{-}NH_4^+$ breakthrough decreased TIN RE of the two MBBRs from 84–86% (P2) to 71–72% (P3) (**Fig. 2**).

At the beginning of P4 (day 94), the DO range was set at 0.2–3 mg L^{-1} for both bioreactors with the objective to recover nitrogen removal. Nevertheless, TIN RE further decreased to 69 (±8) % for MBBR-Ac and 60 (±5) % for MBBR-Et. Decrease in TIN RE was mainly due to loss of D_{eff}, which decreased in both MBBRs by 6–10% and particularly in MBBR-Ac, although N_{eff} recovery in MBBR-Ac led to higher TIN RE compared to MBBR-Et. As shown by NO_3^- profile in the effluent (**Fig.1**), the SPND was not recovered completely. In addition to the high DO levels experienced by the MBBRs for 2 days, adaptation of NOB to low DO levels experienced during IA operation could occur. Previous studies reported an increase of oxygen affinity for NOB after long-term operation at low DO levels [30]. Washout of NOB is difficult to achieve and often requires operational temperatures > 30°C or considerable sludge discharge. Decrease of operational temperature during the study did not favor recovery of the SPDN process.

.

Table 5.2 - Identification at genus level, relative abundance (%) and phylogenetic affiliation of bacteria populating biofilm and suspended biomass of MBBR-Ac and MBBR-Et. Only genera with relative abundance above 4% are listed (except for AOB).

Key functional group	Genus	Phylum	MBBR-Ac				MBBR-Et			
			P1		P2		P1		P2	
			Biofilm	Suspended biomass	Biofilm	Suspended biomass	Biofilm	Suspended biomass	Biofilm	Suspended biomass
DNB	*Thauera*	*Proteobacteria*	7.2	4.5	7.3	5.5	14.2	6.0	6.4	6.5
	Luteimonas	*Proteobacteria*	4.0	5.9	1.9	2.3	1.8	5.6	1.2	0.5
	Flavobacterium	Bacteroidetes	0.4	0.6	5.2	13.5	0.8	0.8	3.4	4.6
	Arenimonas	Proteobacteria	0.2	0.3	6.6	0.3	0.1	0.4	0.3	0.7
	Rhizobium	*Proteobacteria*	15.6	19.2	7.3	12.0	4.8	19.2	3.1	0.9
	Aquamicrobium	*Proteobacteria*	2.5	3.4	1.5	1.6	1.2	3.9	0.9	n.d.
DNB/ putative DNPAOs	*Pseudomonas*	*Proteobacteria*	0.3	2.1	1.1	0.8	8.8	2.8	10.6	1.0
DNB/ putative PAOs	*Acidovorax*	*Proteobacteria*	13.5	13.8	1.5	7.0	n.d.	13.0	0.7	n.d.
	Hydrogenophaga	*Proteobacteria*	2.2	4.2	1.4	1.7	4.4	4.5	0.8	1.3
putative PAOs	*Hyphomicrobium*	*Proteobacteria*	n.d.	1.3	0.9	n.d.	10.4	3.8	2.7	9.1
Anammox	*SM1A02*	*Planctomycetes*	5.0	0.9	8.6	2.2	1.9	0.7	4.1	0.6
	OM190	*Planctomycetes*	0.2	0.7	1.6	0.2	11.3	0.8	2.9	0.1
HAB	*Neochlamydia*	*Verrucomicrobiota*	n.d.	n.d.	n.d.	n.d.	n.d.	n.d.	0.7	12.4
	Parapusillimonas	*Proteobacteria*	2.2	6.0	0.3	2.2	n.d.	6.3	0.2	0.1
	Leadbetterella	*Bacteroidetes*	3.0	1.8	8.0	12.2	2.7	2.0	1.6	3.4
	Bdellovibrio	*Bdellovibrionota*	4.4	7.2	3.1	5.3	2.9	6.1	15.1	34.7
	Uncultured _Anaerolineaceae	*Chloroflexi*	5.6	1.7	9.8	2.7	0.9	1.5	4.3	n.d.
	Dojkabacteria	*Patescibacteria*	5.8	9.6	4.9	1.0	4.7	6.1	4.1	n.d.
AOB	*Nitrosomonas*	*Proteobacteria*	0.7	n.d.	1.4	n.d.	0.3	n.d.	0.6	n.d.

n.d. = not detected

In order to improve D_{eff} and recover TIN RE, at the beginning of P5 the feed C/N ratio was increased to 4.2 (**Table 1**). As a result, D_{eff} in the two MBBRs increased by 7-18 % compared to P3. However, while MBBR-Ac showed stable N_{eff} of 94 (±5) % and TIN RE of 77 (±2) % during P5, MBBR-Et experienced a decrease of N_{eff} from 78 (±6) % (P4) to 68 (±7) % (P5). $N\text{-}NH_4^+$ concentration in the MBBR-Et effluent during P5 was 29% higher than in P4. As a consequence, TIN RE of MBBR-Et was around 10% lower than that of MBBR-Ac (**Fig. 2**). Decrease of N_{eff} in MBBR-Et was likely due to an excess growth of HAB competing with nitrifying bacteria for DO. HAB feature higher growth rate and oxygen affinity compared to nitrifying bacteria and can outcompete them, thus suppressing nitrification inside the biofilm [6,31].

The concentration of carrier-attached biomass during the study remained stable at 2.0 (±0.4) and 2.1 (±0.4) mg VSS $carrier^{-1}$ for MBBR-Ac and MBBR-Et biofilm, respectively. However, while the MBBR-Ac biofilm looked always compact and thin, the MBBR-Et during P5 appeared thick and porous, which could be due to a higher abundance of heterotrophic and filamentous bacteria [32]. This likely limited DO diffusion within the biofilm and hampered nitrification.

In this work, effluent TIN concentrations during continuous operation were nearly always ≤ 10 mg L^{-1} and never exceeded 12 mg L^{-1} at all tested conditions. These concentrations comply with the Italian and European legislation (Urban Wastewater Treatment Directive 98/15/EC), which has set a threshold for total nitrogen in urban wastewater of 10–15 mg L^{-1} depending on the size of the urban center, i.e. 10 mg L^{-1} for population equivalent (PE) >100000 and 15 mg L^{-1} for PE <100000. Despite the satisfactory TIN removal, NO_2^- levels observed in the effluent might be of concern for aquatic life being often higher than 0.6 mg $N\text{-}NO_2^-$ L^{-1} [33] and increase chlorine demand during disinfection. Therefore, adjustment of DO cycle would be required for process upscaling, e.g. by applying longer microaerobic periods which could improve D_{eff} and reduce effluent NO_2^- levels.

5.3.3 Phosphorus removal

During the study, between 62% and 95% of feed $P\text{-}PO_4^{3-}$ was removed by the two MBBRs (**Fig. 3**). Average $N\text{-}NO_2^-$ concentrations in the effluent remained below 3 mg L^{-1}, being lower than levels reported as inhibitory for aerobic P uptake (>10 mg $N\text{-}NO_2$ L^1) [5,34].

During P1, $P\text{-}PO_4^{3-}$ concentration in MBBR effluents was stable at around 1 mg L^{-1}, resulting in average REs ≥ 80% (**Fig. 3**). The decrease of feed $N\text{-}NO_3^-$ concentration from

18 mg L^{-1} (start-up) to around 1 mg L^{-1} determined an increase of $P\text{-}PO_4^{3-}$ RE from 35 (±1) % to 83 (±3) % for MBBR-Ac and from 39 (±1) % to 86 (±6) % for MBBR-Et, which can be attributed to the decreased competition between DNB and PAOs for the available organic carbon. At the end of P1, bacteria belonging to *Hydrogenophaga*, *Acidovorax* and *Pseudomonas* were detected with high relative abundances in the biofilm and suspended biomass of both MBBRs (**Table 2**). Members of these genera are often classified as putative PAOs due to the ability to form and store polyphosphate [20,35] and may have played a key role in P removal in the two MBBRs. In a previous study, Iannacone et al. [5] found that *Hydrogenophaga* was the dominant species in the biofilm of a continuous-flow MBBR combining N and P removal under IA conditions. According to Ge et al. [20], there is strong evidence that the genus *Hydrogenophaga* includes bacteria with P-accumulating ability.

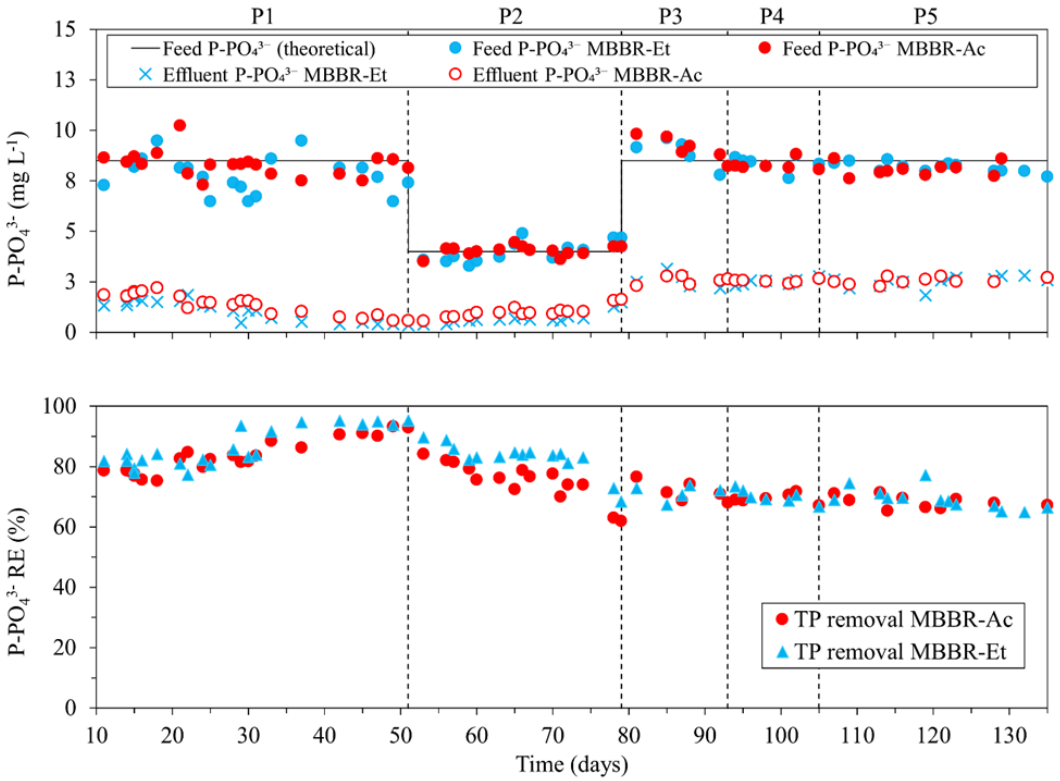

Figure 5.3 - Temporal profiles of influent and effluent $P\text{-}PO_4^{3-}$ concentrations and $P\text{-}PO_4^{3-}$ REs in the MBBR-Ac and MBBR-Et.

Phosphorus removal in the two MBBRs was achieved under continuous feeding conditions and without the presence of the anaerobic stage, which is commonly foreseen for EBPR in SBR as it allows the conversion of complex organic matter to VFAs and establishes a feast phase triggering PAO metabolism. In both MBBRs operated in this

study, NO_3^- concentrations during the first 69 operational days were negligible. Therefore, microaerobic/aerobic operation in the two MBBRs may have induced the alternation of anaerobic and (micro)aerobic conditions in the inner layers of the biofilm and promoted PAO metabolism. However, it should be highlighted that the anaerobic phase is not mandatory for EBPR. Several studies have highlighted the possibility to carry out P removal when the electron donor (VFAs or alcohols) and the electron acceptor (oxygen) are present simultaneously [18]. Pijuan et al. [23] showed that the alternation of feast/famine phases can occur also under strictly aerobic conditions in concomitance with the availability (feast) and absence (famine) of VFAs in the reactor operated as SBR.

At the beginning of P2, the feed C/P ratio in the two MBBRs was nearly doubled by decreasing the feed P-PO_4^{3-} concentration from 8 to 4 mg L^{-1} (**Table 1**). The increase of feed C/P ratio determined a decrease of P-PO_4^{3-} RE to 77 (±4) % for MBBR-Ac and to 84 (±2) % for MBBR-Et (**Fig. 3**). Low COD/P-PO_4^{3-} ratios are recommended in EBPR systems for achieving high P-PO_4^{3-} RE, as high values favor the proliferation of heterotrophic bacteria other than PAOs [21,36]. Sequencing analysis revealed that during P2 the populations of *Hydrogenophaga* and *Acidovorax* decreased significantly both in the biofilm and suspended biomass of the MBBRs and an overall increase of HAB (such as *Leadbetterella* and *Bdellovobrio*) was observed (**Table 2**).

From P3 to P5, P-PO_4^{3-} concentration in the effluent of the two MBBRs was stable at around 3 mg L^{-1}, which was about 2-fold higher than that observed during P2. As a result, P-PO_4^{3-} RE decreased to around 70 % in both MBBRs (**Fig. 3**). Decrease of DO levels during P3 may have favored denitrifiers over PAOs for the available DOC, reducing P-PO_4^{3-} RE. Restoring the DO regime to 0.2–3 mg L^{-1} (P4) and increasing the feed C/P ratio to 13 (P5) did not improve P-PO_4^{3-} removal, which can be attributed to the competition with HAB for the available DOC.

Decrease of P-PO_4^{3-} RE can be expected when treating real wastewater due to the presence of complex and low-biodegradable organic matter. Longer microaerobic phases may induce anaerobic zones in the deeper layers of the biofilm, allowing partial conversion of complex organics to VFA and supporting P-PO_4^{3-} removal.

5.3.4 Microbial community structure in MBBRs performing SPND

The microbial communities of the two MBBRs during the first two operational periods (P1 and P2) were similar. *Proteobacteria* were the dominant phylum in both biofilm and suspended biomass, being present at relative abundances between 39% and 60% in the

biofilm and between 36% and 74% in suspended biomass. *Proteobacteria* include species typical of wastewater treatment systems and often related to nitrogen removal [14,37]. The phyla *Bacteroidetes*, *Bdellovibrionota* and *Planctomycetes* were also present at all operational periods in both biofilm and suspended biomass with relative abundances in the range of 7–31%, 3–35% and 2–11%, respectively. The relative abundances of *Bdellovibrionota* in MBBR-Et at the end of P2 (15–35%) were significantly higher than those observed in the same bioreactor at the end of P1 (3–6%) and in MBBR-Ac in both periods (4–7%). *Bdellovibrionota* are heterotrophic and obligate aerobic bacteria that can prey upon gram-negative bacteria. The increase of HAB during P2 was a consequence of the higher feed C/P ratio applied in P2 compared to P1 (**Table 1**). In contrast, the population of *Chloroflexi* in suspended biomass of MBBR-Et at the end of P2 decreased below the detection limit, while a higher relative abundance (8%) compared to previous period (5%) was observed in the biofilm. *Bacteroidotes* and *Chloroflexi* were reported to dominate EBPR systems and include DNPAOs [21]. *Planctomycetes*, which were detected during P1 and P2 in the biofilm and suspended biomass of both MBBRs, are typical of anammox systems and their presence could be attributed to the concomitance of ammonia, nitrite and high operational temperatures [38]. The relative abundance of these bacteria in the biofilm was much higher than in the suspended biomass (**Table 2**), suggesting that anaerobic conditions occurred in the inner layers of the biofilm.

At class level, the microbial communities of the two MBBRs during P1-P2 were dominated by *Gammaproteobacteria* and *Alphaproteobacteria*, which were present in biofilm and suspended biomass at relative abundances of 20–42% and 15–32% in respective order. The only exception is represented by the MBBR-Et suspended biomass during P2, being dominated by *Bdellovibrionia* (35%) and *Gammaproteobacteria* (20%).

Fig. 4 shows the taxonomic composition at genus level of the microbial communities in the MBBR biofilm and suspended biomass, while a phylogenetic classification of the functional groups including AOB, DNB, HAB and putative PAOs/DNPAOs is shown in **Table 2**. At the end of P1, the most abundant bacterial genera in the MBBR-Ac biofilm were *Rhizobium* (15.6%), *Acidovorax* (13.5) and *Thaurea* (7.2%). Members of these genera have been reported to possess denitrifying ability [14,39,40]. Other DNB included *Luitemonas* (4.0%) *Aquamicrobium* (2.5%) and *Hydrogenophaga* (2.2%) [41–43] (**Table 2**, **Fig. 4**). The genera *Hydrogenophaga* and *Acidovorax,* belonging to the family of *Comamonadaceae,* have been indicated as putative PAOs due to the ability to form and store polyphosphate [20]. In particular, *Hydrogenophaga* was proven to accumulate P under aerobic conditions [44] and was the dominant genus in a continuous-flow MBBR

performing combined SND and P removal under microaerobic/aerobic conditions [5]. Glycogen accumulating organisms (GAOs) were not detected in the MBBR biofilm or suspended biomass probably due to absence of an anaerobic phase within the aeration cycle. *Nitrosomonas* (0.7%) was the only representative of autotrophic AOB in the MBBR biofilm. However, it cannot be excluded that *Thaurea* and *Pseudomonas* played a role in nitrification, as members of these genera were reported among heterotrophic nitrifiers-aerobic denitrifiers [45]. Typical NOB such as *Nitrobacter*, *Nitrospira* and *Nitrosospira* were never detected in the MBBR biofilm and suspended biomass during the study, indicating that the alternation of microaerobic and aerobic conditions following cultivation at high pH and temperature and low SRT was effective for NOB suppression. Regarding MBBR-Et, the dominant genera in the biofilm were *Thauera* (14.2%), *Hyphomicrobium* (10.4%), *OM190* (11.3%) and *Pseudomonas* (8.8%) (**Table 2**). *Hyphomicrobium* and *Pseudomonas* includes putative PAOs/DNPAOs [37,46]. *Hydrogenophaga* was detected also in the MBBR-Et biofilm with a relative abundance of 4.2%.

The microbial composition of suspended biomass in the two MBBRs during P1 was quite similar and dominated by DNB such as *Rhizobium* (19.2%), *Acidovorax* (13.0–13.8%) and *Luitemonas* (5.6–5.9%). High relative abundances of bacteria involved in degradation of organic matter such as *Bdellovibrio* (6.1-7.2%), *Parapusillimonas* (6.0–6.3%) and *Dojnabacteria* (6.1–9.6%) [47] were also observed (**Table 2**). Interesting is the absence of AOB, which indicates that suspended biomass was mostly a pool of heterotrophic bacteria, while the MBBR biofilm included all functional groups carrying out the SPND process.

Biofilm composition changed significantly during P2 following the decrease of feed C/P ratio. The relative abundances of *uncultured_Anaerolineaceae*, *SM1A02*, *Arenimonas* and *Flavobacterium* increased by 1.0–6.4% (**Table 2**). In contrast, the relative abundance of *Hydrogenophaga*, *Luitemonas*, *Aquamicrobium* and *Rhizobium* showed a decrease between 0.3% and 8.3%. *Flavobacterium* and *Arenimonas* are reported among DNB [43,48]. *SM1A02*, a genus belonging to *Planctomycetes*, has been indicated as a potential anammox bacteria, being found at high abundances in anammox systems [49,50]. The relative abundance of *Nitrosomonas* in the microbial community of biofilm doubled in both MBBRs, which explains the higher N_{eff} observed in P2 (97%) compared to P1 (87%). The population of *Hydrogenophaga* significantly decreased in the biofilm of both MBBRs and especially in MBBR-Et (from 4.4% to 0.8%), which is in agreement with the decrease of P-PO_4^{3-} RE in P2 (**Table 1**).

Increase of C/P ratio stimulated HAB growth in suspended form during P2. The overall increase of HAB relative abundance was estimated to be 9.3% and 42.3% for MBBR-Ac and MBBR-Et, respectively. In particular, the population of *Bdellovibrio* and *Neochlamydia* in MBBR-Et suspended biomass increased dramatically, reaching relative abundances of 34.7% and 12.4%, respectively. In contrast, the relative abundances of *Acidovorax*, *Hydrogenophaga*, *Pseudomonas*, *Rhizobium*, *Luteimonas* and *Parapusillimonas* decreased by 1.3-18.3% (**Table 2**), which could also contribute to the decrease of P-PO_4^{3-} RE in P2 (**Fig.3**).

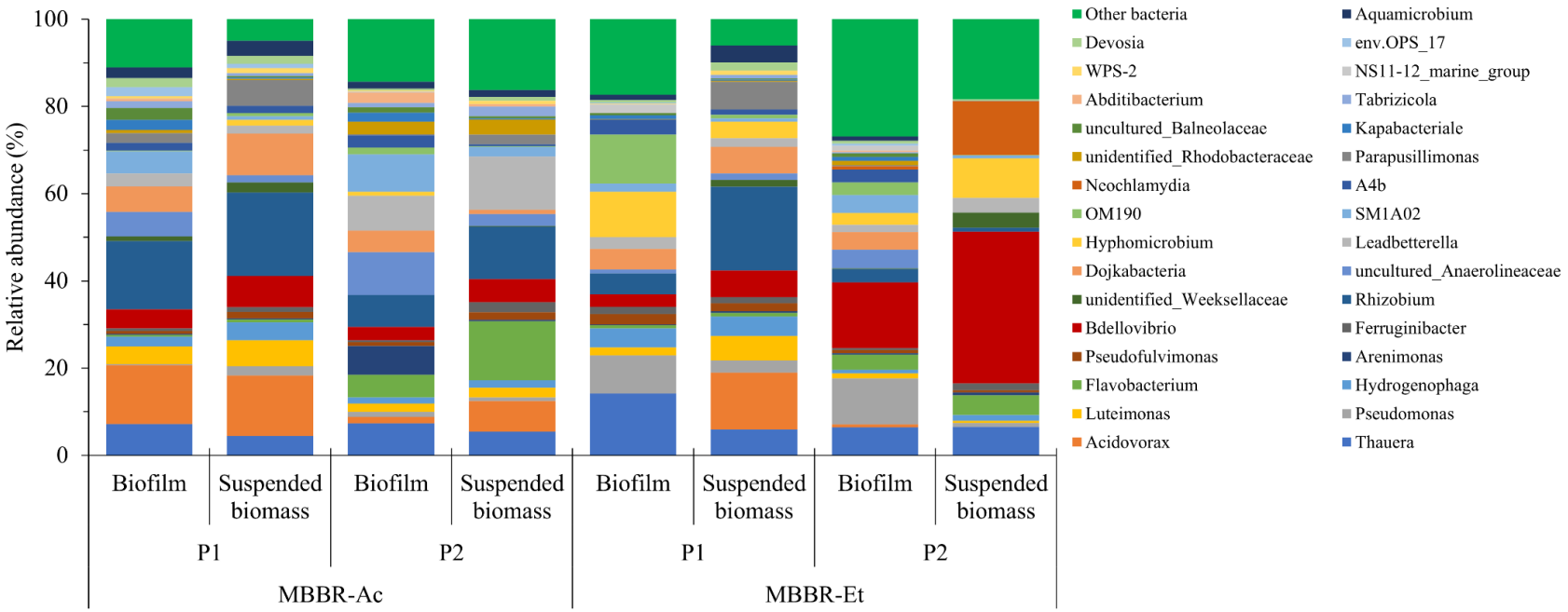

Figure 5.4 - Microbial community composition of the MBBR-Ac (a) and MBBR-Et (b) biofilm and suspended biomass at genus level at relative abundances above 2%.

5.4 Conclusions

SPND with average TIN, N_{eff} and D_{eff} REs > 80% was maintained in continuous-flow intermittently-aerated MBBRs at DO levels between 0.2 and 3 mg L^{-1}. Biomass cultivation at pH 8.2, SRT 4 days and 26–28°C and IA operation effectively inhibited NOB growth and maintained SPND in the MBBRs. Acetate was preferable to ethanol as resulted in a more diversified microbial community. P-PO_4^{3-} REs > 80% were achieved without an anaerobic stage. Microaerobic/aerobic MBBR is a promising technology for combined C, N and P removal, although the impact of complex organics and reduction of effluent NO_2^- levels need further investigation.

5.5 Supplementary materials

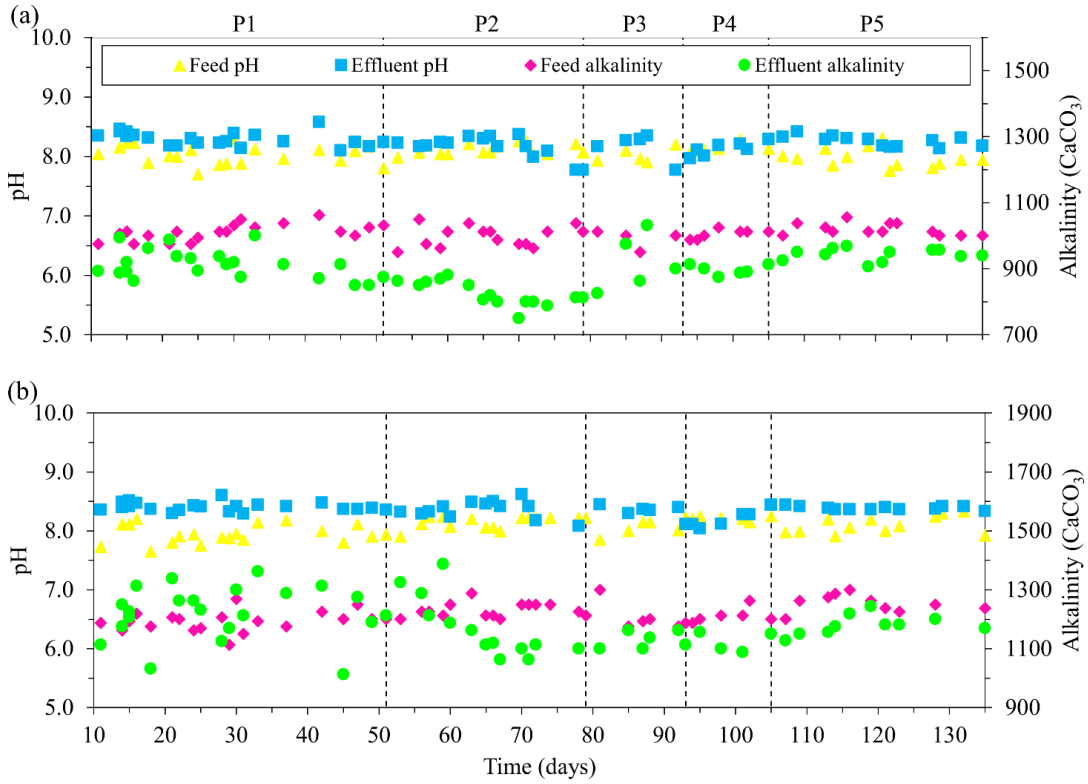

Figure S5.5 - Profiles of effluent pH and alkalinity concentration during continuous MBBR-Ac (a) and MBBR-Et (b) operation.

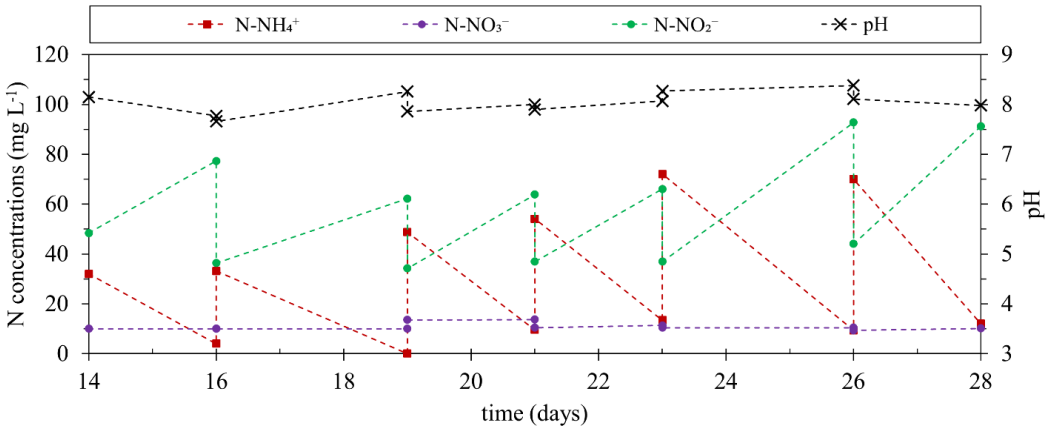

Figure S5.6 - The evolution of N-NH_4^+, N-NO_3^-, N-NO_2^- concentrations and pH during AOB cultivation.

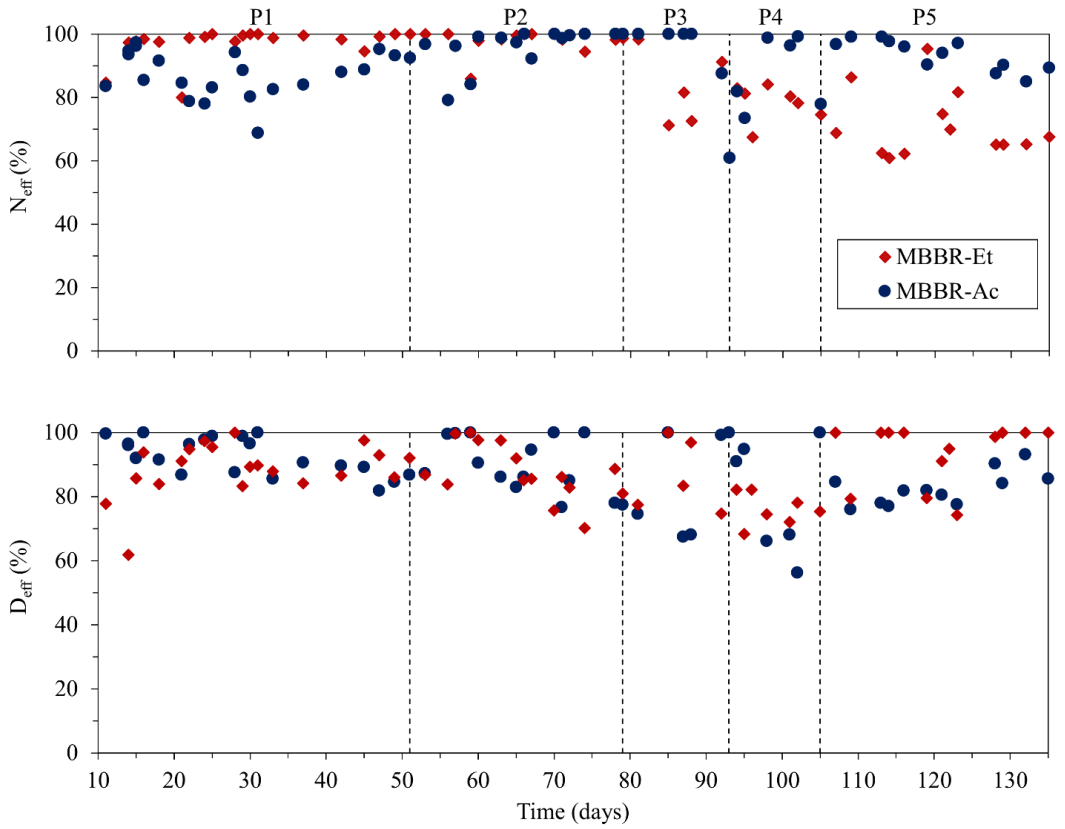

Figure S5.7 - Efficiencies of nitrification (N_{eff}) and denitrification (D_{eff}) during continuous MBBR-Ac and MBBR-Et operation.

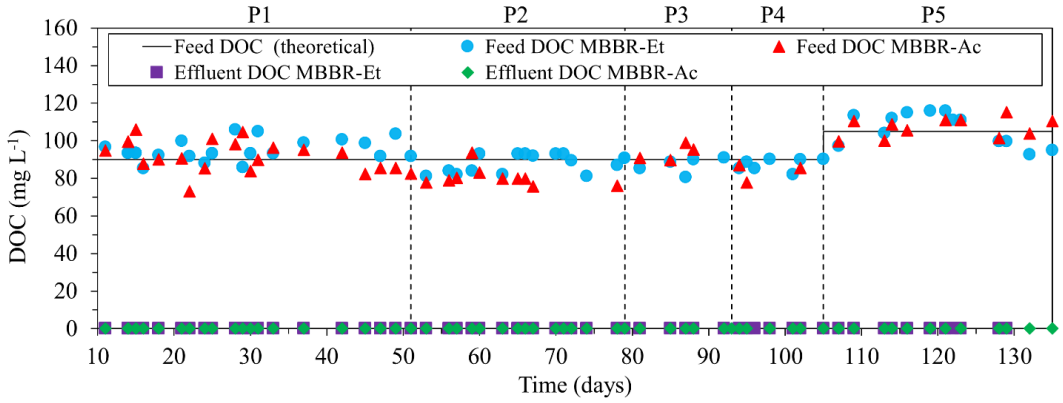

Figure S5.8 - Temporal profiles of influent and effluent DOC concentrations during continuous MBBR-Ac (a) and MBBR-Et (b) operation.

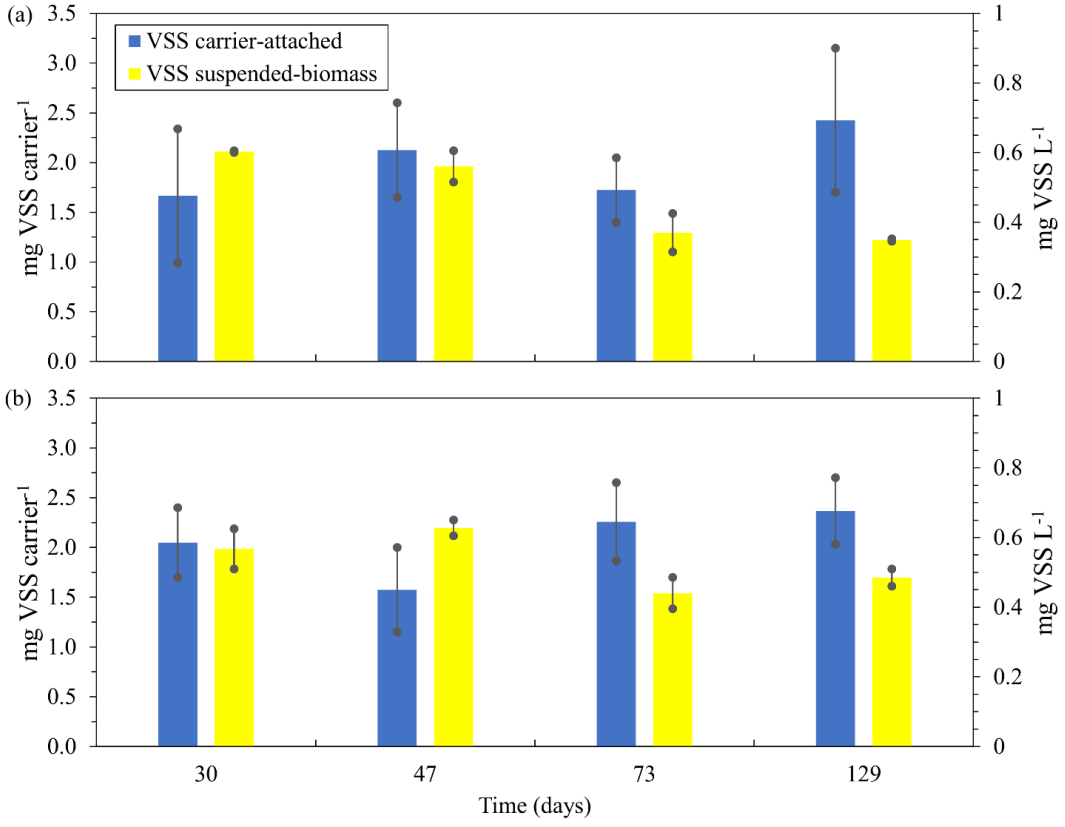

Figure S5.9 - Concentrations of carrier-attached and suspended biomass during continuous MBBR-Ac (a) and MBBR-Et (b) operation.

5.6 References

[1] P.J.T.M. van Puijenbroek, A.H.W. Beusen, A.F. Bouwman, Global nitrogen and phosphorus in urban waste water based on the Shared Socio-economic pathways, *J. Environ. Manage.* 231 (2019) 446–456.

[2] G. Bertanza, L. Menoni, G. Umberto, R. Pedrazzani, Promoting biological phosphorus removal in a full scale pre-denitrification wastewater treatment plant, *J. Environ. Manage.* 254 (2020) 109803.

[3] F. Jaramillo, M. Orchard, C. Muñoz, M. Zamorano, C. Antileo, Advanced strategies to improve nitrification process in sequencing batch reactors - a review, *J. Environ. Manage.* 218 (2018) 154–164.

[4] S. Rahimi, O. Modin, I. Mijakovic, Technologies for biological removal and recovery of nitrogen from wastewater, *Biotechnol. Adv.* 43 (2020) 107570.

[5] F. Iannacone, F. Di Capua, F. Granata, R. Gargano, G. Esposito, Simultaneous nitrification, denitrification and phosphorus removal in a continuous-flow moving bed biofilm reactor alternating microaerobic and aerobic conditions, *Bioresour. Technol.* (2020) 123453.

[6] F. Iannacone, F. Di Capua, F. Granata, R. Gargano, F. Pirozzi, G. Esposito, Effect of carbon-to-nitrogen ratio on simultaneous nitrification denitrification and phosphorus removal in a microaerobic moving bed biofilm reactor, *J. Environ. Manage.* 250 (2019) 109518.

[7] L. Chu, J. Wang, Comparison of polyurethane foam and biodegradable polymer as carriers in moving bed biofilm reactor for treating wastewater with a low C/N ratio, *Chemosphere.* 83 (2011) 63–68.

[8] Y. Jia, M. Zhou, Y. Chen, Y. Hu, J. Luo, Insight into short-cut of simultaneous nitrification and denitrification process in moving bed biofilm reactor: effects of carbon to nitrogen ratio, *Chem. Eng. J.* 400 (2020) 125905.

[9] S. Yang, F. Yang, Nitrogen removal via short-cut simultaneous nitrification and denitrification in an intermittently aerated moving bed membrane bioreactor, J. *Hazard. Mater.* 195 (2011) 318–323.

[10] W. Huang, Z. She, M. Gao, Q. Wang, C. Jin, Y. Zhao, L. Guo, Effect of anaerobic/aerobic duration on nitrogen removal and microbial community in a

simultaneous partial nitrification and denitrification system under low salinity, *Sci. Total Environ.* 651 (2019) 859–870.

[11] Y. Peng, G. Zhu, Biological nitrogen removal with nitrification and denitrification via nitrite pathway, *Appl. Microbiol. Biotechnol.* 73 (2006) 15–26.

[12] X. Liu, M. Kim, G. Nakhla, M. Andalib, Y. Fang, Partial nitrification-reactor configurations, and operational conditions: performance analysis, *J. Environ. Chem. Eng.* 8 (2020) 103984.

[13] A. di Biase, M.S. Kowalski, T.R. Devlin, J.A. Oleszkiewicz, Moving bed biofilm reactor technology in municipal wastewater treatment: a review, *J. Environ. Manage.* 247 (2019) 849–866.

[14] L. Yan, S. Liu, Q. Liu, M. Zhang, Y. Liu, Y. Wen, Z. Chen, Improved performance of simultaneous nitrification and denitrification via nitrite in an oxygen-limited SBR by alternating the DO, *Bioresour. Technol.* 275 (2019) 153–162.

[15] R. Campo, S. Sguanci, S. Caffaz, L. Mazzoli, C. Lubello, T. Lotti, Efficient carbon, nitrogen and phosphorus removal from low C/N real domestic wastewater with aerobic granular sludge, *Bioresour. Technol.* 305 (2020) 122961.

[16] C. Tan, F. Ma, S. Qiu, Impact of carbon to nitrogen ratio on nitrogen removal at a low oxygen concentration in a sequencing batch biofilm reactor, *Water Sci. Technol.* 67 (2013) 612–618.

[17] P. Roots, F. Sabba, A.F. Rosenthal, Y. Wang, Q. Yuan, L. Rieger, F. Yang, J.A. Kozak, H. Zhang, G.F. Wells, Integrated shortcut nitrogen and biological wastewater: process operation and modeling, *Environ. Sci. Technol.* 6 (2019) 566–580.

[18] S.Y. Gebremariam, M.W. Beutel, D. Christian, T.F. Hess, Research advances and challenges in the microbiology of enhanced biological phosphorus removal - a critical review, *Water Environ. Res.* 83 (2011) 195–219.

[19] J. Jena, R. Kumar, A. Dixit, T. Das, Anoxic – aerobic SBR system for nitrate, phosphate and COD removal from high-strength wastewater and diversity study of microbial communities, *Biochem. Eng. J.* 105 (2016) 80–89.

[20] H. Ge, D.J. Batstone, J. Keller, Biological phosphorus removal from abattoir wastewater at very short sludge ages mediated by novel PAO clade *Comamonadaceae*, *Water Res.* 69 (2014) 173–182.

[21] Q. He, J. Zhou, Q. Song, W. Zhang, H. Wang, L. Liu, Elucidation of microbial characterization of aerobic granules in a sequencing batch reactor performing simultaneous nitrification, denitrification and phosphorus removal at varying carbon to phosphorus ratios, *Bioresour. Technol.* 241 (2017) 127–133.

[22] M. Vargas, C. Casas, J.A. Baeza, Maintenance of phosphorus removal in an EBPR system under permanent aerobic conditions using propionate, *Biochem. Eng. J.* 43 (2009) 288–296.

[23] M. Pijuan, A. Guisasola, J.A. Baeza, J. Carrera, C. Casas, J. Lafuente, Aerobic phosphorus release linked to acetate uptake: influence of PAO intracellular storage compounds, *Biochem. Eng. J.* 26 (2005) 184–190.

[24] L.S. de S. Rollemberg, Q.L. De Oliveira, A.R.M. Barros, V.M.M. Melo, P.I.M. Firmino, A.B. do. Santos, Effects of carbon source on the formation, stability, bioactivity and biodiversity of the aerobic granule sludge, *Bioresour. Technol.* 278 (2019) 195–204.

[25] D. Ucar, T. Yilmaz, F. Di, G. Esposito, E. Sahinkaya, Comparison of biogenic and chemical sulfur as electron donors for autotrophic denitrification in sulfur-fed membrane bioreactor (SMBR), *Bioresour. Technol.* 299 (2020) 122574.

[26] F. Di Capua, M.C. Mascolo, F. Pirozzi, G. Esposito, Simultaneous denitrification, phosphorus recovery and low sulfate production in a recirculated pyrite-packed biofilter (RPPB), *Chemosphere.* (2020) 126977.

[27] J.J. Classen, W.J. Chandler, R.S. Huie, J.A. Osborne, A centrifuge-based procedure for suspended solids measurements in Lagoon sludge, *Am. Soc. Agric. Biol. Eng.* 56 (2013) 747–752.

[28] S. Ge, S. Wang, X. Yang, S. Qiu, B. Li, Y. Peng, Detection of nitrifiers and evaluation of partial nitrification for wastewater treatment: a review, *Chemosphere.* 140 (2015) 85–98

[29] H. Chai, Y. Xiang, R. Chen, Z. Shao, L. Gu, L. Li, Q. He, Enhanced simultaneous nitrification and denitrification in treating low carbon-to-nitrogen ratio wastewater: treatment performance and nitrogen removal pathway, *Bioresour. Technol.* 280 (2019) 51–58.

[30] G. Liu, J. Wang, Long-term low DO enriches and shifts nitrifier community in activated sludge, *Environ. Sci. Technol.* 47 (2013) 5109–5117.

[31] S. Zhu, S. Chen, Effects of organic carbon on nitrification rate in fixed film biofilters, *Aquac. Eng.* 25 (2001) 1–11.

[32] S. Okabe, H. Satoh, Y. Watanabe, In situ analysis of nitrifying biofilms as determined by in situ hybridization and the use of microelectrodes, *Appl. Environ. Microbiol.* 65 (1999) 3182–3191.

[33] C. Dale, V. Water, D. Oliphant, M. Ekenberg, Wastewater treatment using MBBR in cold climates, Proc. Mine Water Solut. Extrem. Environ. Vancouver, Canada. (2015) 1–17.

[34] P. Jabari, G. Munz, Q. Yuan, J.A. Oleszkiewicz, Free nitrous acid inhibition of biological phosphorus removal in integrated fixed-film activated sludge (IFAS) system, *Chem. Eng. J.* 287 (2016) 38–46.

[35] M. Stokholm-Bjerregaard, S.J. Mcilroy, M. Nierychlo, S.M. Karst, M. Albertsen, P.H. Nielsen, A critical assessment of the microorganisms proposed to be important to enhanced biological phosphorus removal in full-scale wastewater treatment systems, *Front. Microbiol.* 8 (2017) 718.

[36] J. Zhao, X. Wang, X. Li, S. Jia, Q. Wang, Y. Peng, Improvement of partial nitrification endogenous denitrification and phosphorus removal system: balancing competition between phosphorus and glycogen accumulating organisms to enhance nitrogen removal without initiating phosphorus removal deterioration, *Bioresour. Technol.* 281 (2019) 382–391.

[37] S. Du, D. Yu, J. Zhao, X. Wang, C. Bi, J. Zhen, Achieving deep-level nutrient removal via combined denitrifying phosphorus removal and simultaneous partial nitrification-endogenous denitrification process in a single-sludge sequencing batch reactor, *Bioresour. Technol.* 289 (2019) 121690.

[38] T. Ya, S. Du, Z. Li, S. Liu, M. Zhu, X. Liu, Z. Jing, R. Hai, X. Wang, Successional dynamics of molecular ecological network of Anammox microbial communities under elevated salinity, *Water Res.* (2020) 116540.

[39] S. Salehi, K.Y. Cheng, A. Heitz, M.P. Ginige, Simultaneous nitrification, denitrification and phosphorus recovery (SNDPr) - an opportunity to facilitate full-scale recovery of phosphorus from municipal wastewater, *J. Environ. Manage.* 238 (2019) 41–48.

[40] Y.Q. Gu, T.T. Li, H.Q. Li, Biofilm formation monitored by confocal laser scanning microscopy during startup of MBBR operated under different intermittent aeration modes, *Process Biochem.* 74 (2018) 132–140.

[41] L. Li, G. Qian, L. Ye, X. Hu, X. Yu, W. Lyu, Research on the enhancement of biological nitrogen removal at low temperatures from ammonium-rich wastewater by the bio- electrocoagulation technology in lab-scale systems, pilot-scale systems and a full-scale industrial wastewater treatment plant, *Water Res.* 140 (2018) 77–89.

[42] S. Wang, L. Wang, L. Deng, D. Zheng, Y. Zhang, Y. Jiang, H. Yang, Performance of autotrophic nitrogen removal from digested piggery wastewater, *Bioresour. Technol.* 241 (2017) 465–472.

[43] J. Fu, Z. Lin, P. Zhao, Y. Wang, L. He, J. Zhou, Establishment and efficiency analysis of a single-stage denitrifying phosphorus removal system treating secondary effluent, *Bioresour. Technol.* 288 (2019) 121520.

[44] S.K. Jørgensen, A.S.L. Pauli, Polyphosphate accumulation among denitrifying bacteria in activated sludge, *Anaerobe.* 1 (1995) 161–168.

[45] L. Zhang, G. Fu, Z. Zhang, Long-term stable and energy-neutral mixed biofilm electrode for complete nitrogen removal from high-salinity wastewater: mechanism and microbial community, *Bioresour. Technol.* 313 (2020) 123660.

[46] Q. Wang, D. Yu, X. Wang, G. Chu, T. He, J. Zhao, Development of novel denitrifying nitrite accumulation and phosphorus removal (DNAPR) process for offering an alternative pretreatment to achieve mainstream Anammox, *Bioresour. Technol.* 319 (2021) 124164.

[47] X. Huang, P. Lee, Shortcut nitrification/denitrification through limited-oxygen supply with two extreme COD/N-and-ammonia active landfill leachates, *Chem. Eng. J.* 404 (2021) 126511.

[48] W. Xing, Y. Wang, T. Hao, Z. He, F. Jia, H. Yao, pH control and microbial community analysis with HCl or CO_2 addition in H_2 -based autotrophic denitrification, *Water Res.* 168 (2020) 115200.

[49] J. Zhang, L. Zhang, Y. Miao, Y. Sun, Q. Zhang, L. Wu, Y. Peng, Enhancing sewage nitrogen removal via anammox and endogenous denitrification: significance of anaerobic/oxic/anoxic operation mode, *Bioresour. Technol.* 289 (2019) 121665.

[50] Z. rui Chu, K. Wang, X. kun Li, M. ting Zhu, L. Yang, J. Zhang, Microbial characterization of aggregates within a one-stage nitritation-anammox system using high-throughput amplicon sequencing, *Chem. Eng. J.* 262 (2015) 41–48.

CHAPTER 6.

General Discussion

6.

6.1 Introduction

The water quality of rivers, lakes and estuaries is strongly affected by human activities [1]. The excessive use of nutrients and their subsequent discharge into water bodies is responsible for the eutrophication phenomenon and severely affects the natural aquatic biota. Generally, biological N removal in WWTPs is achieved by two separated biological processes, i.e. nitrification and denitrification, or alternating anaerobic/anoxic/aerobic phases to perform combined N removal and biological P removal (e.g. UCT system). However, the combined removal of these two nutrients in continuous-flow mode, typical of WWPTs, commonly requires the presence of several basins for each oxygen regime applied, or several batch-type bioreactors, i.e. SBRs, working in parallel, resulting in complicated and expensive operation.

SND has been reported as a promising process for N removal, being economically favorable and technically feasible compared to CAS [2]. Biofilm technologies, such as MBBR, FBBR or AGS, are ideal systems to achieve a simultaneous removal of N and P due to the formation of a multispecies biofilm [3]. Biofilm is mainly composed by stratified layers of bacteria and its microbial community composition depends on the inoculated sludge and influent wastewater characteristics [4,5]. The main mechanism of solute substrate transport from the bulk liquid into microbial cell in the biofilm is diffusion [6]. Diffusion limitations generate gradients of electron donors (e.g. organic carbon) and electron acceptors (e.g. DO) within the biofilm, resulting in the formation of aerobic, anoxic and anaerobic zones, enabling the coexistence of nitrifying, denitrifying and heterotrophic bacteria [7]. The microbial interactions are affected by operation factors such as wastewater composition, organic loading rate (OLR), DO and feed C/N ratio.

The aim of this doctoral thesis was to study a compact solution to achieve simultaneous removal of C, N and P compounds in a continuous-flow MBBR. The main purpose was to help small communities struggling with the implementation of wastewater treatment facilities by offering a low-cost and effective treatment solution. The experimental works was organized in three phases. In a first phase, the coexistence of stable bacteria involved in nutrients and carbon removal was studied under stable microaerobic conditions (DO = 1.0 ± 0.2 mg L^{-1}) and different feed C/N ratios (Chapter 3). In a second phase, the aeration strategy was shifted to intermittent mode between microaerobic and aerobic conditions and different DO ranges were investigated (Chapter 4). In a third phase, the feasibility of performing combined SPND and biological P removal in continuous-flow intermittently-

aerated MBBRs and the impact of organic carbon source (i.e. ethanol and acetate) on the process was investigated (Chapter 5).

6.2 Aeration strategy choice

The right choice of aeration strategy is fundamental to ensure the activities of the different microbial families involved in C, N and P removal. DO distribution within the biofilm strongly impact nitrification and denitrification activities [7]. Applying high DO levels in the bulk liquid can allow to fully penetrate the biofilm, which favor nitrification and limit denitrification efficiency [8]. Otherwise, low DO concentrations can inhibit nitrifying activity due to competition between AOB/NOB with HAB for the available DO. Nitrifying bacteria are characterized by a lower growth rate and higher affinity constant to oxygen compared to HAB. As a consequence, HAB can limit the existence of nitrifyers within the biofilm [9].

The MBBRs operated under IA were characterized by an accelerated start-up phase compared to MBBR operated under microaerobic conditions (mMBBR). As described in Chapter 3, during start up period, DO concentrations in the mMBBR were gradually decreased to 1.0 mg L^{-1} in order to facilitate the adaptation of nitrifying bacteria. This was suggested by previous experiments in which a severe inhibition of nitrifying activity was observed when microaerobic conditions were set at the beginning of reactor operation. In contrast, IA operation rapidly enabled the simultaneous activities of nitrifying and denitrifying bacteria in MBBRs. IA consists in the alternation of aeration and non-aeration phases in order to stimulate nitrifying activity under aerobic conditions, while under non-aeration phase denitrification is allowed due to decrease of DO concentrations to low values [10]. In Chapters 4 and 5, IA was ensured by fixing DO setpoints and ranges (0.2–2 mg L^{-1}, 0.2–3 mg L^{-1} and 0.2–4 mg L^{-1}). The different DO regimes tested significantly influenced the nitrifying and denitrifying activities of the IAMBBR biofilm, resulting in dynamic trends of NH_4^+, NO_3^- and NO_2^- concentrations in the effluent during the experimental activity. In addition, the different DO ranges tested impacted the microbial community inside biofilm, revealing how this environmental variable is an important factor affecting SND and SPND process [11]. Applying a DO range of 0.2–2 mg L^{-1} determined a relative abundance of nitrifying bacteria lower than 2%, being responsible of effluent NH_4^+ concentrations up to 9 mg L^{-1} at a feed C/N ratio of 2.8 (Chapter 4). The increase of DO range to 0.2–3 mg L^{-1} favored the proliferation of nitrifiers, i.e. *Nitrosomonas*, showing an increase of relative abundance from 1% to 4.2% and allowing to achieve higher NH_4^+ REs. However, aeration should be controlled.

Applying DO levels between 0.2–4 mg L^{-1} resulted in poor denitrification and nitrification activities due to an excessive proliferation of HAB, e.g. *Chryseolinea*. Excess HAB proliferation results in the shortage of organic carbon which affects both DNB and PAO activities, while nitrifying bacteria such *Nitrosomonas* registered a sharply decrease of relative abundance from 4.8% to 2.5% due to an increased competition with HAB for DO and $N\text{-}NH_4^+$ (Chapter 4).

IA was also an effective approach to inhibit *nitratation* ($NO_2^- \rightarrow NO_3^-$) and achieve a SPND process (Chapter 5). The alternation between anoxic and aerobic conditions has been reported as a possible strategy to inhibit NOB activity and favor NO_2^- accumulation [12,13]. Under anoxic conditions, both NOB and AOB activities are inhibited, whereas under aerobic conditions AOB activity recovers faster than NOB activity determining NO_2^- accumulation [14]. The comparison between SND and SPND performances of MBBRs will be discussed in **Section 6.4**.

Finally, it should be highlighted that IA strategy can limit the energy cost compared to continuous aeration [15]. Of course, effective evaluation of cost saving must be evaluated with a full-scale experimental approach.

6.3 Effect of feed C/N ratio

The feed C/N ratio directly affect TIN RE, since low values can limit denitrification efficiency due to lack of carbon source, while high values can determine an excess growth of HAB leading to poor nitrification activity due to competition between HAB and AOB/NOB for DO and $N\text{-}NH_4^+$ [16]. Generally, municipal wastewater is characterized by low C/N ratios, requiring additional carbon source to improve denitrification [13]. The SND process is reported able to reduce carbon demand by almost 30% compared to the conventional pre-denitrification cycle [17].

Chapter 3 illustrates the effects of three different feed C/N ratios (2.7, 4.2 and 5.6) on SND in MBBR under microaerobic conditions. The lowest TIN REs (on average) were achieved at feed C/N ratios of 2.7 (46%) and 5.6 (51%), while TIN REs up to 68% were achieved at a feed C/N ratio of 4.2 (65%). The low TIN removal obtained at feed C/N ratio of 2.7 was attributed to the lack of electron donor for denitrification, as about 14 mg L^{-1} of $N\text{-}NO_x^-$ were averagely observed in the effluent. At the same time, the highest nitrifying activity (316 mg N $gVSS^{-1}$ d^{-1}) was achieved after cultivation at feed C/N ratio of 2.7 [18]. In a similar way, feed C/N ratio of 2.6 resulted in poor TIN RE in the IAMBBR working at DO levels between 0.2 and 3 mg L^{-1} due to lack of carbon source, while increasing the feed C/N ratio from 2.6 to 3.6 determined an increase of TIN RE

from 40% to 62%. The increase of feed C/N ratio from 2.7 to 3.6 also had a beneficial effect on the removal of $P\text{-}PO_4^{3-}$, resulting in an increase of $P\text{-}PO_4^{3-}$ RE from 66% to 75% (Chapter 4). The overall growth of DNB abundance and the enhancement of $P\text{-}PO_4^{3-}$ RE have suggested a possible DNB involvement in P removal.

6.4 SND via nitrate vs SND via nitrite

SND via nitrite (or SPND) is based on complete inhibition of NO_2^- oxidation (*nitratation*), thus NO_2^- are directly reduced by DNB. This results in a cost savings in terms of energy required for aeration during aerobic phase and a lower demand for organic matter under anoxic condition [19].

The SPND process was studied in two continuous-flow MBBRs under microaerobic/aerobic conditions fed with different carbon source, one with acetate (MBBR-Ac) and one with ethanol (MBBR-Et). Alkaline pH (≈8.2), temperatures between 26 and 28°C and an SRT of 4 days were adopted to suppress NOB during cultivation phase (Chapter 5). MBBRs performing SPND (MBBR-Et and MBBR-Ac) reached average TIN REs of around 81–88%, showing an efficiency increase of almost 20% compared to that achieved in MBBR performing SND under similar IA conditions (DO=0.2–3 mg L^{-1}) and feed C/N ratios (3.6) (Chapter 4). *Nitrosomonas* genus was the only nitrifying bacteria detected by Illumina sequencing analysis on MBBR-Et and MBBR-Ac biofilm and suspended biomass, while no typical NOB was detected [20]. Continuous-flow MBBRs performing SPND could be a compact or an upgrading solution for small community wastewater treatment plants, often characterized by low TIN RE and small footprint.

One drawback of SPND is the possibility of NOB adaptation to low DO concentrations resulting in a complete nitrification [21]. This can be explained by a "r-strategist" approach of some nitrifying bacteria such as *Nitrospira*, which are able to thrive at low DO concentrations, being different from k-strategist such as *Nitrobacter* that thrive at high DO levels [22,23]. Results illustrated in Chapter 4 show that *Nitrospira* were never detected during the first 108 days of IAMBBR operation. However, relative abundance of this genus at end of the study almost doubled those of *Nitrosomonas*, demonstrating a long-term adaptation to low DO concentrations. Although satisfactory SPND process could by maintained for almost 70 days under IA conditions, increase of DO levels due to malfunctioning of the control system might threaten the process and could result in rapid NO_3^- occurrence in the effluent (Chapter 5).

6.5 Phosphorus removal: to be or not be due to PAO?

During this study, TIP RE ranging from 16 to 95% was observed in the MBBRs. P-PO_4^{3-} required for cell growth can be evaluated based on C:N:P ratio of 100:5:1 reported by Thompson et al. [24]. Based on this ratio, values between 2–32% of feed P could be used for growth by biomass, revealing a luxury P uptake by microorganisms with probably accumulating ability. Illumina sequencing analysis revealed the presence of putative PAOs such as *Hydrogenophaga*, *Acidovorax* and *Pseudomonas* with high relative abundances, suggesting their key roles in biological P uptake [25]. Biological P removal is commonly achieved alternating anaerobic and aerobic/anoxic conditions by microorganisms able to store more PO_4^{3-} than required for growth [26,27]. However, MBBRs were operated in continuous-flow without an anaerobic phase due to the presence of DO and/or N-NO_x in the bulk. In literature, biological P removal has been found to occur under strictly aerobic conditions, or to continue when the anaerobic/aerobic alternation is switched to continuous aerobic conditions in presence of VFAs [28–30]. However, it cannot be excluded that the alternation between microaerobic and aerobic conditions generated transient anaerobic zones in the biofilm promoting PAO activity. The presence of an anaerobic microenvironment inside the biofilm was suggested by the presence of anammox-related bacteria (i.e. *SM1A02* and *OM190*), detected with high abundances in MBBR-Et and MBBR-Ac.

Low TP REs were observed in chapter 4 (16–25%) likely induced by high N-NO_2^- concentrations (15 mg L^{-1}) achieved in the effluent. Saito et al. (2004) investigated the effects of N-NO_2^- concentrations on biological P uptake by PAOs, showing how inhibitory effects can be observed at 2 mg L^{-1}, while value higher than 6 mg L^{-1} can totally inhibit P uptake under aerobic condition [22,32].

Finally, competition between microorganism with P accumulating ability and HAB must be controlled. The change of DO range from 0.2–3 mg L^{-1} to 0.2–4 mg L^{-1} determined an increase of P-PO_4^{3-} concentrations higher than influent values (Chapter 4). The release of P-PO_4^{3-} in the bulk solution was probably induced by a lack of carbon source due to an excessive proliferation of HAB and a concomitant decrease of *Hydrogenophaga* relative abundance from 9.5% to 6.8%. The competition between PAOs and HAB was further investigated in Chapter 5, doubling the feed C/P ratio from 11 to 22 by decreasing influent P-PO_4^{3-} concentrations. The increase of feed C/P ratios affecting both TP REs and microbial community. The decreasing of TP REs were followed by a decrease of putative PAOs relative abundance (*Hydrogenophaga* and *Acidovorax*) and an

overall increase of HAB. High feed COD/P-PO_4^{3-} may be responsible of an excessive proliferation of HAB and result in outcompetition of PAOs [33].

6.6 Key functional group in nitrogen and phosphorus removal

The bacterial community structures of IAMBBR, MBBR-Ac and MBBR-Et were studied at different trophic levels (Chapter 4–5). At, phylum level, *Proteobacteria* and *Bacteroidetes*, which are mainly related to N and P removal in wastewater treatment system [34,35], showed the highest relative abundances in the biofilms, while at class level. AOB were represented exclusively by the genus *Nitrosomonas*. NOB genera, such as *Nitrospira* and *Nitrosospira*, were only detected in IAMBBR performing SND, while these genera were not detected in biofilm and suspended biomass of MBBRs performing SPND (Chapter 5). The denitrifying bacteria community was the most abundant in each reactor with a variety of representative genera, such as *Thaurea*, *Flavobacterium*, *Rhizobium*, *Pseudomonas*, and *Luitemonas*. The genus *Thaurea* was predominant both in biofilm and suspended biomass performing SPND coupled to P removal (4.5–14.2%), consistent with the existing reports on SPND process [11]. The genera *Hydrogenophaga*, *Acidovorax* and *Pseudomonas* have been indicated as putative PAO by several studies [25,36,37] and were likely responsible to P-PO_4^{3-} RE. These genera were found capable to form and store poly-P, a key ability of PAOs. The *Hydrogenophaga*, conventionally classified as DNB, was a dominant species of IAMBBR biofilms and suspended biomass, with relative abundances ranging from 0.8% to 4.4% and from 1.3% to 4.5%, respectively.

Carbon source was another factor affecting the microbial community in bioreactors [38]. Acetate favored a more diversified microbial community, while ethanol stimulated the growth of heterotrophs (Chapter 5). Sequencing results showed a strong increase of HAB such as *Bdellovibrio* and *Neochlamydia* genera in MBBR-Et when the C/P ratio was increased from 11 to 22 with relative abundances reaching of 34.7% and 12.4%, respectively.

6.7 Future research and practical applications

In this study, simultaneous N removal coupled to P removal was studied in MBBRs operating under different aeration strategies and feed C/N ratios. Municipal synthetic wastewater was used to study the effect of different concentration of C, N and P. The carbon sources used were represented by readily available substrates such as VFA (i.e.

acetate) and alcohol (i.e. ethanol) [39]. In contrast, real municipal wastewater contains almost 50% of non-diffusible particulate form of total COD [40]. Hence, understanding the effect of real wastewater on TIN and $P\text{-}PO_4^{3-}$ RE is crucial to assess the suitability of the studied bioreactor system to real scale application. Reactor scale-up is necessary also to evaluate operational issue and costs of the IAMBBR technology. However, readily available organic carbon in full-scale WWTPs could be provided by establishing an anaerobic phase placed upstream the IAMBBR or by channeling part of the first-stage supernatant from a two-stage anaerobic digestion to the IAMBBR basin. In the future, trials could be performed for extending this solution to pre-existing and larger facilities (> 2000 PE) requiring additional treatment to achieve discharge limits.

Literature lacks a hydrodynamic study describing the motion field of the MBBR carriers during the microaerobic/aerobic conditions. This is the subject an ongoing study conducted on a lab-scale MBBR realized in the laboratory LIA (*Laboratio di Ingegneria delle Acque*, San Vittore (Fr)) (**Fig. 6.1**). The realized lab-scale MBBR is 5 m long, 2 m wide and 2 m high, corresponding to a working volume of 10 m^3. Fine bubble diffuser pipes (DBMT, ecoplants) and a mixer (Mx-ii 21154, SCM Tecnologie) have been installed on the bottom of MBBR and nearby the small wall on the left, respectively. The diffuser pipes were designed and realized in order to have two aeration mode: uniform aeration and one-side aeration. Almost 7 m^3 of Carriers Biomaster 0.12KLS (Amitec s.r.l, Milano) have been purchased. Carriers (12.5 mm x 12.5 mm) are characterized by a density and specific surface area of 1.03 g cm^{-3} and 500 $m^2\,m^{-3}$, respectively.

Figure 6.1 - MBBR lab-scale set-up with 30% filling ratio.

The MBBR is a complex multiphase system, making it also challenging to identify a technique that can allow a full study of the interaction between air, water and carrier [41].

The main objective of the hydrodynamic study will be to achieve a homogeneous carrier distribution in MBBR, optimizing the filling ratio and aeration conditions, thus avoiding stagnant zones directly responsible for the formation of zones where anaerobic processes could be triggered. Future experimental activities could be pursued through different approaches. As a first pathway, computational fluid dynamics (CFD) simulations could be used to study the hydrodynamic behavior of the carriers, while the results could be verified directly on lab-scale MBBR. One of the main drawbacks of using CFDs could be the time required to simulate a scenario due to the complexity of the problem. A second possible pathway is to use a modified-carrier with a transponder to allow the track by means of Radio Frequency Identification (RIFD) technology. RFID is an automatic technology often used from industrial tracking to access control and composed by a reader and a transponder [42]. The reader generates an electromagnetic field at different frequencies used to track the transponder or tags, smart devise characterized by a code to be easily identified [43]. Finally, the tags are realized in several shapes and materials, making them adaptable to carriers. Overall, the hydrodynamic study will support the optimization of mixing conditions in the bioreactors with potential benefits on the biological process and reduction of operational costs.

6.8 References

[1] L. Li, G. Qian, L. Ye, X. Hu, X. Yu, W. Lyu, Research on the enhancement of biological nitrogen removal at low temperatures from ammonium-rich wastewater by the bio- electrocoagulation technology in lab-scale systems, pilot-scale systems and a full-scale industrial wastewater treatment plant, *Water Res.* 140 (2018) 77–89.

[2] Z. Xia, Q. Wang, Z. She, M. Gao, Y. Zhao, L. Guo, C. Jin, Nitrogen removal pathway and dynamics of microbial community with the increase of salinity in simultaneous nitrification and denitrification process, *Sci. Total Environ.* 697 (2019) 134047.

[3] T. Liu, G. Jia, J. Xu, X. He, X. Quan, Simultaneous nitrification and denitrification in continuous flow MBBR with novel surface-modified carriers, *Environ. Technol.* (2020).

[4] R. Khanongnuch, F. Di Capua, A.M. Lakaniemi, E.R. Rene, P.N.L. Lens, Long-term performance evaluation of an anoxic sulfur oxidizing moving bed biofilm reactor under nitrate limited conditions, *Environ. Sci. Water Res. Technol.* 5 (2019) 1072–1081.

[5] Y.Q. Gu, T.T. Li, H.Q. Li, Biofilm formation monitored by confocal laser scanning microscopy during startup of MBBR operated under different intermittent aeration modes, *Process Biochem*. 74 (2018) 132–140.

[6] D. Taherzadeh, C. Picioreanu, H. Horn, Mass transfer enhancement in moving biofilm structures, *Biophys. J.* 102 (2012) 1483–1492.

[7] M. Layer, M. Garcia, A. Hernandez, E. Reynaert, E. Morgenroth, N. Derlon, Limited simultaneous nitrification-denitrification (SND) in aerobic granular sludge systems treating municipal wastewater: mechanisms and practical implications, *Water Res. X*. 7 (2020) 100048.

[8] J. Zhou, H. Yu, K. Ye, H. Wang, Y. Ruan, J. Yu, Optimized aeration strategies for nitrogen removal efficiency: application of end gas recirculation aeration in the fixed bed biofilm reactor, *Environ. Sci. Pollut. Res.* 26 (2019) 28216–28227.

[9] S. Matsumoto, A. Terada, S. Tsuneda, Modeling of membrane-aerated biofilm: Effects of C/N ratio, biofilm thickness and surface loading of oxygen on feasibility of simultaneous nitrification and denitrification, *Biochem. Eng. J.* 37 (2007) 98–107.

[10] J. Lim, P. Lim, C. Seng, Enhancement of nitrogen removal in moving bed sequencing batch reactor with intermittent aeration during REACT period, *Chem. Eng. J.* 197 (2012) 199–203.

[11] L. Yan, S. Liu, Q. Liu, M. Zhang, Y. Liu, Y. Wen, Z. Chen, Improved performance of simultaneous nitrification and denitrification via nitrite in an oxygen-limited SBR by alternating the DO, *Bioresour. Technol.* 275 (2019) 153–162.

[12] S. Yang, F. Yang, Nitrogen removal via short-cut simultaneous nitrification and denitrification in an intermittently aerated moving bed membrane bioreactor, *J. Hazard. Mater.* 195 (2011) 318–323.

[13] R. Campo, S. Sguanci, S. Caffaz, L. Mazzoli, C. Lubello, T. Lotti, Efficient carbon, nitrogen and phosphorus removal from low C/N real domestic wastewater with aerobic granular sludge, *Bioresour. Technol.* 305 (2020) 122961.

[14] E.M. Gilbert, S. Agrawal, F. Brunner, T. Schwartz, H. Horn, S. Lackner, Response of different *Nitrospira* species to anoxic periods depends on operational DO, *Environ. Sci. Technol.* 48 (2014) 2934–2941.

[15] R.B. Moura, M.H.R.Z. Damianovic, E. Foresti, Nitrogen and carbon removal from synthetic wastewater in a vertical structured-bed reactor under intermittent aeration, *J. Environ. Manage.* 98 (2012) 163–167.

[16] J. Wang, H. Rong, Y. Cao, C. Zhang, Factors affecting simultaneous nitrification and denitrification (SND) in a moving bed sequencing batch reactor (MBSBR) system as revealed by microbial community structures, *Bioprocess Biosyst. Eng.* 43 (2020) 1833–1846..

[17] W. Ma, Y. Han, W. Ma, H. Han, H. Zhu, C. Xu, K. Li, D. Wang, Enhanced nitrogen removal from coal gasification wastewater by simultaneous nitrification and denitrification (SND) in an oxygen-limited aeration sequencing batch biofilm reactor, *Bioresour. Technol.* 244 (2017) 84–91.

[18] H. Wang, Q. Song, J. Wang, H. Zhang, Q. He, W. Zhang, J. Song, Simultaneous nitrification, denitrification and phosphorus removal in an aerobic granular sludge sequencing batch reactor with high dissolved oxygen: effects of carbon to nitrogen ratios, *Sci. Total Environ.* 642 (2018) 1145–1152.

[19] W. Huang, Z. She, M. Gao, Q. Wang, C. Jin, Y. Zhao, L. Guo, Effect of anaerobic/aerobic duration on nitrogen removal and microbial community in a simultaneous partial nitrification and denitrification system under low salinity, *Sci. Total Environ.* 651 (2019) 859–870.

[20] Q. He, J. Zhou, Q. Song, W. Zhang, H. Wang, L. Liu, Elucidation of microbial characterization of aerobic granules in a sequencing batch reactor performing simultaneous nitrification, denitrification and phosphorus removal at varying carbon to phosphorus ratios, *Bioresour. Technol.* 241 (2017) 127–133.

[21] X. Liu, M. Kim, G. Nakhla, M. Andalib, Y. Fang, Partial nitrification-reactor configurations, and operational conditions: performance analysis, *J. Environ. Chem. Eng.* 8 (2020) 103984.

[22] S. Rahimi, O. Modin, I. Mijakovic, Technologies for biological removal and recovery of nitrogen from wastewater, *Biotechnol. Adv.* 43 (2020) 107570.

[23] G. Liu, J. Wang, Long-term low DO enriches and shifts nitrifier community in activated sludge, *Environ. Sci. Technol.* 47 (2013) 5109–5117.

[24] L.J. Thompson, V. Gray, D. Lindsay, A. Von Holy, Carbon:nitrogen:phosphorus ratios influence biofilm formation by *Enterobacter cloacae* and *Citrobacter freundii*, *J. Appl. Microbiol.* 101 (2006) 1105–1113.

[25] H. Ge, D.J. Batstone, J. Keller, Biological phosphorus removal from abattoir wastewater at very short sludge ages mediated by novel PAO clade *Comamonadaceae*, *Water Res.* 69 (2014) 173–182.

[26] S.Y. Gebremariam, M.W. Beutel, D. Christian, T.F. Hess, Research advances and challenges in the microbiology of enhanced biological phosphorus removal — a critical review, *Water Environ. Res.* 83 (2011) 195–219.

[27] J.T. Bunce, E. Ndam, I.D. Ofiteru, A. Moore, D.W. Graham, A review of phosphorus removal technologies and their applicability to small-scale domestic wastewater treatment systems, *Front. Environ. Sci.* 6 (2018).

[28] M. Pijuan, A. Guisasola, J.A. Baeza, J. Carrera, C. Casas, J. Lafuente, Aerobic phosphorus release linked to acetate uptake: influence of PAO intracellular storage compounds, *Biochem. Eng. J.* 26 (2005) 184–190.

[29] M. Vargas, C. Casas, J.A. Baeza, Maintenance of phosphorus removal in an EBPR system under permanent aerobic conditions using propionate, *Biochem. Eng. J.* 43 (2009) 288–296.

[30] D. Yadav, N. Kumar, V. Pruthi, P. Kumar, Ensuring sustainability of conventional aerobic wastewater treatment system via bio-augmentation of aerobic bacterial consortium: an enhanced biological phosphorus removal approach, J. *Clean. Prod.* 262 (2020) 121328.

[31] T. Saito, D. Brdjanovic, M.C.M. Van Loosdrecht, Effect of nitrite on phosphate uptake by phosphate accumulating organisms, *Water Res.* 38 (2004) 3760–3768.

[32] P. Jabari, G. Munz, Q. Yuan, J.A. Oleszkiewicz, Free nitrous acid inhibition of biological phosphorus removal in integrated fixed-film activated sludge (IFAS) system, *Chem. Eng. J.* 287 (2016) 38–46.

[33] J. Zhao, X. Wang, X. Li, S. Jia, Q. Wang, Y. Peng, Improvement of partial nitrification endogenous denitrification and phosphorus removal system: balancing competition between phosphorus and glycogen accumulating organisms to enhance nitrogen removal without initiating phosphorus removal deterioration, *Bioresour. Technol.* 281 (2019) 382–391.

[34] S. Du, D. Yu, J. Zhao, X. Wang, C. Bi, J. Zhen, Achieving deep-level nutrient removal via combined denitrifying phosphorus removal and simultaneous partial nitrification-endogenous denitrification process in a single-sludge sequencing batch reactor, *Bioresour. Technol.* 289 (2019) 121690.

[35] J. Fu, Z. Lin, P. Zhao, Y. Wang, L. He, J. Zhou, Establishment and efficiency analysis of a single-stage denitrifying phosphorus removal system treating secondary effluent, *Bioresour. Technol.* 288 (2019) 121520.

[36] M. Stokholm-Bjerregaard, S.J. Mcilroy, M. Nierychlo, S.M. Karst, M. Albertsen, P.H. Nielsen, A critical assessment of the microorganisms proposed to be important to enhanced biological phosphorus removal in full-scale wastewater treatment systems, *Front. Microbiol.* 8 (2017) 718.

[37] S.K. Jørgensen, A.S.L. Pauli, Polyphosphate accumulation among denitrifying bacteria in activated sludge, *Anaerobe*. 1 (1995) 161–168.

[38] L.S. de S. Rollemberg, Q.L. De Oliveira, A.R.M. Barros, V.M.M. Melo, P.I.M. Firmino, A.B. do. Santos, Effects of carbon source on the formation, stability, bioactivity and biodiversity of the aerobic granule sludge, *Bioresour. Technol.* 278 (2019) 195–204.

[39] N. Derlon, J. Wagner, R. Helena, E. Morgenroth, Formation of aerobic granules for the treatment of real and low-strength municipal wastewater using a sequencing batch reactor operated at constant volume, *Water Res.* 105 (2016) 341–350.

[40] M. Layer, A. Adler, E. Reynaert, A. Hernandez, M. Pagni, E. Morgenroth, Organic substrate diffusibility governs microbial community composition, nutrient removal performance and kinetics of granulation of aerobic granular sludge, *Water Res. X.* 4 (2019) 100033.

[41] J. Wang, X. Ying, Y. Huang, Y. Chen, D. Shen, X. Zhang, H.J. Feng, Numerical study of hydrodynamic characteristics in a moving bed biofilm reactor, *Environ. Res*. (2020) 110614.

[42] D. Bertoni, G. Sarti, G. Benelli, A. Pozzebon, Radio frequency identification (RFID) technology applied to the definition of underwater and subaerial coarse sediment movement, *Sediment. Geol.* 228 (2010) 140–150.

[43] N. Goseberg, I. Nistor, J. Stolle, Tracking of "Smart" debris location based on RFID technique, Coast. Struct. Solut. to Coast. Disasters 2015 TsunamisAt Boston, USA. (2017).